

1996

Preparation and characterization of sol-gel derived titania-silica thin films

Young Min Kwon
San Jose State University

Follow this and additional works at: https://scholarworks.sjsu.edu/etd_theses

Recommended Citation

Kwon, Young Min, "Preparation and characterization of sol-gel derived titania-silica thin films" (1996). *Master's Theses*. 1317.
DOI: <https://doi.org/10.31979/etd.tbv6-svv6>
https://scholarworks.sjsu.edu/etd_theses/1317

This Thesis is brought to you for free and open access by the Master's Theses and Graduate Research at SJSU ScholarWorks. It has been accepted for inclusion in Master's Theses by an authorized administrator of SJSU ScholarWorks. For more information, please contact scholarworks@sjsu.edu.

INFORMATION TO USERS

This manuscript has been reproduced from the microfilm master. UMI films the text directly from the original or copy submitted. Thus, some thesis and dissertation copies are in typewriter face, while others may be from any type of computer printer.

The quality of this reproduction is dependent upon the quality of the copy submitted. Broken or indistinct print, colored or poor quality illustrations and photographs, print bleedthrough, substandard margins, and improper alignment can adversely affect reproduction.

In the unlikely event that the author did not send UMI a complete manuscript and there are missing pages, these will be noted. Also, if unauthorized copyright material had to be removed, a note will indicate the deletion.

Oversize materials (e.g., maps, drawings, charts) are reproduced by sectioning the original, beginning at the upper left-hand corner and continuing from left to right in equal sections with small overlaps. Each original is also photographed in one exposure and is included in reduced form at the back of the book.

Photographs included in the original manuscript have been reproduced xerographically in this copy. Higher quality 6" x 9" black and white photographic prints are available for any photographs or illustrations appearing in this copy for an additional charge. Contact UMI directly to order.

UMI

A Bell & Howell Information Company
300 North Zeeb Road, Ann Arbor MI 48106-1346 USA
313/761-4700 800/521-0600

**PREPARATION AND CHARACTERIZATION OF SOL-GEL DERIVED
TITANIA-SILICA THIN FILMS**

A Thesis

Presented to

The Faculty of the Department of Materials Engineering

San Jose State University

In Partial Fulfillment

of the Requirements for the Degree

Master of Science

by

Young-Min Kwon

August 1996

UMI Number: 1381428

**Copyright 1996 by
Kwon, Young-Min**

All rights reserved.

**UMI Microform 1381428
Copyright 1996, by UMI Company. All rights reserved.**

**This microform edition is protected against unauthorized
copying under Title 17, United States Code.**

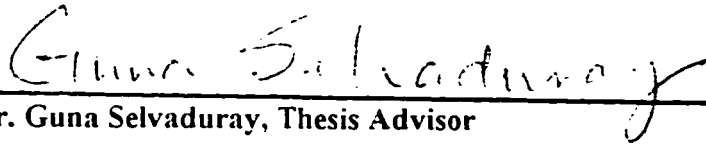
UMI
300 North Zeeb Road
Ann Arbor, MI 48103

@ 1996

Young-Min Kwon

ALL RIGHTS RESERVED

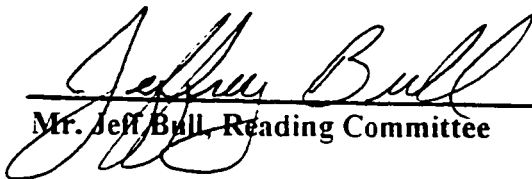
APPROVED FOR THE DEPARTMENT OF MATERIALS ENGINEERING



Dr. Guna Selvaduray, Thesis Advisor



Dr. Michael Jennings, Reading Committee



Mr. Jeff Bull, Reading Committee

APPROVED FOR THE UNIVERSITY



ABSTRACT

PREPARATION AND CHARACTERIZATION OF SOL-GEL DERIVED TITANIA-SILICA THIN FILMS

by Young-Min Kwon

Sol-gel derived titania-silica thin films were prepared on silicon wafers by dip coating. The deposited films were characterized by measuring the thickness, refractive index and spectral reflectance. This coating provided antireflectivity over almost the entire spectral range of the silicon wafer. The dependence of the thickness and refractive index of the films on processing conditions were investigated as a function of coating rate, the number of coating cycles and heat-treatment temperature. The pore structures of the films were inferred from the porosity measurements of very thin bulk gels. The pore characteristics of gels, influenced by different processing parameters, were studied by measuring the adsorption isotherm, pore volume, pore size, surface area and pore size distribution. The pore structures of resultant bulk gels were found to be process dependent. The porosity of the gel varied as a function of water concentration, aging times, addition of polyethylene glycol and heat-treatment temperature.

ACKNOWLEDGEMENTS

First of all, I would like to thank Dr. Guna Selvaduray, my thesis advisor, for his advice and assistance during the course of this work. I also wish to express my appreciation to Dr. Michael Jennings and Mr. Jeff Bull for their support and suggestions as my thesis committee members. Next, I am greatly thankful to Mr. Kay-Nam Chun for his helpful guidance, assistance and valuable suggestions during this study. I also wish to extend my gratitude to Dr. Peter Gwozdz for providing the silicon wafers for my experiments. I am also grateful to Hansen Fong for his helpful assistance in performing the experiment. Finally, my deepest appreciation goes to my parents, wife, and daughter for their endless tolerance, encouragement and support throughout the duration of this study.

TABLE OF CONTENTS

	PAGE
ABSTRACT	iv
ACKNOWLEDGEMENTS	v
TABLE OF CONTENTS	vi
LIST OF FIGURES	viii
LIST OF TABLES	xii
LIST OF ABBREVIATIONS / ACRONYMS	xiv
CHAPTER 1 INTRODUCTION	1
CHAPTER 2 BACKGROUND	6
2.1. Sol Preparation	6
2.2. Sol-Gel Deposition Methods	19
2.3. Thickness Control in Dip Coating Process	22
2.4. Microstructure Control in Sol-Gel Derived Films	31
2.5. Antireflective Films with Tailored Refractive Index	40
CHAPTER 3 EXPERIMENTAL OBJECTIVES	47
CHAPTER 4 EXPERIMENTAL PROCEDURE	48
4.1. Preparation of Coating Solution	52
4.2. Coating Method	55
4.3. Preparation of Bulk Gels	56
4.4. Characterization Methods	57
CHAPTER 5 RESULTS AND DISCUSSION	58
5.1. Thickness Control of Films	58
5.2. Effect of Drain Rate and Heat-treatment on Refractive Index	64
5.3. Effect of PEG added to Solution	64
5.4. Effect of Water Concentration	79

5.5. Effect of Aging Times	85
5.6. Effect of Heat-treatment Temperature After Deposition	87
5.7. Effect of Alkoxide Composition	93
CHAPTER 6 CONCLUSIONS	97
CHAPTER 7 REFERENCES	99
APPENDIX A Ellipsometry	103
APPENDIX B Reflection Measurement by Reflectometer	106
APPENDIX C Porosity Measurement with Quantachrome Autosorb-1	108
APPENDIX D Calculation for % Change in Thickness of Films	115
APPENDIX E Ellipsometric Measurements for Thickness and Refractive Index	117
APPENDIX F Reflectivity Measurements	133
APPENDIX G Autosorb-1 Data	137

LIST OF FIGURES

FIGURE	PAGE
Fig. 1. Illustrations of general sol-gel steps and applications.	7
Fig. 2. Elements used to date in the sol-gel process.	8
Fig. 3. Schematic representation of hydrolysis and polycondensation reactions in alkoxide solution.	11
Fig. 4. Regions of stable titanium alkoxide solution as a function of water concentration.	14
Fig. 5. Thickness of sol-gel films prepared from various starting solvent during heat-treatments.	15
Fig. 6. Stages of the dip coating process.	21
Fig. 7. Stages of the spin coating process.	23
Fig. 8. The steady-state dip coating process.	24
Fig. 9. Coating thickness vs. substrate withdrawal speed.	26
Fig. 10. Coating thickness vs. viscosity at different withdrawal speed.	28
Fig. 11. Effect on film thickness with partial replacement of ethanol by t-butanol.	29
Fig. 12. Coating thickness vs. the number of deposition layers at different dip coating rates.	30
Fig. 13. Variation in coating thickness with heat-treatment temperature.	32
Fig. 14. Schematic representations of structures of gel and film.	34

Fig. 15. Effects of water soluble polymers on gel structure.	39
Fig. 16. Change in pore morphology after heat-treatment.	41
Fig. 17. Change in refractive index during heat-treatment temperature.	42
Fig. 18. Reflection of incident light on a glass surface (a) and on a glass surface coated with a single film (b).	43
Fig. 19. Effect of porosity on the refractive indices of oxides.	46
Fig. 20. Preparation procedure of TiO ₂ -SiO ₂ sol-gel films.	49
Fig. 21. Preparation procedure of TiO ₂ -SiO ₂ bulk gels.	50
Fig. 22. Photographs of the surface of films with various coating conditions.	59
Fig. 23. Effect of drain rate on the thickness of sol-gel derived titania-silica films.	61
Fig. 24. Effect of the number of coating cycles on the thickness of titania-silica films.	62
Fig. 25. Effect of heat-treatment temperature on the thickness of titania-silica films.	63
Fig. 26. Effect of drain rate on the refractive index of titania-silica sol-gel films.	65
Fig. 27. Effect of heat-treatment temperature on the refractive index of titania-silica sol-gel films.	66
Fig. 28. Schematic illustration of DSC curves of PEG containing gels.	68
Fig. 29. Effect of the addition of PEG on the thickness of titania-silica sol-gel films.	69
Fig. 30. Effect of the addition of PEG on the shrinkage of titania-silica sol-gel films.	71
Fig. 31. Effect of the addition of PEG on the refractive index of titania-silica sol-gel films.	72
Fig. 32. Effect of the addition of PEG on the reflectivity of titania-silica sol-gel films.	74

Fig. 33. N ₂ adsorption/desorption isotherms of titania-silica bulk gels prepared from sol with and without PEG (volume percentage).	76
Fig. 34. Pore size distribution of titania-silica bulk gel prepared by 2 vol. % PEG containing sol and sol without PEG.	78
Fig. 35. N ₂ adsorption/desorption isotherms of titania-silica bulk gels at various water concentrations.	82
Fig. 36. Pore size distribution of titania-silica bulk gels at various water concentrations.	83
Fig. 37. Effect of water concentration on the reflectivity of titania-silica sol-gel films.	84
Fig. 38. N ₂ adsorption/desorption isotherms of titania-silica bulk gels at various aging times.	87
Fig. 39. Pore size distribution of titania-silica bulk gels at various aging times.	88
Fig. 40. Effect of aging times on the reflectivity titania-silica sol-gel films.	89
Fig. 41. N ₂ adsorption/desorption isotherms of titania-silica bulk gels at at various heat-treatment temperature.	92
Fig. 42. Pore size distribution of titania-silica bulk gels at various heat-treatment temperature.	93
Fig. 43. Refractive index as a function of alkoxide composition (TiO ₂ / SiO ₂).	95
Fig. 44. Effect of alkoxide composition on the reflectivity of titania-silica sol-gel films.	96

Fig. 45. Ellipsometer component at measurement	105
Fig. 46. Typical configuration of Dyn-optics 224 Reflectometer.	107
Fig. 47. Quantachrome Autosorb-1	110
Fig. 48. A typical BET plot	111
Fig. 49. Isotherm types classified by BDDT.	115

LIST OF TABLES

TABLE	PAGE
Table 1. Alkoxides used in sol-gel technology.	10
Table 2. Effect of the HCl content on gelation properties and spinnability of TMOS solution.	18
Table 3. Refractive index, % porosity, pore size, and surface area of multicomponent silicate films versus sol aging times prior to film deposition.	36
Table 4. List of raw materials.	51
Table 5. Composition and aging times of titania-silica solutions	53
Table 6. Porosity of bulk titania-silica gels and refractive index of films on Si wafers as a function of the addition of PEG.	73

Table 7.	81
Porosity of bulk titania-silica gels and refractive index of films on Si wafers as a function of water concentration.	
Table 8.	86
Porosity of bulk titania-silica gels and refractive index of films on Si wafers as a function of aging times.	
Table 9.	91
Porosity of bulk titania-silica gels and refractive index of films on Si wafers as a function of heat-treatment temperature.	

LIST OF ABBREVIATIONS / ACRONYMS

A. C. S.	American Chemical Society
AR	Antireflective
BET	Brunauer-Emmett-Teller
BDDT	Brunauer-Deming-Deming-Teller
bp	Boiling point
d	Density of liquid compound or solid inorganic compound
DSC	Differential Scanning Calorimetry
EtOH	Ethanol
FW	Formula weight based on carbon mass = 12.011
M (OR) ₄	Metal alkoxide with valence 4
M.W.	Weight-average molecular weight of a polymer
n	Refractive index
PEG	Poly(ethylene glycol)
R	Reflectivity (%)
R-OH	An alcohol
RT	Room temperature
TEOS	Tetraethylorthosilicate
TMOS	Tetramethoxysilane

T_m Melting temperature

·
vol. Volume

wt Weight

< Less than

> Greater than

CHAPTER 1

INTRODUCTION

The formation of sol-gel derived thin oxide coatings on various substrates, such as glasses, metals, plastics and semiconductors, has been shown to be one of the most promising coating techniques for many industrial applications including optical, electronic and protective purposes.⁽¹⁾ In general, a "sol" is a solution of soluble organometallic precursors, whereas a "gel" is a macroscopically rigid network built through polymerization of the sol. The sol-gel method refers to the preparation of inorganic materials by chemical reactions of hydrolysis and polycondensation of sols at a relatively low temperature.⁽²⁾ The transparent and homogeneous sols prepared from these reactions are used as coating solutions to obtain pure oxide films. The sol-gel coating process is quite simple. These coating solutions can be applied onto a substrate by dipping or spinning. Sols are typically prepared by mixing a metal alkoxide, a suitable amount of water for partial hydrolysis of the alkoxide, and an alcohol as a co-solvent. Thus, structural variations of final products can be obtained by well controlled hydrolysis and polycondensation reactions of metal alkoxides.

The sol-gel method is not new, but much attention has been paid recently to the synthesis of various types of advanced materials in the form of films, fibers, monoliths, powders, composites and porous media.⁽³⁾ Among them, certainly one of the most commercially promising applications of sol-gel techniques, is the thin film coating

prepared at room temperature, though most need to be calcined and densified by heating. The sol-gel coating method has many advantages over conventional thin film deposition methods such as chemical vapor deposition (CVD), sputtering and evaporation, in that they are suitable for the deposition of coatings on irregularly shaped substrates with large surface areas at relatively low processing temperatures.⁽⁴⁾ Compared to other coating methods, the sol-gel method requires no expensive equipment and may be one of the simplest coating techniques. In addition, the sol-gel method is very useful for the preparation of advanced materials with high purity and homogeneity. The most important advantage of the sol-gel method over conventional coating methods is the microstructural and compositional tailoring of the films before or during deposition.⁽¹⁾ Although the sol-gel method is very attractive, several problems still exist. The disadvantages of the sol-gel method include the relatively higher cost of starting materials (metal alkoxide versus oxides), cracking that often occurs due to large shrinkage during the removal of the solvent within the gel, difficulty in reproducible processing and long processing times.⁽⁵⁾

However, in the case of thin film formation, the advantages of the sol-gel method are relatively easy to secure and most of the disadvantages can be minimized. The sol-gel coating process does not have serious cracking problems because as the film dries all the shrinkage occurs in the direction normal to the surface of substrate. This leads to relatively uniform shrinkage due to the constraint of the film in the plane of the substrate. Rapid drying methods can be employed without the development of cracking.⁽⁶⁾ In sol-gel coating methods such as dipping or spinning, the raw material cost is relatively

unimportant because only small amounts of metal alkoxide are used for the desired coatings. The coating solution can be used for sufficiently long periods by further diluting the solution with an alcohol. Therefore, the sol-gel derived thin film formation is economically suitable because thin films can be made without expensive equipment.

There are many applications for sol-gel derived films in optical, microelectronic, protective and sensor applications.^(6, 7) Among them, optical coatings, which can alter the reflectance, transmission and absorption of the substrates, have been widely developed over the past several decades. One specific example of the earliest commercial applications of the sol-gel coating method is a transparent and highly antireflective thin oxide coating for sun-shielding windows, automobile rear view mirrors and silicon solar cells. The sol-gel derived thin films have been investigated extensively for the development of a cheap antireflective (AR) coating which reduces the reflectance at the substrate surface.⁽⁸⁾ AR coatings to reduce reflection losses at the surface have been used widely for cathode-ray-tube (CRT) face plates, solar cells and glass picture frames. One major advantage of the sol-gel coating method is that the AR coating can be densified at relatively low temperatures which do not cause excessive damage to the silicon solar cell.

Thin film coatings based on sol-gel derived SiO_2 and TiO_2 have been extensively investigated for optical and protective applications.^(1, 6, 8) The optical coatings must be highly transparent and stable. Titanium dioxide (TiO_2) has been found to be highly versatile and suitable for the preparation of optical coatings due to many interesting physical properties such as good transmittance in the visible region as well as good

mechanical and chemical stability. One important parameter in AR coatings is the refractive index. Since TiO_2 has a high refractive index (~ 2.30), in order to obtain a suitable AR coating with low refractive index, another oxide such as SiO_2 (~ 1.46) can be incorporated. With proper control of composition, desired microstructure, refractive indices, and controlled thicknesses of the films for the AR coatings can be obtained. The sol-gel derived TiO_2 - SiO_2 thin films have many actual and potential applications. Such films have been deposited to enhance the efficiency of silicon solar cells and are considered to serve as a passivation coating for soda lime-silica glass plates. These films also significantly improve the weathering resistance of the substrate.⁽⁹⁾

The most significant advantage of the sol-gel coating method over other film forming techniques is the ability to control the refractive index of the film prior to deposition. In order to obtain suitable refractive indices for AR coatings, it is necessary to introduce porosity in the films.⁽¹⁰⁾ Controlled introduction of porosity can reduce the refractive index of the sol-gel derived thin films. The desired properties of the sol-gel derived films can be obtained by tailoring the gel properties such as pore volume, pore size and surface area.

The optical properties and pore characteristics of sol-gel derived TiO_2 - SiO_2 thin films are process dependent. The physical nature of the film such as thickness and surface morphology can also be controlled by varying the process conditions. This research was aimed to prepare antireflective TiO_2 - SiO_2 thin films using the sol-gel dip coating process on silicon wafers and to study the processing parameters which may influence the

properties of films. Investigation of the pore structure of the coating, which can be tailored by process conditions, is very useful for a better understanding of the porosity-optical properties relationship. In order to prepare optimal sol-gel derived thin films for optical applications, the relationship between process parameters and the resultant optical properties and microstructure of the films is essential. In this study, the effects of specific process parameters, such as water concentration, aging times of sols, addition of water soluble polymers and heat-treatment temperatures after deposition, on the properties of the sol-gel derived $\text{TiO}_2\text{-SiO}_2$ thin films were studied.

The principles of the sol-gel method and the fundamental physics and chemistry underlying thin film formation are first briefly reviewed in Chapter 2. The experimental objectives and procedures employed in this research are discussed in Chapter 3 and 4, respectively, and the results obtained are presented in Chapter 5. The conclusions of this study and future research are contained in Chapter 6.

CHAPTER 2

BACKGROUND

2.1. Sol Preparation

The term “sol-gel” refers to two physico-chemical states. The “sol,” which is a colloidal dispersion of solids in liquid, is a solution of precursor materials needed to make the final product.^(1,6) The basis for the sol-gel coating process is the preparation of transparent and homogeneous sols; these sols should be stable for a long time in order to build up successive films to the desired thickness. In general, sols are prepared by controlled chemical reactions of metal alkoxides with water in mutual solvents such as alcohols. The sol can then be transformed into a rigid gel by one of several processes such as evaporation of the liquid in the sol. The gel consists of a continuous solid network surrounding and supporting a continuous liquid phase. The gel is a very porous solid exhibiting a jelly-like structure in which the pores are predominantly interconnected. This gel is so active that it can be easily densified at very low temperatures. Figure 1 illustrates general sol-gel processing steps and potential applications.⁽⁶⁾

The most important reagents for the preparation of sols are the class of materials known as metal alkoxides because they react readily with water. Figure 2 shows the elements that have been used in sol-gel processing to date.⁽¹¹⁾

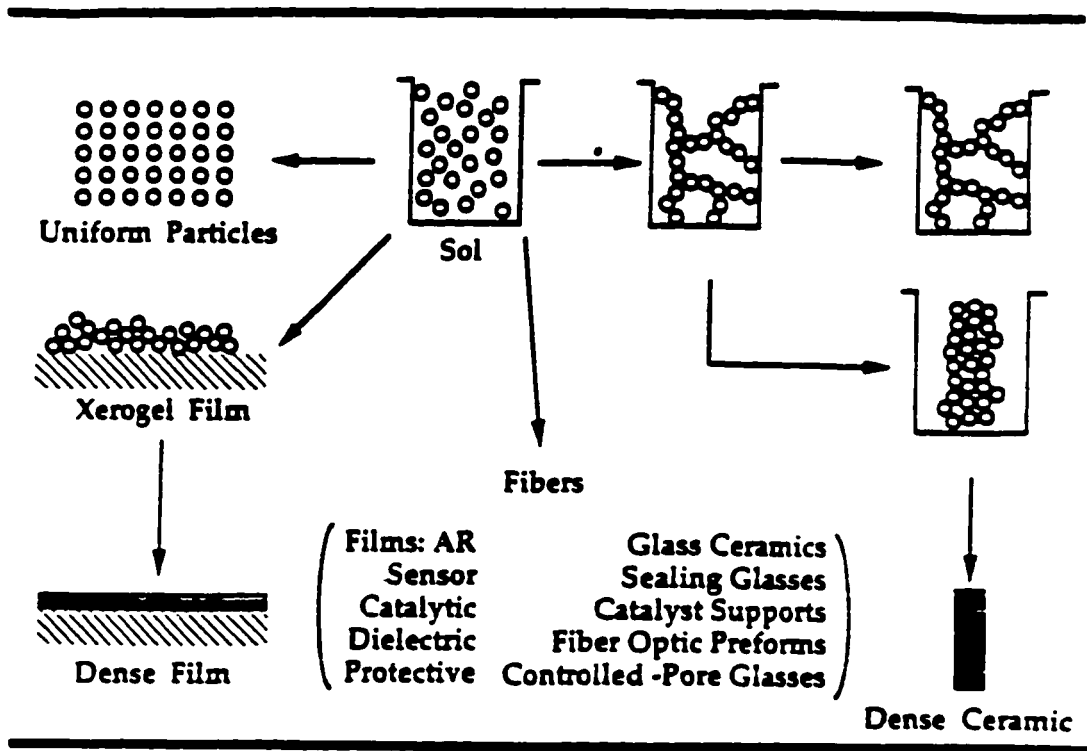


Fig. 1. Illustrations of general sol-gel steps and applications.⁽⁶⁾

IA	IIA	IIIB	IVB	VB	VIB	VII B	VIII B	IB	IIB	IIIA	IVA	VA	VIA	VIIA	VIIIA		
H															He		
Li	Be									B	C	N	O	F	Ne		
Na	Mg									Al	Si	P	S	Cl	Ar		
K	Ca	Sc	Ti	V	Cr	Mn	Fe	Co	Ni	Cu	Zn	Ga	Ge	As	Se	Br	Kr
Rb	Sr	Y	Zr	Nb	Mo	Tc	Ru	Rh	Pd	Ag	Cd	In	Sn	Sb	Te	I	Xe
Cs	Ba	La	Hf	Ta	W	Re	Os	Ir	Pt	Au	Hg	Tl	Pb	Bi	Po	At	Rn
Fr	Ra	Ac	(Ung)	(Unp)													
⁵⁸ Ce	⁵⁹ Pr	⁶⁰ Nd	⁶¹ Pm	⁶² Sm	⁶³ Eu	⁶⁴ Gd	⁶⁵ Tb	⁶⁶ Dy	⁶⁷ Ho	⁶⁸ Er	⁶⁹ Tm	⁷⁰ Yb	⁷¹ Lu				
⁹⁰ Th	⁹¹ Pa	⁹² U	⁹³ Np	⁹⁴ Pu	⁹⁵ Am	⁹⁶ Cm	⁹⁷ Bk	⁹⁸ Cf	⁹⁹ Es	¹⁰⁰ Fm	¹⁰¹ Md	¹⁰² No	¹⁰³ Lr				

Fig. 2. Elements that have been used in the sol-gel process.⁽¹⁰⁾

Almost any metal can form an alkoxide which has the following general formula: $M(OR)_n$, where M is the metal with a valence n and R is an alkyl group, C_xH_{2x-1} . The list of the most widely used metal alkoxides in the sol-gel method is shown in Table 1.⁽¹⁰⁾

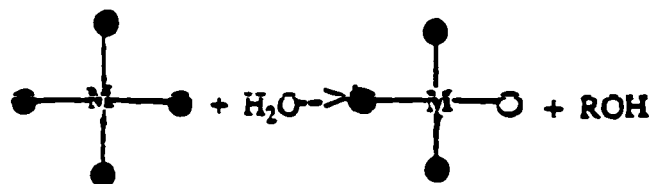
In alcoholic solutions containing water, metal alkoxides are rapidly hydrolyzed into the corresponding hydroxides with or without the addition of catalysts. Subsequent polycondensation reactions of hydroxides with each other or unhydrolyzed alkoxides make two or three dimensional networks composed of inorganic oxide linkages (M-O-M). In general, it is possible that the polycondensation reaction starts at different stages of the hydrolysis of the metal alkoxide, depending on the process conditions. These two chemical reactions (hydrolysis and polycondensation) are shown in Figure 3. The parameters that influence the chemical reactions are temperature, pH, concentration of water, type of solvent used, and precursor.⁽¹²⁾

The structure and properties of sols are usually affected by the concentration of water in the metal alkoxide solutions.^(13, 14) The water concentration, $H_2O/M(OR)_n$, not only affects the sol but also the nature of the resultant products. It can determine the molecular size and polymer morphology in the sol. The number of OH groups per metal ion should increase with increased concentration of water.

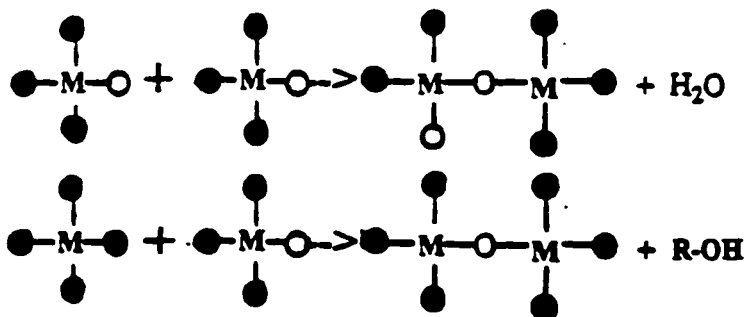
Since an increase of water content increases the number of sites to be hydrolyzed, the hydrolysis is promoted by using excess water. This results in highly cross-linked final products. With under-stoichiometric addition of water, the condensation mechanism is biased towards producing an alcohol as a by product whereas over-stoichiometric

Table. 1 Alkoxides used in the sol-gel method. ⁽¹⁰⁾

Cation	M (OR)_n	Description
Si	Si (OC ₂ H ₅) ₄	Tetraethylorthosilicate or Tetraethoxysilane
	Si (OCH ₃) ₄	Tetramethylorthosilicate or Tetramethoxysilane
Al	Al (O- <i>iso</i> -C ₃ H ₇) ₃	Aluminum isopropoxide
	Al (O- <i>sec</i> -C ₄ H ₉) ₃	Aluminum secondary butoxide
Ti	Ti (O-C ₂ H ₅) ₄	Titanium ethoxide
	Ti (O- <i>iso</i> -C ₃ H ₇) ₄	Titanium isopropoxide
	Ti (O-C ₄ H ₉) ₄	Titanium tetrabutoxide
	Ti (O-C ₃ H ₇) ₄	Titanium tetramyloxide
B	B (OCH ₃) ₃	Trimethylborate
Ge	Ge (O-C ₂ H ₅) ₄	Germanium ethoxide
Zr	Zr (O- <i>iso</i> -C ₃ H ₇) ₄	Zirconium isopropoxide
	Zr (O-C ₄ H ₉) ₄	Zirconium tetratertiary butoxide
Y	Y (O-C ₂ H ₅) ₃	Yttrium ethoxide
Ca	Ca (O-C ₂ H ₅) ₂	Calcium ethoxide



Hydrolysis



Condensation (Polymerization)



Fig. 3. Schematic representation of hydrolysis and polycondensation reactions in an alkoxide solution.

addition of water leads to the formation of water as a by-product.⁽¹²⁾ Excess water is deliberately added to promote hydrolysis and polycondensation, but water is also present in the atmosphere and as a by-product of these two reactions. Even in excess water, the reaction does not go to completion. Therefore, an appropriate concentration of water is a very important factor that influences the overall sol-gel process. Sols prepared with high water content produce highly cross-linked polymer structures. Conversely, a decrease in water content increases the chance of polymerization of only partially hydrolyzed alkoxide groups, producing less cross-linked polymers. In some alkoxide systems such as titanium alkoxides, which are rapidly hydrolyzed with addition of water, the gelling time is drastically reduced with increased water, resulting in an unstable solution viscosity. One factor which can present a problem in a multicomponent system (e.g., TiO₂-SiO₂ binary system) is the different hydrolysis rates of each alkoxide.⁽¹⁵⁾ A more rapid hydrolysis of one alkoxide compared to the other can lead to the precipitation of hydroxides in the sol. This can be overcome by adding water slowly or partial hydrolysis of each alkoxide before mixing the two. Sols obtained using low water content tend to form opaque and discontinuous films because of their low oxide contents. Although the hydrolysis is promoted by increased concentration of water, too much water concentration results in too much dilution of the sol, leading to poor wettability of the coating solution with the substrate. The use of a suitable amount of water and equivalent oxide content results in clear and stable sols. The equivalent oxide content of metal oxide is given by the ratio $MO_2/M(OR)_n$ where M is a Group IV metal.

Figure 4 shows the stability regions for $\text{Ti}(\text{OC}_2\text{H}_5)_4$ and $\text{Ti}(\text{OC}_4\text{H}_9)_4$ sols, as a function of oxide content and concentration of water, $[\text{H}_2\text{O}/\text{Ti}(\text{OR})_4]$.⁽¹⁶⁾ Different concentrations of water are needed for desired hydrolysis of metal alkoxide. Clear and stable sols can be prepared if the equivalent oxide concentration and $[\text{H}_2\text{O}]/[\text{Ti}(\text{OR})_4]$ value lie under the appropriate curve. The equivalent oxide content of titanium oxide is given by $\text{TiO}_2/\text{Ti}(\text{OR})_4$. The oxide content of the hydrolysis products from metal alkoxides can never be 100 % oxide since this would require an infinite polymer with no terminal bonds.⁽¹⁵⁾

The sol-gel process is generally carried out by using various solvents, usually alcohols. Since some metal alkoxides (e.g., silicon alkoxides) are immiscible with water, a co-solvent is needed to prevent liquid-liquid phase separation. Prior dilution of the metal alkoxide by alcohols also prevents uncontrolled hydrolysis during the mixing of all ingredients needed to make sols. Thus, the selection of the solvent is very important to obtain the desired coating solutions. The type of solvent used has a significant effect on both the nature of the sols and the properties of the films.⁽¹⁶⁾ The viscosity of the sol produced is dependent upon the type of solvent used. A higher viscosity alcohol such as butanol ($\text{C}_4\text{H}_9\text{OH}$) leads to the deposition of thicker coatings due to a decrease in the rate of convective outflow from the substrate. Figure 5 shows the dependence of thickness on the type of solvent used for preparing the sol.⁽¹⁷⁾ The sols prepared using methanol (CH_3OH) lead to less uniformity and regions of poor wetting in the films due to the high evaporation rate of methanol. Thus, films prepared from ethanol ($\text{C}_2\text{H}_5\text{OH}$) or propanol ($\text{C}_3\text{H}_7\text{OH}$) are more uniform because these sols are more stable with time and have a

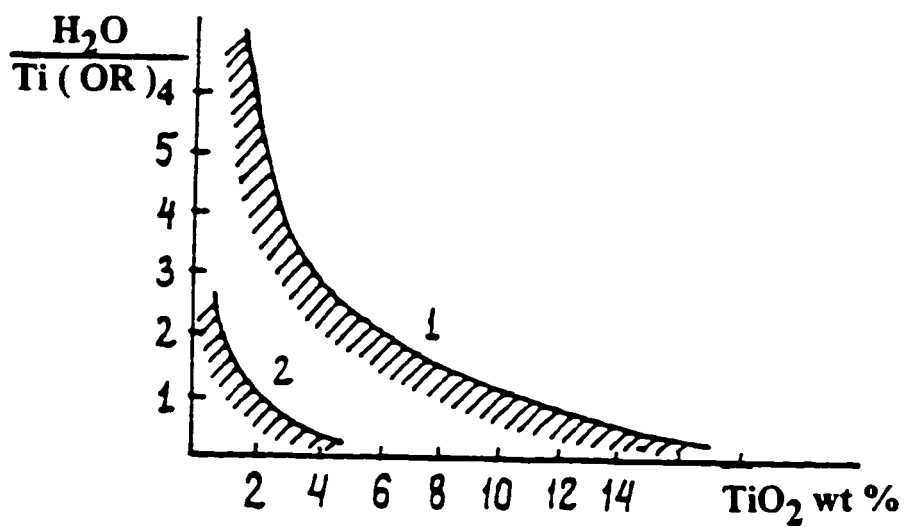


Fig. 4. Regions of stable titanium alkoxide solution as a function of water concentration.⁽¹⁶⁾ 1: titanium butoxide ($\text{Ti}(\text{OC}_4\text{H}_9)_4$) in butanol solution; 2: tetraethylorthosilicate ($\text{Ti}(\text{OC}_2\text{H}_5)_4$) in ethanol solution.

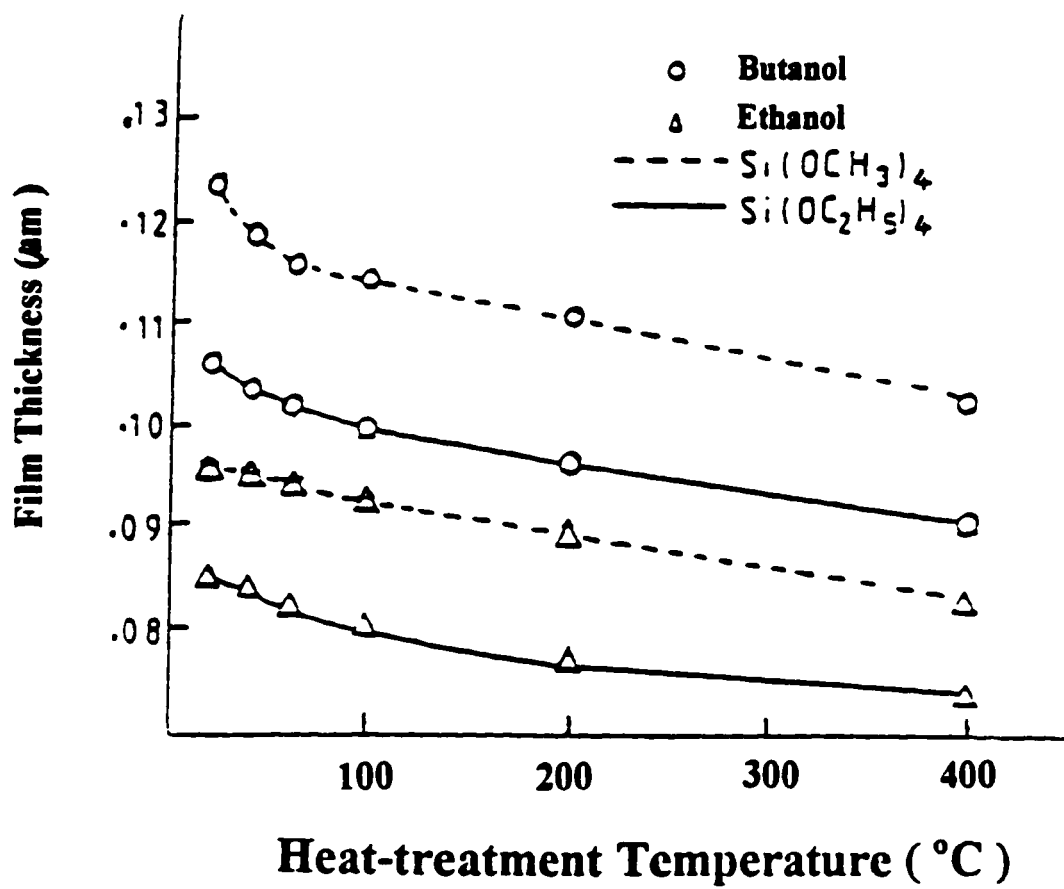


Fig. 5. Thickness of sol-gel films prepared from various starting solvent during heat-treatments.⁽¹⁷⁾

suitable viscosity for the coating process. The sols prepared using ethanol or propanol also have a higher equivalent oxide content due to a greater extent of polymerization.

Since metal alkoxides have different structures, depending on the types of alkyl groups used, the properties of sols are also different. The rates of hydrolysis and polycondensation reactions are dependent upon the chain length or molecular weight of the alkyl groups.⁽¹⁷⁾ The rate of hydrolysis decreases with increasing size of the alkyl groups within the alkoxide whereas the gelling time of the solution increases with increasing size of the alkyl group.⁽¹⁷⁾ Higher rates of hydrolysis and condensation reactions are obtained from monomeric alkoxides rather than from oligomeric alkoxides due to lower steric hindrance from the monomeric alkoxides.^(16, 18) In terms of precursors, long-chain organic groups give slower reaction rates and methyl groups give the fastest rates. The sols prepared using tetramethoxysilane (TMOS), $\text{Si}(\text{OCH}_3)_4$, gelled faster than those prepared using tetraethylorthosilicate (TEOS), $\text{Si}(\text{OC}_2\text{H}_5)_4$ because more branched polymers are formed in TMOS-based sols. Typically, as in the case of solvents, ethanol or propanol-based alkoxides are more widely used in the coating process.⁽¹⁶⁾

The type of catalyst, if used in the preparation of the sol, is also an important parameter. The hydrolysis of the metal alkoxide can be accelerated when acidic catalysts are used. Many researchers have reported that mineral acids, such as HCl or HNO_3 , are more effective catalysts for the hydrolysis than equivalent concentrations of basic catalysts.⁽¹⁹⁾ Aelion et al. showed that the rate of hydrolysis was influenced more by the strength and concentration of the catalysts than the type of the solvent.⁽²⁰⁾ Sols prepared

with high concentrations of acidic catalyst, however, have poor coating properties, such as difficulty in spinning, as shown in Table 2.⁽¹²⁾ The rate of the polycondensation reaction is greatly increased by using basic catalysts such as ammonium hydroxide (NH_4OH), which usually results in an increased viscosity of the alkoxide solution. When a strong basic catalyst is added to an alkoxide solution, relatively fast gelation can occur during sol preparation. Since the sol suddenly loses its fluidity and takes on the appearance of an elastic solid, the sols prepared by using basic catalysts are not useful for the preparation of good quality coating solutions. In general, HCl is also needed to avoid flocculation or precipitation of colloidal particles when a rapidly hydrolyzable alkoxide is added to an alcoholic solution.⁽²¹⁾ Ji-pin Zhong et al. have shown that when a strong acid is added, the precipitation gradually disappears and the sol becomes clear.⁽²²⁾ This disappearance implies that the zeta potential, which causes a repulsion between colloidal particles, has increased and stabilized the particles in the solution.⁽²²⁾

The structure and properties of the sols continue to change due to continuing polycondensation reactions through the aging of the sol in a sealed container. The aging may result in the growth of precursor particles in the sol, which leads to coarsening of the pores within the films prepared from this sol.⁽²³⁾ During the aging carried out in a closed container, the solvent evaporates very slowly, maintaining a fairly constant volume of solvent in the solution. Continued condensation leads to slightly increased viscosity of the solution. In most alkoxide systems the sol should be aged for a few hours to a few days to stabilize it and increase its wettability.

Table 2 Effect of HCl content on gelation properties and spinnability of TMOS solution ⁽¹²⁾

Composition (mol)		Appearance at Gelation	Gelling time (hr)	Spinnability
H ₂ O/TMOS	HCl/TMOS			
2.00	0.01	Transparent	12.6	Yes
2.00	0.40	Transparent	0.6	No
1.70	0.01	Transparent	13.4	Yes
1.70	0.40	Opalescent	1.0	No
1.44	0.01	Transparent	17.2	Yes
1.44	0.40	Opalescent (sedimentation)	(1.4) ^b	Yes ^c
1.53	0.01	Transparent	14.5	Yes
1.53	0.15	Opalescent	3.6	No
1.53	0.20	Opalescent	2.9	No
1.53	0.25	Opaque	2.5	No
1.53	0.30	Opaque	1.9	No
1.53	0.35	Opaque (sedimentation)	(1.6) ^b	No
1.53	0.40	Opaque (sedimentation)	(1.3) ^b	No

^aCH₃OH/TMOS was kept constant at 2.

^bNo clear determination was made, since gelation took place during sedimentation.

^cBottom phase.

The aging process can be assisted by increasing the temperature of the sol.

Some water soluble organic polymers such as poly(ethylene glycol) $[H(OCH_2CH_2)_nOH]$ or diethanolamine $[(HOCH_2CH_2)_2NH]$ can be used to avoid precipitation of hydroxides from alcoholic solutions of metal alkoxides with high rates of hydrolysis and condensation.⁽²⁴⁾ When these polymers are added to the solution, large amounts of water can be added to control the viscosity of the solution. The premature gelation of the coating solution prior to deposition can be prevented with the addition of water soluble polymers. This delay of the gelling time in the polymer-incorporated solution may be accounted for by the hindrance of the polymerization of hydrolyzed species by the added polymeric molecules as well as the dilution effects.⁽²⁴⁾

2.2. Sol-Gel Deposition Methods

Two kinds of sol-gel coating methods, namely dipping and spinning coating, are widely used to form thin oxide films. They are based on the linear and centrifugal spreading of an alkoxide solution onto the substrate, respectively.⁽²⁵⁾ The dipping method is probably the most useful for the fabrication of multilayers, especially for the deposition of thin oxide films, with a high degree of uniformity, planarity and surface quality on irregularly shaped substrates.^(1, 6, 25) This coating method is also more adaptable to the size of substrate. The dip coating method is the most favored sol-gel film forming technique, and it uses less expensive equipment. Dip coating is a relatively simple way of depositing a thin film from a sol onto the substrate by immersion and subsequent withdrawing of the

substrate. Figure 6 is a schematic representation of the dip coating process.⁽²⁵⁾

The substrate is first chemically cleaned then dipped into a coating bath containing a metal alkoxide solution and uniformly withdrawn into any atmosphere, e.g., vacuum or moist air. The liquid film steadily flows down the substrate after wetting the substrate. The cleanliness of the substrate is therefore an important factor for proper adhesion of the films. Since the liquid film wets the surface, it adheres to the substrate and solidifies rapidly through the evaporation of the solvent. At this stage, the film undergoes rapid drying, followed by further condensation and gelation, simultaneously. The deposited film can then be densified by heat-treatment in a furnace. The thickness of the coating layer is determined by the coating rate, i.e., the speed of substrate withdrawal from the coating solution.^(24, 25) The film thickness increases with increasing withdrawal speeds. The thickness also depends on the concentration of the solution, its viscosity, surface tension of the solution and relative humidity above the coating bath.^(1, 25) Other parameters affecting the coating thickness are the angle of withdrawal, which is normally 90°, and the number of coating cycles.

Besides the dip coating method, other techniques can be employed for thin film deposition from the sol-gel process. Spin coating is often used for one-sided coating. The spin coating method is a technology that has been well developed by the microelectronics industry for the application of thin films of photoresist onto silicon wafers. In the spin coating process, the coating solution is dripped onto the center of the substrate, which is spinning at a high speed, and spreads evenly.⁽²⁵⁾

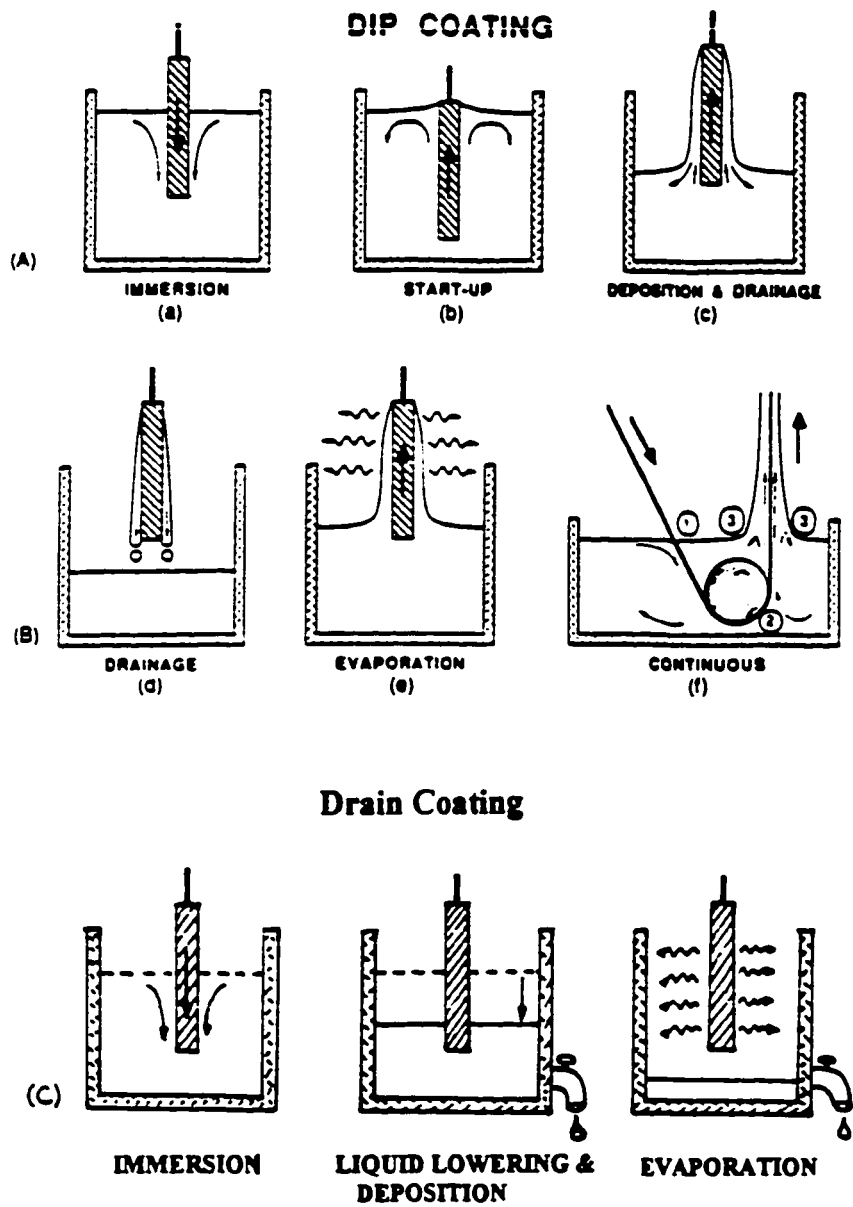


Fig. 6. Stages of the dip coating process. ⁽²⁵⁾

Figure 7 is a representation of the spin coating process, which is divided into four stages: deposition, spin-up, spin-off and evaporation. Spin coating is probably the most suitable for the coating of small disks or lenses with circular shapes. The disadvantages include an edge effect on non-circular shaped substrates, centrifugally stressed surface layers and mechanical problems associated with spinning large substrates. In the case of spin coating, external stresses are applied during film formation due to the high shear rates. A final sol-gel deposition method is spray coating, which may be the least effective way of the three. In this case, the use of material is less efficient and the films tend to be rough. It is possible to spray the coating solution onto a hot substrate and obtain a very rapid reaction between the solution and substrate. This spraying method has potential as a hot coating technique for applying coatings onto glass surfaces.⁽²⁶⁾ However, this method does not result in a uniform layer thickness which is required for optical coatings.

2.3. Thickness Control in Dip Coating Process

In the dip coating method, the film is deposited from a coating solution by dipping and then withdrawing the substrate at a constant speed, as shown in Figure 8. The coating solution is concentrated on the substrate surface by gravitational draining, followed by vigorous evaporation and further polycondensation reactions.^(23, 25) The liquid film has an approximate wedge-like shape due to the evaporation and draining of the solvent.

STAGES OF THE BATCH SPINNING PROCESS

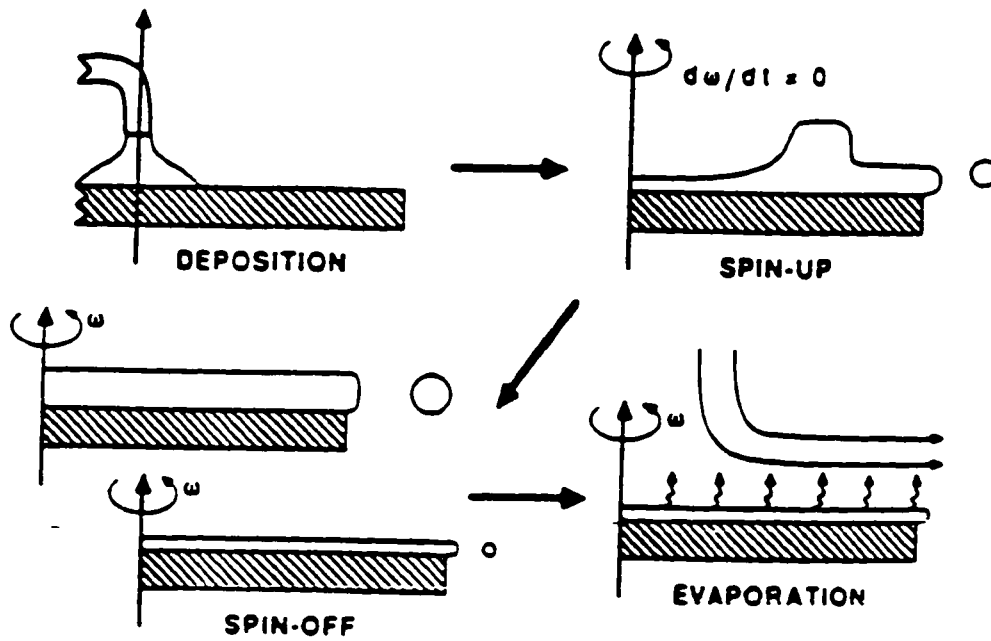


Fig. 7. Stages of the spin coating process. ⁽⁶⁾

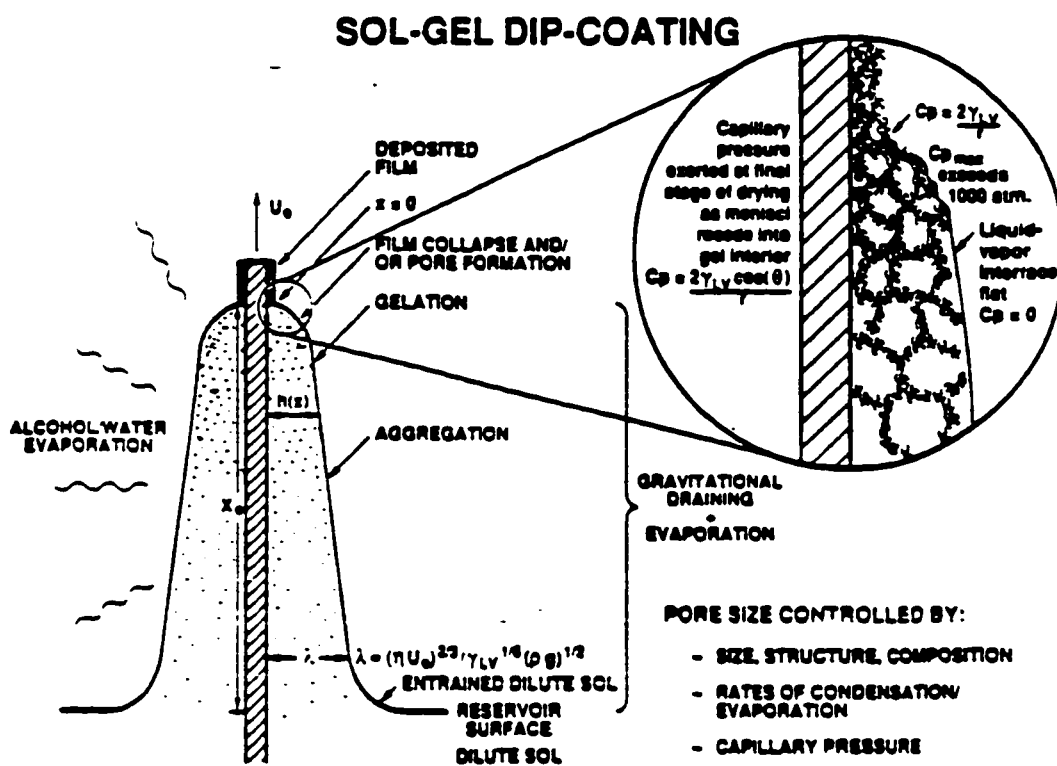


Fig. 8. The steady-state dip coating process. ⁽²³⁾

The thickness of the deposited film is determined by a competition among several forces, which are: (1) viscous drag, which is proportional to liquid viscosity and withdrawal speed, (2) gravity which is proportional to liquid density, and (3) resultant force of surface tension in concavely curved menisci. Among the three forces, the surface tension is not important when the liquid viscosity and withdrawal speed are high enough to hold the meniscus curvature down. Thus, the thickness of the deposited film in this case can be governed by a competition between viscous drag and gravity.

When the viscous drag, $\eta U_0 / h$, and gravity, $\rho g h$, are in balance, the thickness h of the deposited film can be represented by the following equation.^(23, 25)

$$h = C_1 (\eta U_0 / \rho g)^{1/2} \quad [1]$$

where U_0 is the withdrawal speed, η is the solution viscosity, ρ is the liquid density, g is the gravitational acceleration, and $C_1 = 0.81$ for Newtonian liquids. However, since the withdrawal speed and liquid viscosity are typically low in the case of sol-gel dip coating, the thickness is represented by three forces of viscous drag, gravity and surface tension. A relationship derived by Landau and Levich shows that the film thickness is proportional to the 2/3 power of the withdrawal speed.^(27, 28)

$$h = 0.94 (\eta U_0)^{2/3} / \gamma_{LV}^{1/6} (\rho g)^{1/2} \quad [2]$$

where γ_{LV} is the liquid-vapor surface tension. Figure 9 shows the coating thickness as a function of withdrawal speed in the dip coating process.⁽⁶⁾ Greater overlap of the deposition and drying stages can be obtained by decreasing the withdrawal speed. Thinner films can be obtained with a slower coating rate.

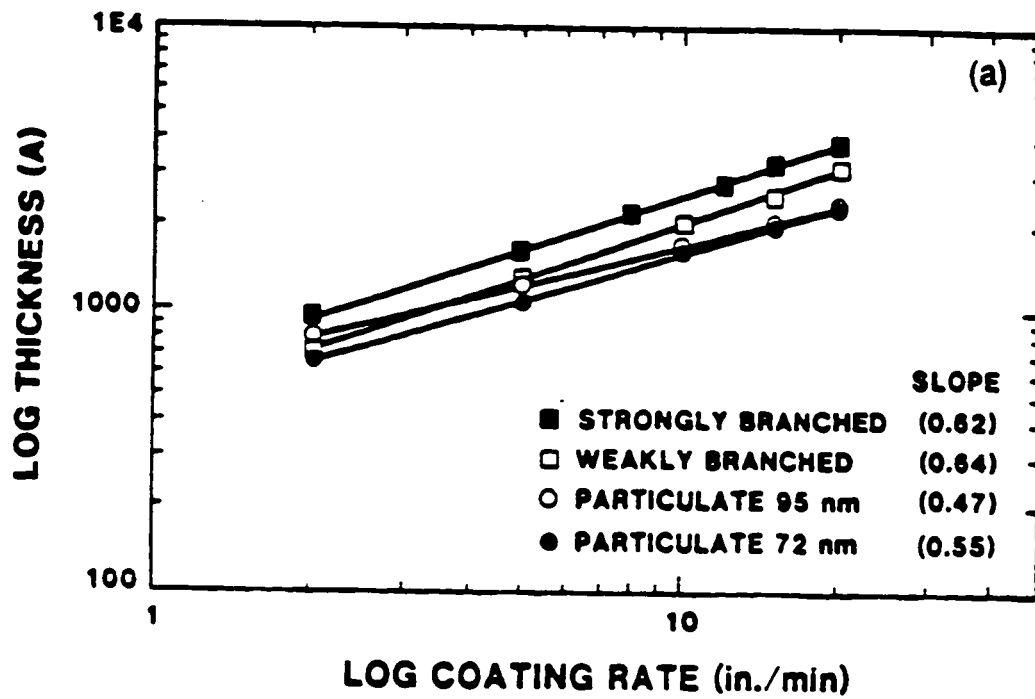


Fig. 9. Coating thickness vs. substrate withdrawal speed. ⁽⁶⁾

The withdrawal speed should be very constant in order to avoid striations.

In addition to the withdrawal speed (or coating rate), the coating thickness also depends on the viscosity of the solution, the number of coating cycles and the temperature of heat-treatment after deposition.^(1, 6, 25) The thickness of the film deposited is dependent on the solution viscosity, which is affected by the concentration changes, the extent of hydrolysis, and type of solvent used.⁽²⁶⁾ Although the composition of the liquid bath may be unaffected by the evaporation in a closed container, the evaporation of the solvent during thin film deposition significantly increases the concentration of precursor species in the liquid film. Thus, the viscosity progressively increases due to both an increased concentration and further polycondensation reaction promoted by the increased concentration. The coating thickness increases with increased viscosity, as shown in Figure 10. Since higher viscosity of the solution leads to a decrease in the rate of outflow, less liquid flows off the substrate, resulting in thicker coatings. The type of solvent in the coating solution has an effect on the coating thickness due to differences in the viscosities of the solvents used. A higher viscosity alcohol, such as butanol, leads to a deposition of thicker coatings, as shown in Figure 11.⁽³⁰⁾ Good quality films with the desired thickness can be obtained by the consecutive deposition and heat-treatment of thinly deposited layers, at a relatively low withdrawal speed, from dilute coating solutions. As can be seen from Figure 12, for a given withdrawal speed the coating thickness is proportional to the number of deposited layers.⁽³¹⁾

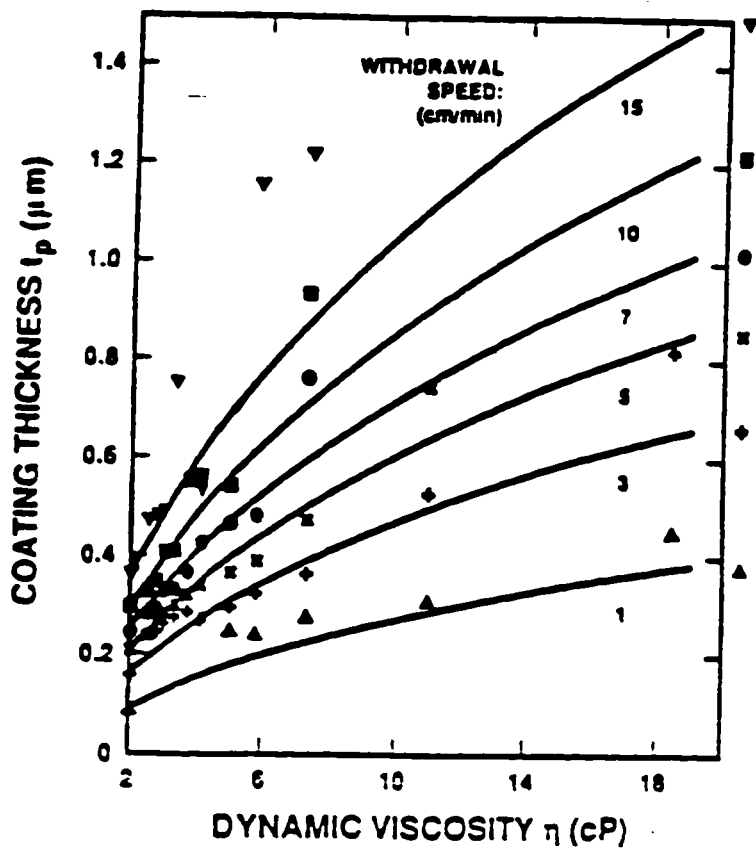


Fig. 10. Coating thickness vs. viscosity at different withdrawal speed. ⁽⁶⁾

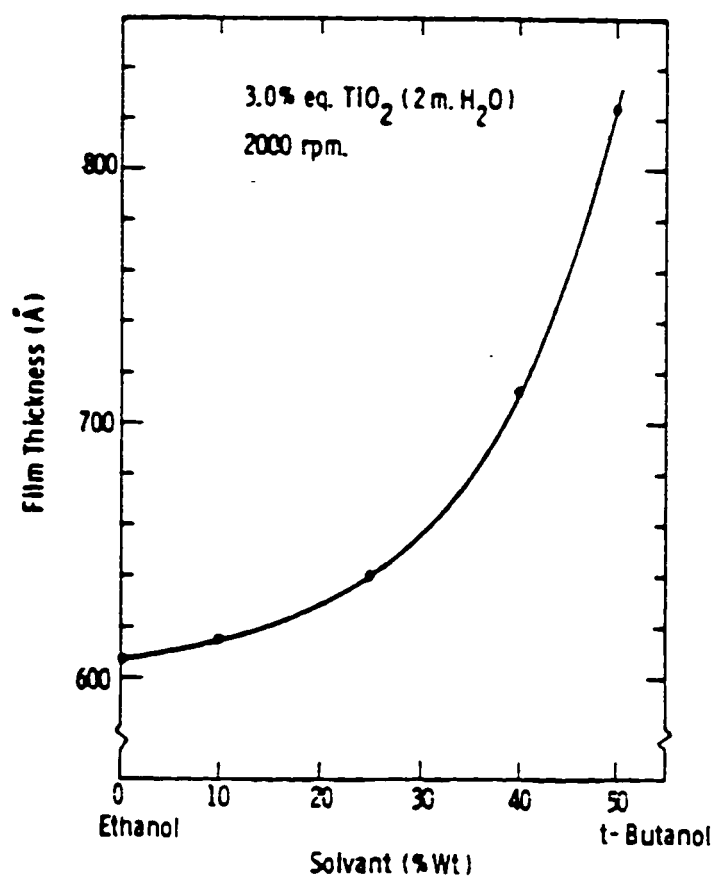


Fig. 11. Effect on film thickness of partial replacement of ethanol by t-butanol. ⁽³⁰⁾

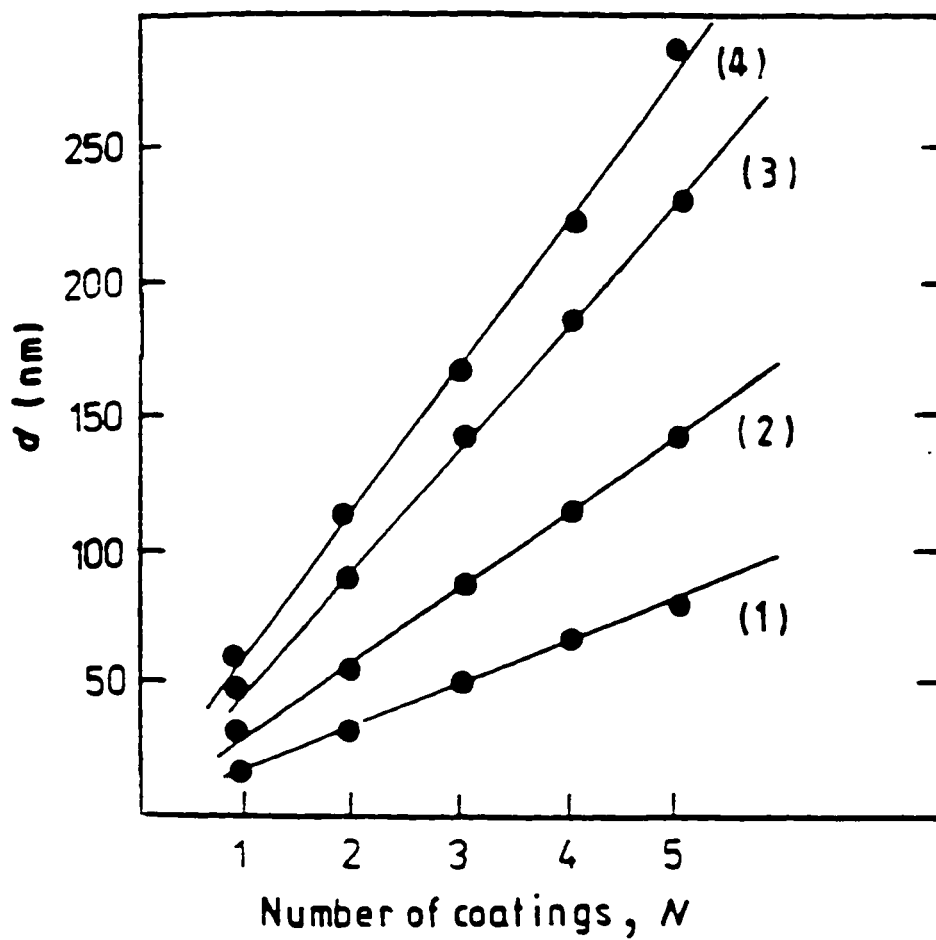


Fig. 12. Coating thickness vs. the number of deposition layers at different dip coating rates. coating rates: (1) 6 mm/min, (2) 120 mm/min, (c) 240 mm/min (4) 600 mm/min. ⁽³¹⁾

The temperature and the duration of the heat-treatment of as-deposited films have a significant effect on the thickness of the final films. The coating thickness decreases during heat-treatment, suggesting a sintering and densification process.⁽³²⁾ As the temperature increases, the film shrinks and the porosity within the film decreases. Since almost all as-deposited films have the same thickness under the same deposition conditions, the thinner coatings after heat-treatment are more dense than the thicker coatings. Thus, increasing heat-treatment temperature increases the film density. This makes the films tougher and more resistant to scratching. Figure 13 shows the change in film thickness as a function of heat-treatment temperature.

2.4. Microstructure Control in Sol-Gel Derived Films

The ability to tailor the microstructure of the film is the most important advantage sol-gel derived films have over films prepared by conventional coating methods.^(1, 6) The microstructure of the sol-gel derived films can be controlled for specific applications, such as antireflective coatings and porous films in the fields of sensors or catalysis. In literature reviews of current sol-gel research, it was found that the microstructure of the deposited films, such as pore volume, pore size and surface area, can easily be controlled by varying process parameters such as water concentration and aging times. The microstructures of the sol-gel derived films depend on the structures of precursors in the solution and process conditions such as the coating solution and heat-treatment after deposition. The relative rates of evaporation and polycondensation during deposition also affect the microstructure

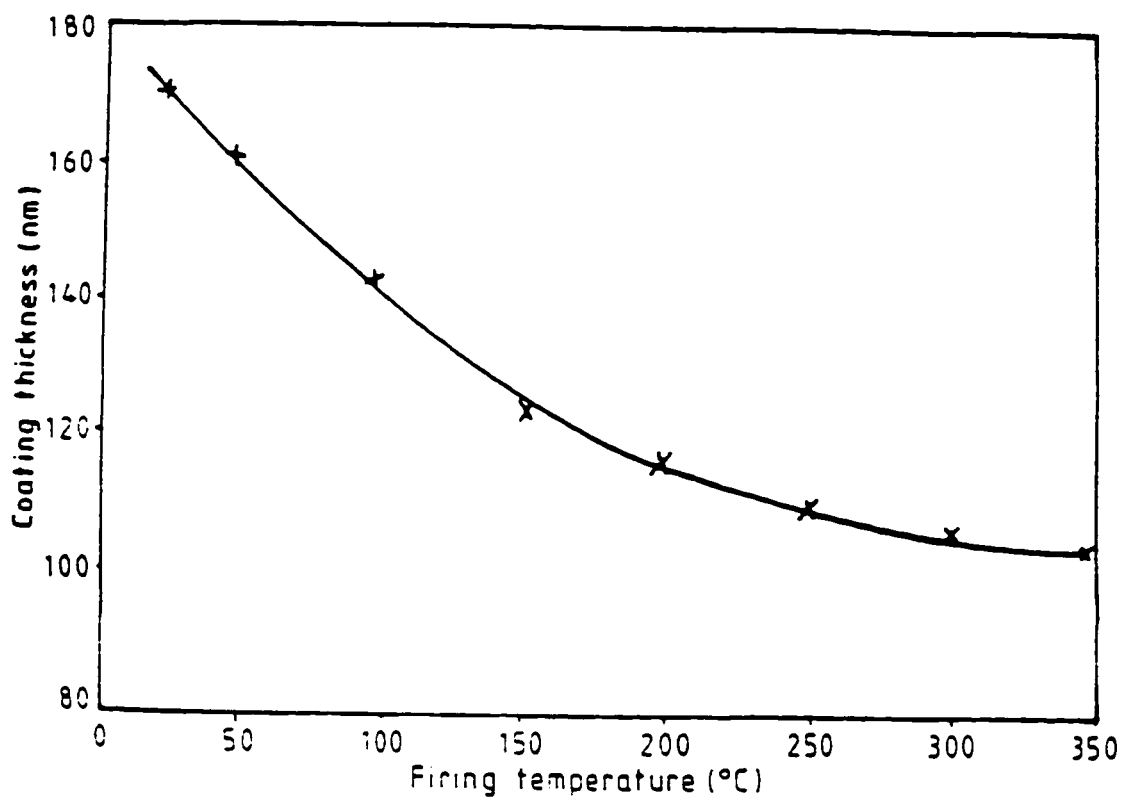


Fig. 13. Variation in coating thickness with heat-treatment temperature. ⁽³²⁾

of the film. In sol-gel deposition, gelation, drying, and further polycondensation stages are normally not separated. Thus, the overlap of the deposition and drying stages causes the films to experience a competition between evaporation and further polycondensation reactions.^(1, 6, 33) Since the evaporation densifies the film structure while the continuing condensation reaction stiffens the structure, the resistance to compactness increases.⁽³³⁾ When the deposited film is sufficiently stiff to withstand flow, further evaporation may collapse the film or generate pores within the film. Since pores are formed by solvent evaporation, the pore structure of the film depends on the relative rates of evaporation and continued polycondensation reactions. During deposition, the condensation and evaporation rates can be controlled by varying the pH values of the coating solution and the partial pressure of the solvent in the coating ambient, respectively.⁽³³⁾

It is possible to prepare sols in which the structures of the precursor species range from entangled linear polymeric species to uniform colloidal particles that are either aggregated or remain non-aggregated.^(1, 34) The structure of precursor species in the solution depends on several factors, which include the nature of the starting materials, pH, water concentration, solvent composition and aging of the solution.⁽¹⁾ Various types of sols are used to prepare different gel structures for many applications in the areas of protective, antireflective and highly porous coatings. The structural changes in films from various types of sol-gel structures are schematically illustrated in Figure 14. The sols with unaggregated entangled precursor species lead to gels with low porosity, resulting from a large number of interparticle contacts. On the other hand, the sols containing aggregated

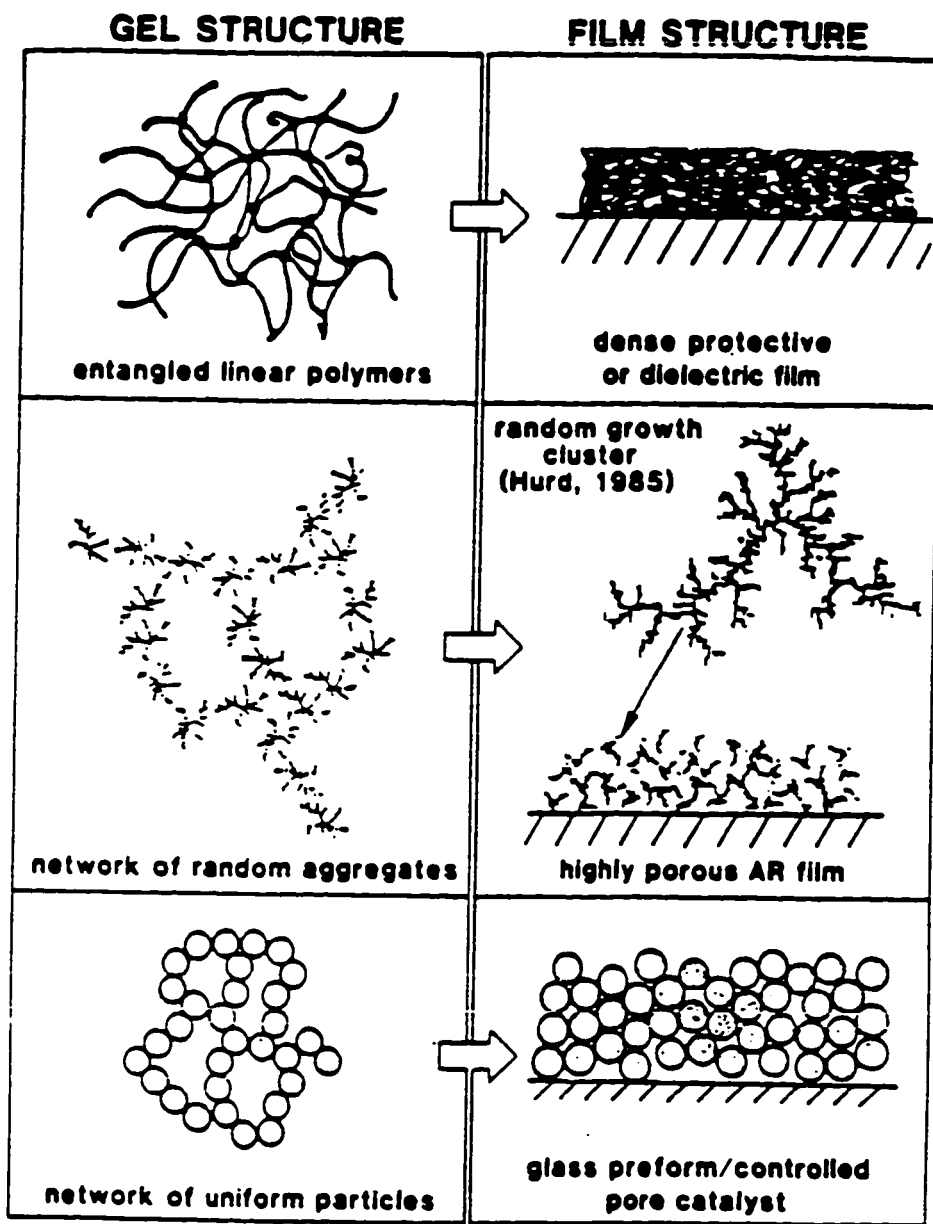


Fig. 14. Schematic representations of structures of gel and film. ⁽³⁶⁾

colloidal particles result in highly porous film structures, due to the relatively open structures in the sols. Unaggregated, highly-entangled sols yield dense protective films. In contrast, highly porous antireflective layers can be formed from aggregated sols.

Since the pore structure reflects to some extent the size and topology of the precursor in the sol, microstructure tailoring can be achieved by controlling the polymer growth in the sol prior to film deposition. Brinker et al. demonstrated that the size of the precursor species, which increases with aging times of the sol, has an effect on the pore volume, pore size and surface area of the final film.^(6, 23) The pore volume, average pore size and surface area of the films increase with the size of the precursor species. The aging process prior to deposition leads to a growth of precursor species in the solution. Table 3 shows that the porosity and refractive index of the sol-gel derived films can be tailored by aging the sol prior to film deposition.

The microstructure of the film can also be tailored by varying the water concentration, $H_2O/M(OR)_n$, in the alkoxide solution. The water concentration also affects the relative rates of evaporation and polycondensation reactions during deposition. Thus, this parameter has a significant effect on the densification behavior of the resultant film and eventually determines the pore morphology of the film, which in turn determines the refractive index.^(23, 25) In general, lower water concentration results in linear polymers with long chains, whereas higher water concentration tends to form spherical or irregular shapes. The sols prepared with low water concentration yield rather dense films, whereas porous films are obtained from the use of sols with higher water concentration.⁽³⁶⁾

Table. 3 Refractive index, % porosity, pore size, and surface area of multicomponent silicate films versus sol aging times prior to film deposition. ⁽⁶⁾

Sample Aging Times ^a	Refractive Index	Porosity (%)^b	Median Pore Radius (nm)	Surface Area (m²/g)
Unaged	1.45	0	< 0.2	1.2-1.9
3 day	1.31	16	1.5	146
1 week	1.25	25	1.6	220
2 week	1.21	33	1.9	263
3 week ^c	1.18	52	3.0	245

a) Aging of dilute sol at 50°C and pH 3 prior to film deposition.

b) Determined from N₂ adsorption isotherm.

c) The 3 week sample gelled. It was re-liquefied at high shear rates and diluted with ethanol prior to film deposition.

The sols prepared with under-stoichiometric addition of water cause weakly branched precursor species. In the solution with low water concentration, weakly branched precursor species continually rearrange themselves as the solvent evaporates, leading to efficient packing. Since the condensation rate and extent of branching are very low in the sol with low water concentration, highly concentrated solutions with increased viscosity can be prepared. This increased viscosity of the solution results in the formation of a rather thick film. Since low water gels result in less cross-linked structures, broad pore size distributions are usually observed in these gels. On the other hand, higher water concentration leads to an increased condensation rate, resulting in highly condensed species with highly cross-linked structures. This increased condensation rate also increases the size of the precursor species in the solution.^(6,33) The increase in porosity can be obtained with increasing precursor size due to the rigid gel network which has a tendency to resist compaction during solvent evaporation. Thus, since greater amounts of water increase the size of precursor species, further increase in water concentration causes an increase in porosity, resulting in a reduction of the refractive index.⁽²³⁾

In order to control the porosity of the sol-gel derived films, several water soluble polymers such as poly(ethylene glycol) (PEG) can also be added to the solution. The changes in pore size distribution with the addition of polymers result from their effects on the growth of sol particles.⁽³⁷⁾ Uncharged polymers such as PEG affect only the amount of micropores because these have little influence on sol particle growth. These polymers do not undergo hydrolysis or condensation and so do not become part of the gel network.

Charged polymers, such as polyelectrolytes, significantly increase the number of large mesopores and fine pore structures are found in the gels. The effects of charged polymers can be explained in terms of electrostatic interaction between the sol particles and polyions. The proteins decrease the number of micropores and mesopores and greatly increase the number of macropores due to the growth of sol particles. In Figure 15, the influence of water soluble polymers on the gel structures is schematically illustrated.

Water soluble polymers such as polyvinyl alcohol, PEG and polyethylene imine have been widely used as additives to control gel structures and hardening of the gel films. Among them, polyethylene glycol has been found to be suitable for optical sol-gel coatings because, in the case of optical coatings, only micropores within the film are of importance. Matsuda et al. showed that the combustion of added PEG in the gel films during heat-treatment leads to an increase in porosity within the films, resulting in a decrease in the refractive index and in the hardness of the films.⁽³⁸⁾

The pore structure of the sol-gel derived films can be further modified by heat-treatment after deposition. In general, heat-treatment is carried out initially to change the as-deposited film to a pure organic-free oxide layer and secondly to modify the original pore size. Since the necessary pore size for the AR coating is considerably smaller than the wavelength of light, the initial pore size must be reduced below a critical size without causing pore closure. As the heat-treatment temperature increases, the film shrinks and the initial pore size decreases due to viscous sintering and densification processes.⁽³⁹⁾

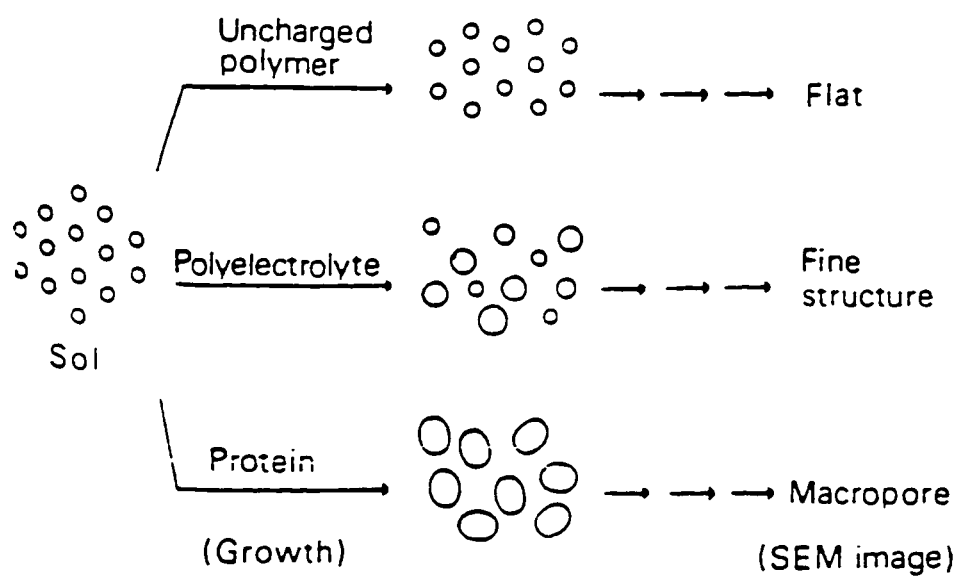


Fig. 15. Effects of water soluble polymers on gel structure. ⁽³⁷⁾

Thus, a uniform reduction in pore size and change in pore morphology can be obtained by heat-treating the deposited film as shown in Figure 16. Figure 17 illustrates that heat-treatment can be used to tailor the refractive index, n , which can be varied according to the pore size.

2.5. Antireflective Films with Tailored Refractive Index

Part of the light passing through a boundary is lost due to reflections which are related to the difference in refractive indices between the two media. The reflectivity, R , of the substrate surface without a coating is given by following expression.

$$R = (n_2 - n_0 / n_2 + n_0)^2 \quad [3]$$

where n_2 and n_0 are the refractive indices of substrate and medium (air), respectively.

For example, at a boundary between air ($n = 1$) and a silicon wafer ($n = 3.85$),

$$R = (3.85 - 1.0 / 3.85 + 1.0)^2 = 0.345$$

which means that 35 % of the incident light is reflected from the surface. One way of eliminating this reflection loss is the interference effect by applying a suitable coating to the surface.⁽⁴⁰⁾ If an appropriate thin film with refractive index n_1 is deposited on the surface of the substrate, the reflections can be reduced, as shown in Fig 18. A coating with refractive index n_1 , which separates media with indices n_0 and n_2 , modifies the magnitude of the reflectivity, R .

$$R = (n_1^2 - n_2 n_0 / n_1^2 + n_2 n_0)^2 \quad [4]$$

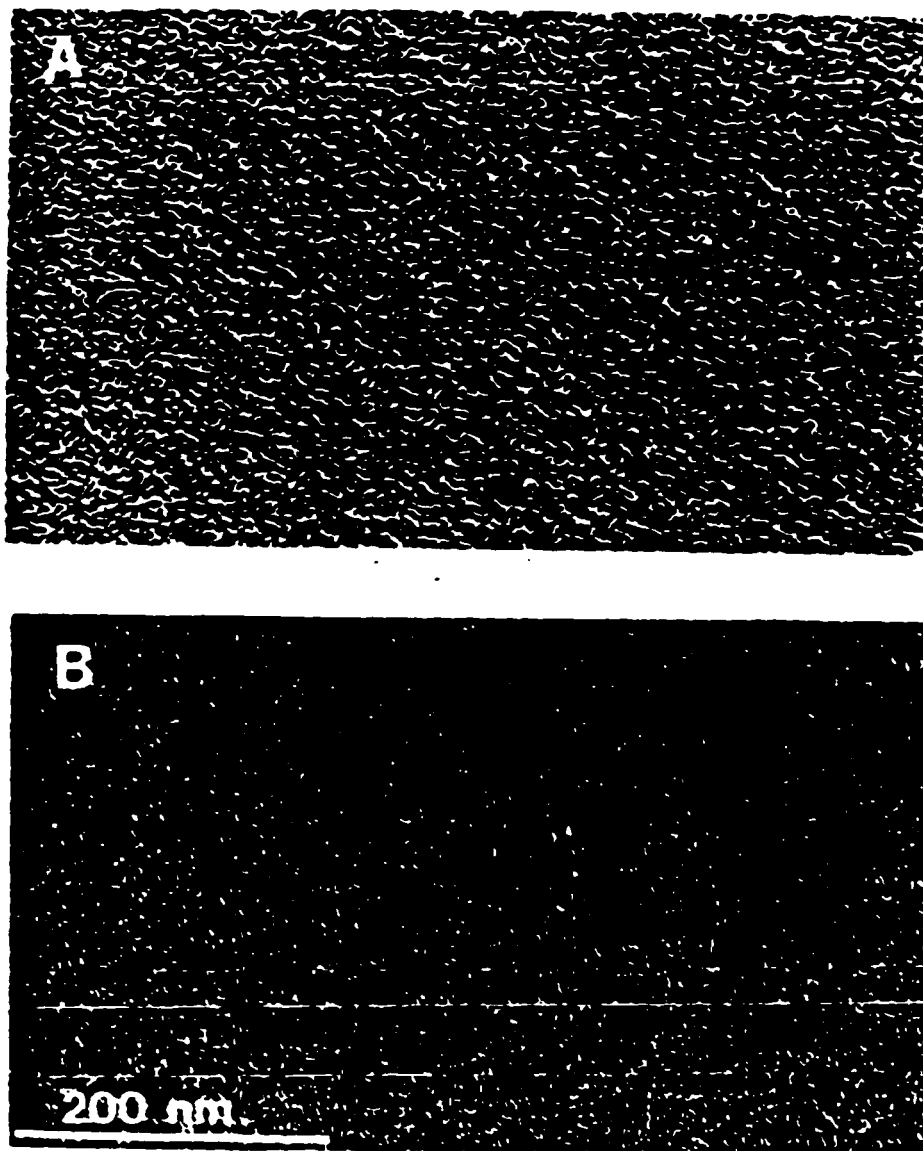


Fig. 16. Change in pore morphology of the sol-gel derived silica glass after heat-treatment at 485°C for 4h. (a) before and (b) after heat-treatment for pore size tailoring.⁽³⁰⁾

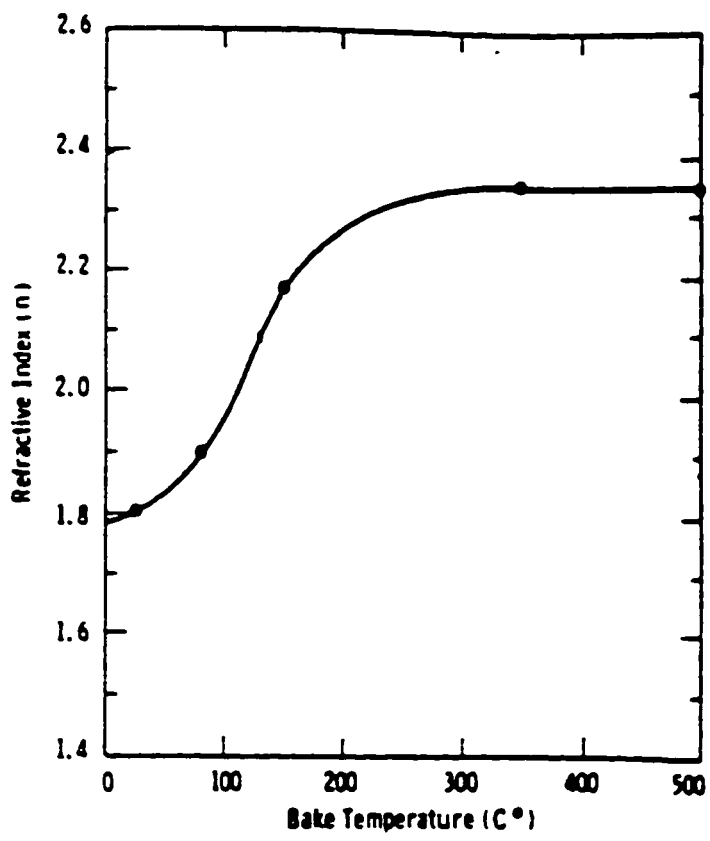


Fig. 17. Change in refractive index during heat-treatment. ⁽⁴⁰⁾

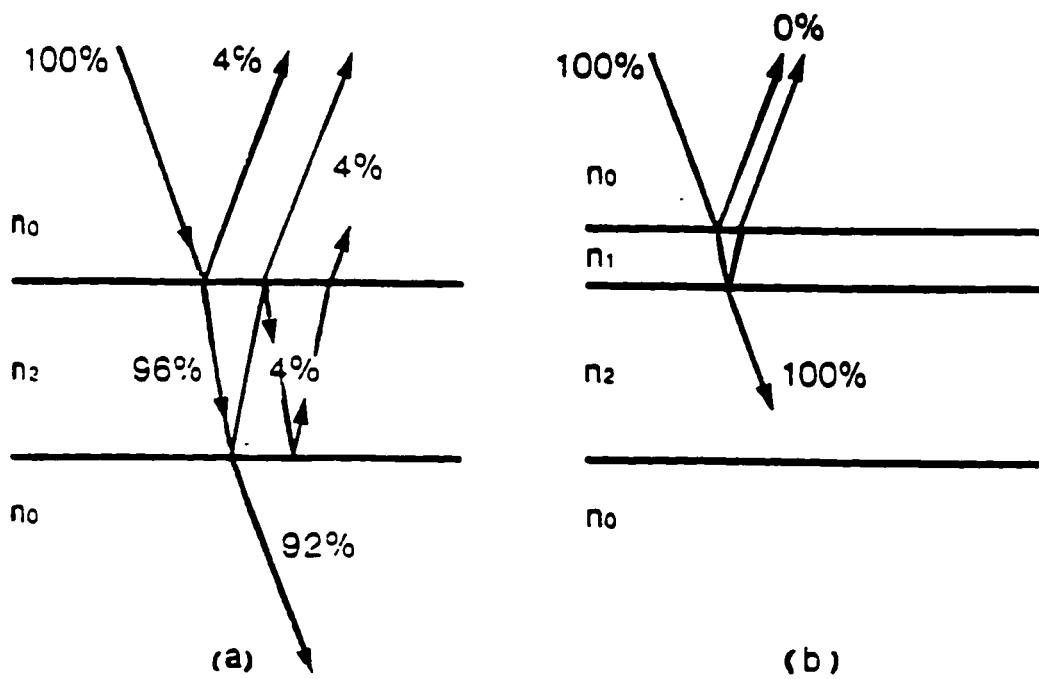


Fig. 18. Reflection of incident light on a glass surface (a) and on a glass surface coated with a single film (b).

Theoretically, in order to obtain zero reflectivity, the refractive index of the coating must satisfy both the amplitude condition and the phase condition. When the light is incident on a substrate surface coated with a suitable thin film, both sides of the film will reflect some of the light. For complete elimination of the two reflected beams, the reflected intensities at the upper and lower boundaries of the film should be equal. The refractive index of the film should be intermediate between the indices of the air and the substrate. The optical thickness of the film should be made one quarter wavelength so that the total difference in phase between the two reflected beams will correspond to twice one quarter wavelength, that is 180° . Thus, for zero reflectivity at wavelength λ , the thickness t and refractive index n_1 of the coating are determined by the following equations:

$$\text{amplitude condition: } n_1 = (n_2 n_0)^{1/2} \quad [5]$$

$$\text{phase condition: } t = \lambda/4n_1 \quad [6]$$

These two conditions result in destructive interference for light reflected from both the front and back sides of the film. Thus, reflected light becomes zero when both amplitude and phase conditions are correct. In general, a relatively low refractive index of film is required for suitable AR coatings. The tailored refractive index is probably the most important factor for the preparation of the desired sol-gel derived AR coatings. Since the refractive index of a material is related to its density, the refractive index can be tailored by proper control of composition and microstructure of the deposited film. The density of a material may be lowered with the introduction of non-scattering porosity. The refractive index, n_p , in a porous structure is given by⁽⁴¹⁾

$$n_p^2 = (n_d^2 - 1) (1 - P) + 1 \quad [7]$$

where n_p and n_d are the refractive indices of the porous and non-porous states of the material, and P is the volume fraction of non-scattering porosity. Thus, the refractive index of AR coatings can be controlled by proper introduction of porosity, as shown in Figure 19.⁽⁴²⁾

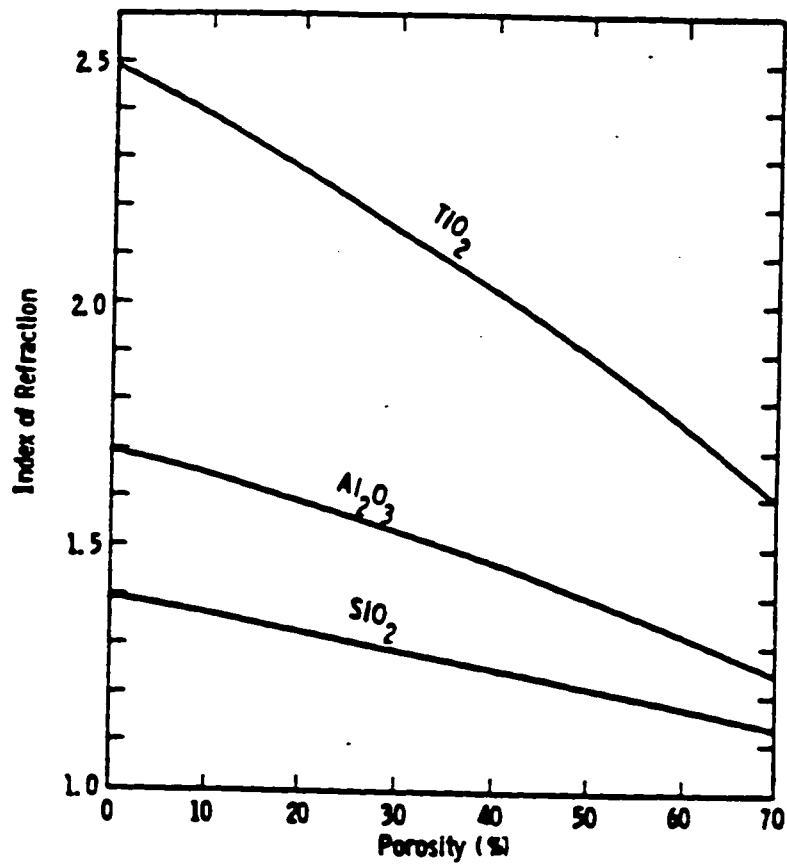


Fig. 19. Effect of porosity on the refractive indices of oxides. ⁽⁴²⁾

CHAPTER 3

EXPERIMENTAL OBJECTIVES

Thin film formation via sol-gel processing is a simple technology in principle but has required considerable effort to be of practical use. Compared to traditional coating methods, sol-gel coating permits microstructural as well as compositional tailoring prior to deposition, as was described in Chapter 2. Several studies have shown that the pore structures, which affect optical properties such as the refractive index of the films, can be controlled by varying process conditions.

The purpose of this study was to prepare sol-gel derived titania-silica thin films and to determine the effects of variations in process conditions on the properties of the films, including thickness, optical properties and porosity. The experimental work consisted of measurements of the thickness, refractive index, and reflectivity of the film as a function of drain rate, heat-treatment temperature, and addition of PEG. The influence of various process conditions such as water concentration, aging times, addition of PEG, and heat-treatment temperature on the porosity of the bulk gel was also investigated.

CHAPTER 4

EXPERIMENTAL PROCEDURE

Titania-silica ($\text{TiO}_2\text{-SiO}_2$) thin films were deposited onto silicon wafers from coating solutions prepared by the hydrolysis and polycondensation reactions of metal alkoxides. Prior to gelation, these coating solutions (or sols) were used by dip coating to form transparent oxide films. Figure 20 shows the overall procedure employed in preparing the titania-silica coating films. All coatings were applied at room temperature in an ambient atmosphere. The coating solutions were also placed in Petri dishes, gelled and dried to produce thin bulk gels. The preparation of the bulk gel is illustrated in Figure 21.

Tetraethylorthosilicate, $\text{Si}(\text{OC}_2\text{H}_5)_4$, titanium isopropoxide, $\text{Ti}(\text{OC}_3\text{H}_7)_4$, anhydrous ethanol, $\text{C}_2\text{H}_5\text{OH}$, deionized water and hydrochloric acid (HCl) were used as raw materials. A list of the raw materials used and their vendors are reported in Table 4. Tetraethylorthosilicate (TEOS) is a highly volatile and slowly hydrolysable alkoxide whereas titanium isopropoxide, $\text{Ti}(\text{O}^i\text{Pr})_4$, is a highly hydrolysable compound. These two alkoxide solutions were each prehydrolyzed separately prior to mixing them together, due to their different hydrolysis rates. The TEOS and $\text{Ti}(\text{O}^i\text{Pr})_4$ sol-gel coating solutions were then combined to prepare the desired sol-gel molar ratios, and aged for the coating experiments. The $\text{TiO}_2\text{-SiO}_2$ thin films were deposited from the coating solution and then heat-treated. Since a pulling apparatus of sufficient steadiness was not available for vibration-free dip coating, the films were deposited by draining the coating solutions away

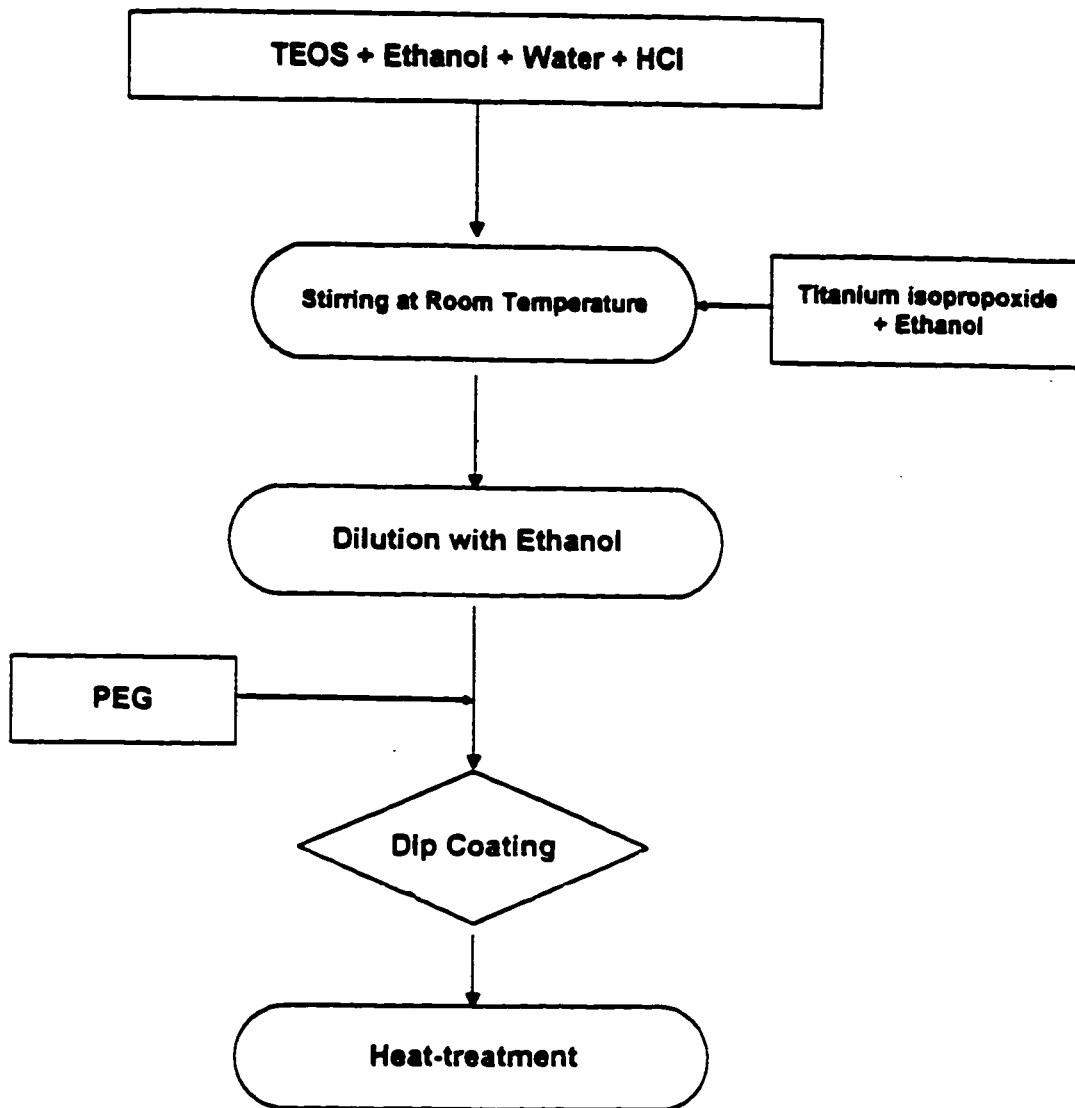


Fig. 20. Preparation procedure of TiO₂-SiO₂ sol-gel films.

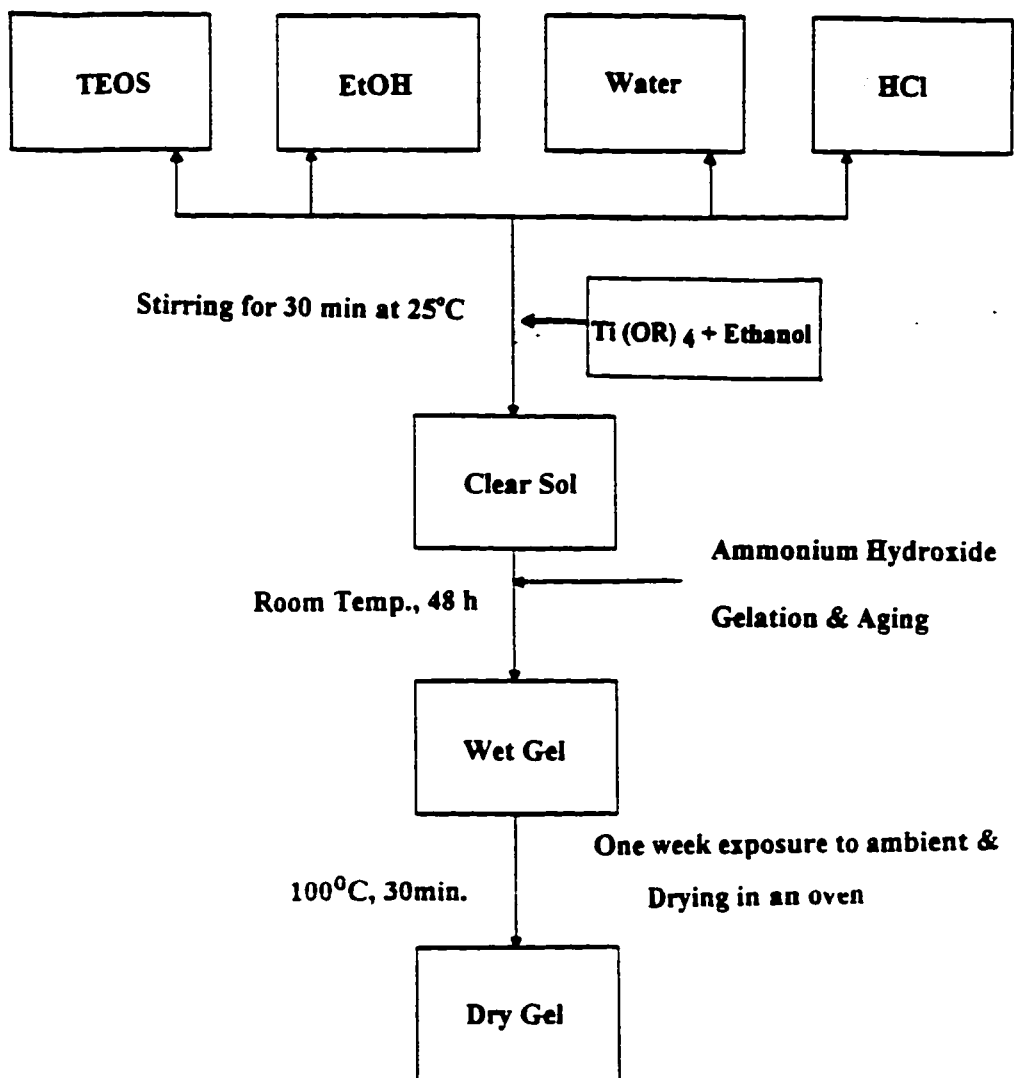


Fig. 21. Preparation procedure of $\text{TiO}_2\text{-SiO}_2$ bulk gels

Table 4 A list of reagents used and their vendors.

Chemicals	Description	Physical Data	Vendor
$\text{Si}(\text{OC}_2\text{H}_5)_4$	Tetraethylorthosilicate	99 %, FW 208.33, bp 168°C	Fisher Scientific
$\text{Ti}(\text{O-iso-C}_3\text{H}_7)_4$	Titanium isopropoxide	98 %, FW 284.26, bp 240°C	Janssen Chimica
$\text{CH}_3\text{CH}_2\text{OH}$	Dehydrated 200 proof Ethyl Alcohol	99 %, FW 47.08, bp 78°C	Quantum Chemical Corporation
H_2O	Distilled and Deionized Water	pH 6-7, FW 18.02, Heavy Metals 0.01ppm	VWR Scientific
HCl	Hydrochloric Acid	A.C.S. Reagent FW 36.46, 0.5 N	VWR Scientific
NH_4OH	Ammonium Hydroxide	A.C.S. Reagent FW 35.05, d 0.900	Fisher Scientific
$\text{H}(\text{OCH}_2\text{CH}_2)_2\text{OH}$	Poly(ethylene glycol)	M.W. 400, Tm -6°C Liquid Viscosity 7.3 centistokes	Janssen Chimica

from around the substrates. The drain-coating technique is a variation on the dip coating method. All deposited samples were used for characterization such as measurement of thickness, refractive index and reflectivity.

4.1. Preparation of Coating Solution

The coating solutions were made by hydrolysis and polymerization reactions from metal alkoxides. The tetraethylorthosilicate (TEOS), $\text{Si}(\text{OC}_2\text{H}_5)_4$, and titanium isopropoxide, $\text{Ti}(\text{OC}_3\text{H}_7)_4$, sol-gel solutions were each prehydrolyzed before mixing together in order to obtain stable precursor species in the solution. The 19 solutions, whose compositions (in volume ratio) are listed in Table 5, were prepared.

A 1:5 volume ratio of TEOS and anhydrous ethanol (EtOH) was mixed with prescribed amounts of water in a 1000 ml round bottom flask. Approximately 200 ml of EtOH was measured using a 250 ml graduated cylinder and then TEOS was added to EtOH in the graduated cylinder so that the final composition would be 1:5 by volume. TEOS/EtOH solution was poured into the flask for further addition of water and catalyst. A certain amount of water ($\text{H}_2\text{O}/\text{TEOS}$ volume ratio = 1.5 to 5) was measured using a 250 ml Erlenmeyer flask. 0.5 N HCl (approximately 20 drops) was added to the water by using a fine point dropper so that the final volume ratio of TEOS to HCl would be 1:0.05. The deionized (DI) water containing hydrochloric acid (HCl) was slowly added to the TEOS solution and then stirred in a covered flask at room temperature for 30 minutes to partially hydrolyze the TEOS.

Table 5 Compositions (in volume ratio)[@] and aging times of titania-silica solutions

Solution Number	TEOS	Ti (OiPr) ₄	H ₂ O	EtOH	HCl	PEG*	Aging Times
A1	4	1	6	20	0.2	0	1 day
A2	4	1	8	20	0.2	0	1 day
A3	4	1	12	20	0.2	0	1 day
A4	4	1	16	20	0.2	0	1 day
B1	4	1	12	20	0.2	0	0 day
B2	4	1	12	20	0.2	0	4 day
B3	4	1	12	20	0.2	0	7 day
B4	4	1	12	20	0.2	0	14 day
C1	4	1	8	20	0.2	0	1 day
C2	3	2	6	20	0.2	0	1 day
C3	2	3	4	20	0.2	0	1 day
C4	1	4	2	20	0.2	0	1 day
D1	4	1	8	20	0.2	0	1 day
D2	4	1	8	20	0.2	0.3	1 day
D3	4	1	8	20	0.2	0.6	1 day
E1	4	1	8	20	0.2	0	1 day
E2	4	1	8	20	0.2	0	1 day
E3	4	1	8	20	0.2	0	1 day
E4	4	1	8	20	0.2	0	1 day
L	4	1	2	20	0.2	0	1 day
H	4	1	24	20	0.2	0	1 day

[@]: Volumes reported in this table are relative volumes

A: Solution for effect of water concentration. **B:** Solution for effect of aging times

C: Solution for effect of alkoxide composition. **D:** Solution for effect of addition of PEG

E: Solution for effect of heat-treatment temperature

*: $M_w = 400$

The $\text{Ti}(\text{O}^i\text{Pr})_4$ solution was prepared by mixing $\text{Ti}(\text{O}^i\text{Pr})_4$, EtOH, DI water, and HCl, with the volume ratio of EtOH/ $\text{Ti}(\text{O}^i\text{Pr})_4$ being 15:1. The volume ratio of $\text{Ti}(\text{O}^i\text{Pr})_4$ to water to HCl was 1:1:0.05. To avoid precipitation of titanium hydroxides, $\text{Ti}(\text{O}^i\text{Pr})_4$, EtOH and HCl were first mixed and then a small amount of water [$\text{H}_2\text{O}/\text{Ti}(\text{O}^i\text{Pr})_4$ volume ratio = 1] was very slowly added to the $\text{Ti}(\text{O}^i\text{Pr})_4$ solution while stirring. The $\text{Ti}(\text{O}^i\text{Pr})_4$ solution was also stirred at room temperature, for at least 15 minutes, to sufficiently hydrolyze the $\text{Ti}(\text{O}^i\text{Pr})_4$. The $\text{Ti}(\text{O}^i\text{Pr})_4$ solution was then poured into the partially hydrolyzed TEOS solution with continued slow stirring for an additional 30 minutes. Finally, poly(ethylene glycol) (PEG) was added to the solution, which was then further stirred for approximately 20 minutes. The molecular weight of PEG used was 400. The chemical compositions and process conditions for preparing the desired sol-gel solutions are shown in Table 5. The clear and transparent solution obtained in this manner was used for the coating experiments and preparation of the bulk gels. The solution was then aged in a closed container for at least one day to stabilize the solution and to obtain good wettability. The viscosity (or fluidity) of the coating solution, based on qualitative judgement, did not significantly change over a period of 7 days, but for every repeated coating experiments, except for the investigation on effects of solution aging, new coating solutions were prepared. The aged coating solution was further diluted with ethanol to control the film thickness and to obtain a useful viscosity of the coating solution.

4.2. Coating Methods

The sol-gel derived titania-silica thin films were deposited onto 1.25 inch diameter (111) Si wafers by dip coating in titanium/silicon alkoxide solutions. The dip coatings were made by the solution lowering process (draining method), in which the parts to be coated remain at rest and the solution level was lowered by opening the drain valve. This solution lowering method was developed for vibration-free dip coatings. The surface of the silicon wafer was coated uniformly by dipping the wafer into the solution and then draining the solution at a constant drain rate. The coating solution was not exposed to the atmosphere during deposition in order to avoid fast evaporation and contamination by air-borne particles. All substrates (Si wafers) were kept in the solution for at least 5 minutes before draining in order to ensure that the surface conditions of the substrates reached steady-state. To obtain good wetting of the substrate, the contact angles formed with the solution have to be sufficiently small. The substrate has to be perpendicular to the coating solution during deposition. The coating operation was completely smooth and shockless and was so slow that the liquid films adhered to the surface of the substrate. The uniformity of the deposited films could be observed by watching the interference fringes which are formed during evaporation of solvent and volatile reaction products on the Si wafer surfaces. During the coating process the fringes were running horizontally at a constant coating rate (drain rate) which could be adjusted from 0.25 to 12 cm/min by changing the flow rate of the solution through the drain valve. The drain rate of 12 cm/min was used mainly for one cycle coating which was comprised of dip coating,

drying, and heat-treatment. Uniform and sufficient thickness of the films could be obtained by multiple coatings carried out at a lower coating rate (2.5 cm/min). After coating, all substrates were dried at room temperature for 15 minutes and then heated up to 300°C with a heating rate of 7°C / min, and kept there for 30 minutes in a furnace. This heating process resulted in uniform and transparent titania-silica thin films. The preparation of the thicker films required 3~5 repetitions of the procedures described above from dipping to heat-treatment.

4.3. Preparation of Bulk Gels

Titania-silica bulk gels were prepared via a two-step acid/base-catalyzed sol-gel process. In the first step, the TiO₂-SiO₂ solution was prepared, with the addition of HCl, under the same conditions as in the preparation of the coating solution. In the second step, 1 ml of 0.05 M ammonium hydroxide (NH₄OH) was added to the solution to accelerate the gelation. The resulting sol was then allowed to gel, in sealed Petri dishes, at room temperature. After gelation, the gels were aged at room temperature for 48 hours. The Petri dishes were then uncapped and the gels were exposed to ambient atmosphere inside a flow hood for drying. After one week of exposure, the aged gels were dried again in an oven at 100°C by covering the Petri dishes with thin aluminum foil punctured with several pin holes to control the evaporation rate of water and alcohol. The gels were heated up to 100°C at a rate 10°C / min, sustained isothermally for 30 minutes and then

slowly cooled down to room temperature. The thickness of the as-dried gels ranged from 0.1 mm to 0.3 mm, as measured by a micrometer.

4.4. Characterization Methods

The thickness and refractive index of the films were measured, as summarized in Appendix A, by using a Gaertner Ellipsometer L117 equipped with a He-Ne laser at a 70° angle of incidence ($\lambda = 632.8\text{nm}$). Ten to fifteen measurements were taken for each specimen. The specular reflectance at normal incidence from 360 to 1000 nm was measured with a Dyn-Optics 224 Reflectometer using the method described in Appendix B. The pore volume, pore size, surface area and pore size distribution of the bulk gels were determined by N_2 adsorption/desorption method described in Appendix C, using a Quanta Chrome Autosorb-1 BET Surface Area Analyzer. The adsorption isotherms were obtained at liquid nitrogen temperature (77 K). All samples were outgassed at room temperature under vacuum for 3 hours prior to analysis. The adsorbed amount is represented as a function of the relative pressure, P/P_0 , where P is the pressure of nitrogen in the gas phase and P_0 is the saturation pressure. Five adsorption points were collected at relative pressures (P/P_0) between 0.05 and 0.30. The total pore volume was determined by a single adsorption point at $P/P_0 \sim 0.995$. The pore size distributions were calculated from the desorption isotherms. Thermochemical changes in PEG containing bulk gels during heat-treatment up to 400°C at a rate of 10°C/min were investigated by differential scanning calorimetry using a Perkin-Elmer differential scanning calorimeter DSC-4.

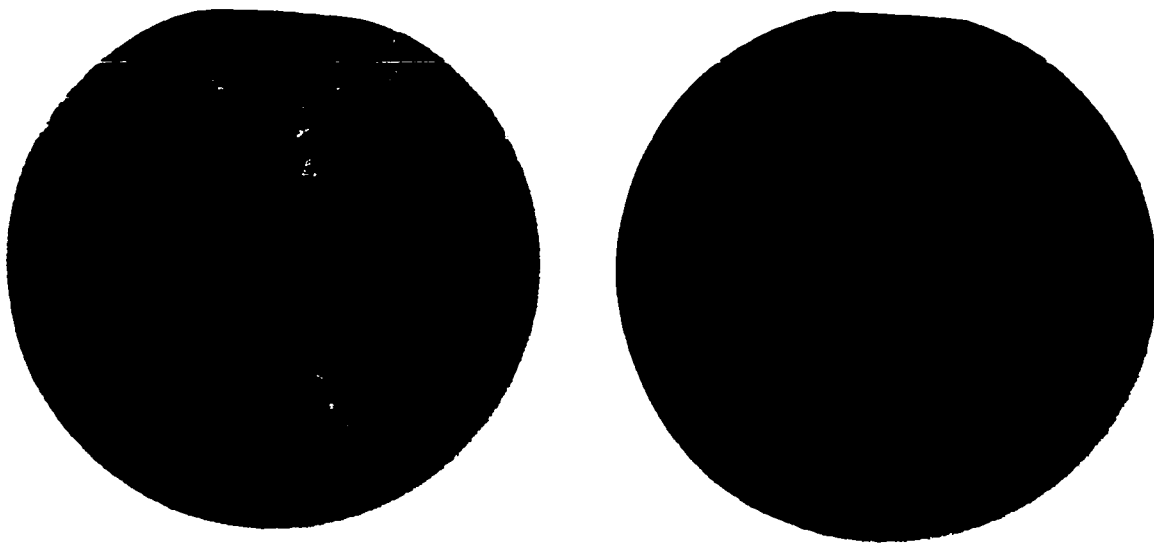
CHAPTER 5

RESULTS AND DISCUSSION

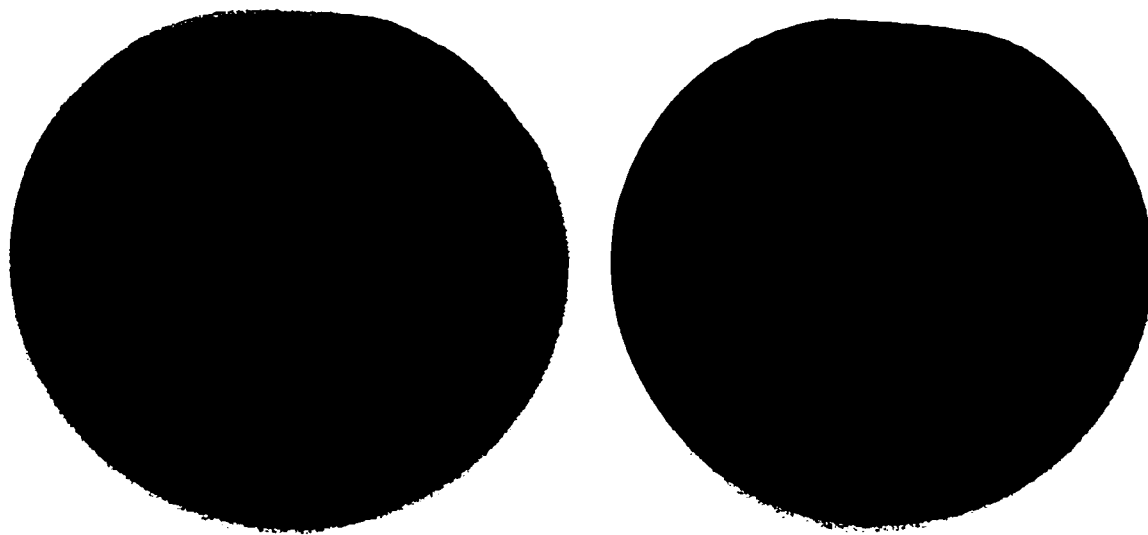
Sol-gel derived TiO₂-SiO₂ thin films were obtained by well controlled sol preparations and careful film deposition processes. A clear Ti (OⁱPr)₄ solution was obtained, only when limited amounts of water and HCl containing ethanol were very slowly added to the alkoxide solution. When larger amounts of water were added, the titanium alkoxide solution quickly became opaque. An increased viscosity of the solution or too much dilution led to poor qualities in the coating films. In order to obtain films which are transparent and homogeneous, the wettability of the solution on the surfaces of the silicon wafers had to be very good. The transparency and uniformity of the coating films could be readily evaluated visually. The coated surfaces of the silicon wafers were first examined visually, an example of which is shown in Figure 22. Titania-silica thin films ranging in thickness from several hundred angstroms to less than five thousand angstroms were deposited under different process conditions. The optical properties of the sol-gel films and the porosity of bulk gels varied with different process parameters.

5.1. Thickness Control of the Films

The film thickness depends on the concentration of the solution, viscosity, coating rate, angle of dipping, the number of coating cycles, and the heat-treatment temperature.



(a) Poor Coatings



(b) Uniform Coatings from Optimal Process Condition

Fig. 22. Photographs of the surfaces of films with various coating conditions.

Among these process variables, the coating rate (drain rate), the number of coating cycles and temperatures of the heat-treatment have a particularly significant influence on control of the film thickness. Figure 23 shows the dependence of film thickness on the drain rate. It was found that as the drain rate increased from 0.25 to 12 cm/min, the thickness of film, deposited by one coating cycle, increased from 266 to 836 Å

In the drain coating, the thickness of the deposited film is proportional to the withdrawal speed (or drain speed) and it can be represented by the following equation.⁽⁴²⁾

$$t = 2V_s\eta^{1/2}/dg \quad [8]$$

In order to obtain desired uniform film thickness, multiple coatings may be used. The film thickness as a function of the number of deposited layers (coating cycles) is shown in Figure 24. It was found that the film thickness was proportional to the number of deposited layers. Furthermore, a linear relationship was found between the thickness increments and the number of coatings. No significant re-dissolution of the deposited films occurred when the coated substrates were dipped into the coating solution for further coatings. The film thickness could also be modified by heat-treatment after deposition. Figure 25 shows the change of the film thickness as a function of heat-treatment temperature. The film thickness decreased during heat-treatment at temperatures between 100°C and 300°C, and then leveled off above 300°C. This is thought to be due to the densification of the film and the decrease in the pore size.

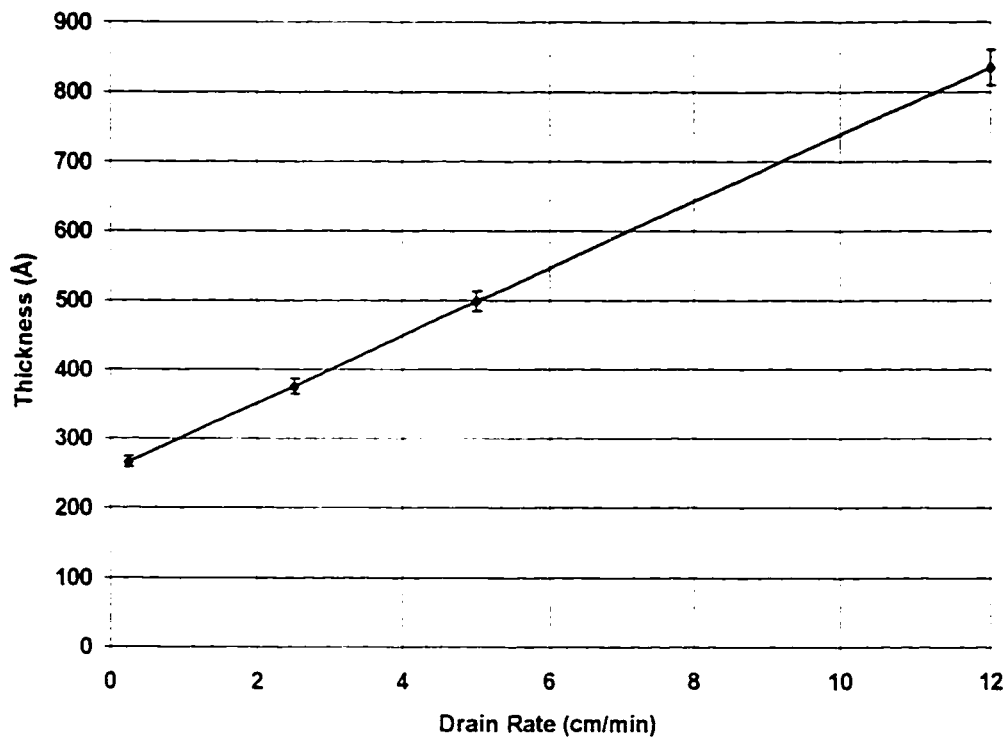


Fig. 23. Effect of drain rate on the thickness of sol-gel derived titania-silica films. (The number of coating cycle was one. Each coating was heat-treated at 300°C for 30 minutes.) Each data point represents the average values obtained from 10 measurements.

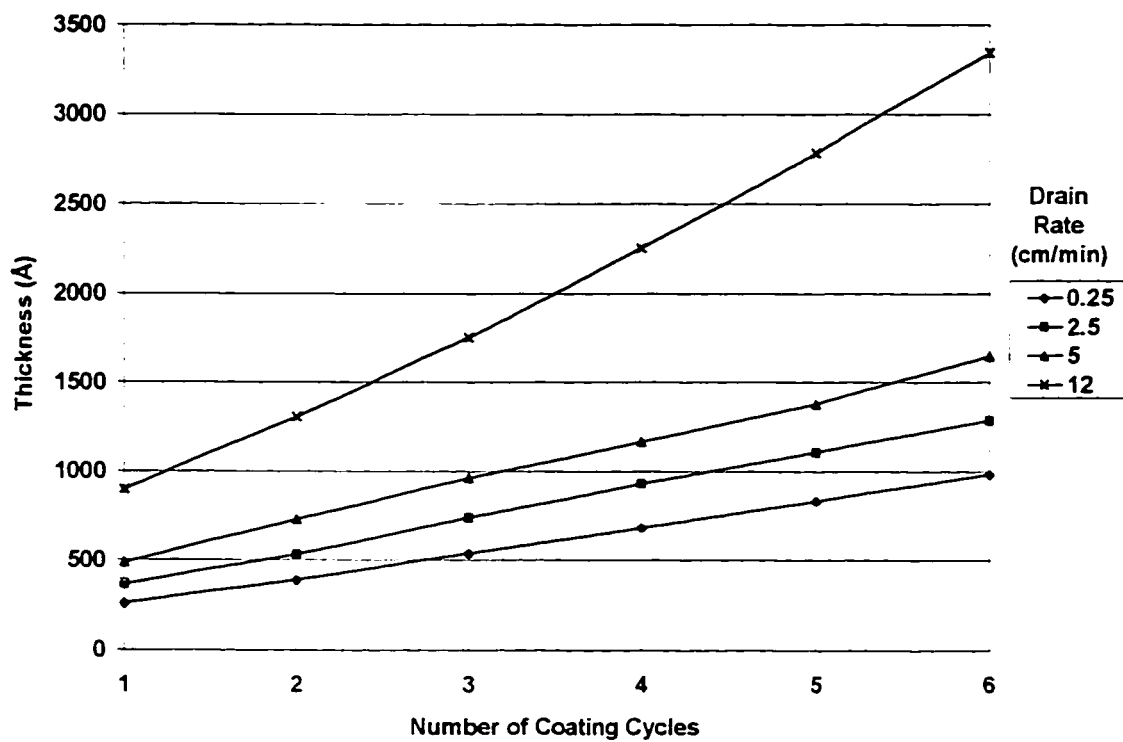


Fig. 24. Effect of the number of coating cycles on the thickness of titania-silica films.
 (The coating films were heat-treated at 300°C for 30 minutes after each coating.)
 Each data point represents the average values obtained from 5 measurements.

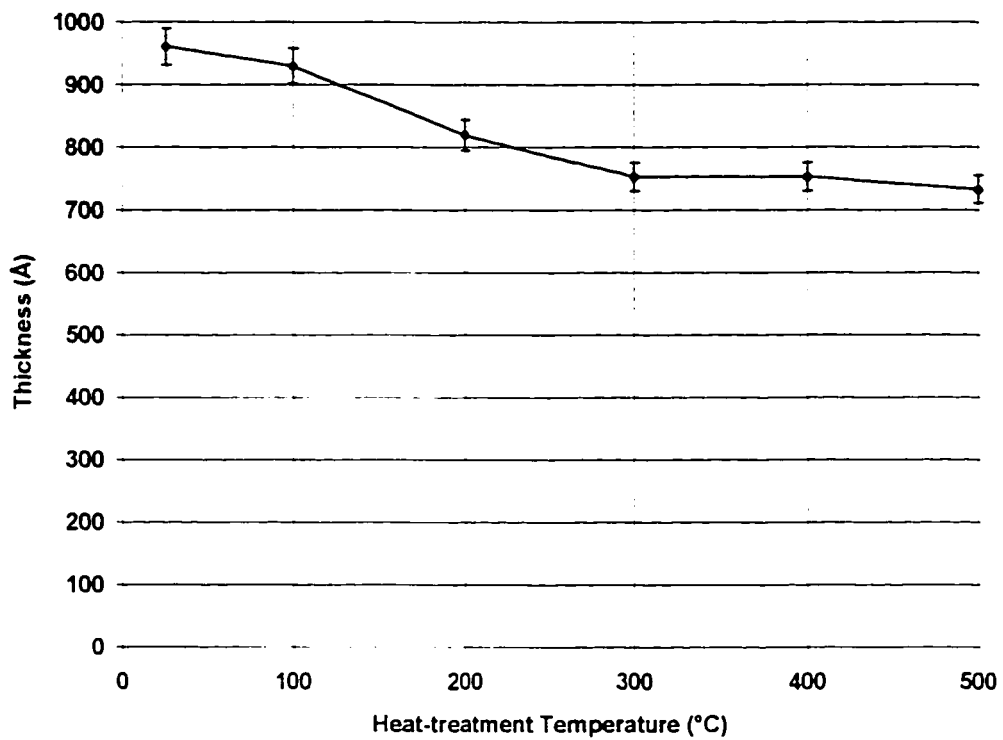


Fig. 25. Effect of heat-treatment temperature on the thickness of titania-silica films.

(The coating rate was 12 cm/min. The heating time was 30 minutes.) Each data point represents the average values obtained from 15 measurements.

5.2. Effect of Drain Rate and Heat-treatment on Refractive Index

Figure 26 shows the refractive index of the sol-gel derived films as a function of the drain rate. Since the refractive index depends on the density of a material, thinner films deposited with a slow drain rate should show a tighter packing of species, and consequently a higher refractive index. In addition to the drain rate, the refractive index was also affected by the heat-treatment temperature as shown in Figure 27. The refractive index may be dependent upon the extent of densification of the coated layer as the temperature increased. The refractive index increased continuously at temperatures between 25°C and 300°C and then remained nearly constant above 300°C. This result indicates that complete densification may be occurring at about 300°C.

5.3. Effect of PEG added to Solution

Poly(ethylene glycol) (PEG) had sufficient solubility in an ethanol-based solution for formulation of the coating solution. The solutions prepared with the addition of PEG were transparent as were the solutions produced without PEG. Over-diluted solutions usually lead to poor quality coatings which spread inhomogeneously on the substrate during drying. Since the addition of organic polymers, such as PEG, increases the viscosity of the coating solution, better wettability could be obtained by adding PEG into the diluted solutions. Small amounts of PEG (2 vol. % <) were added to the solution in order to achieve better control of the film thickness.

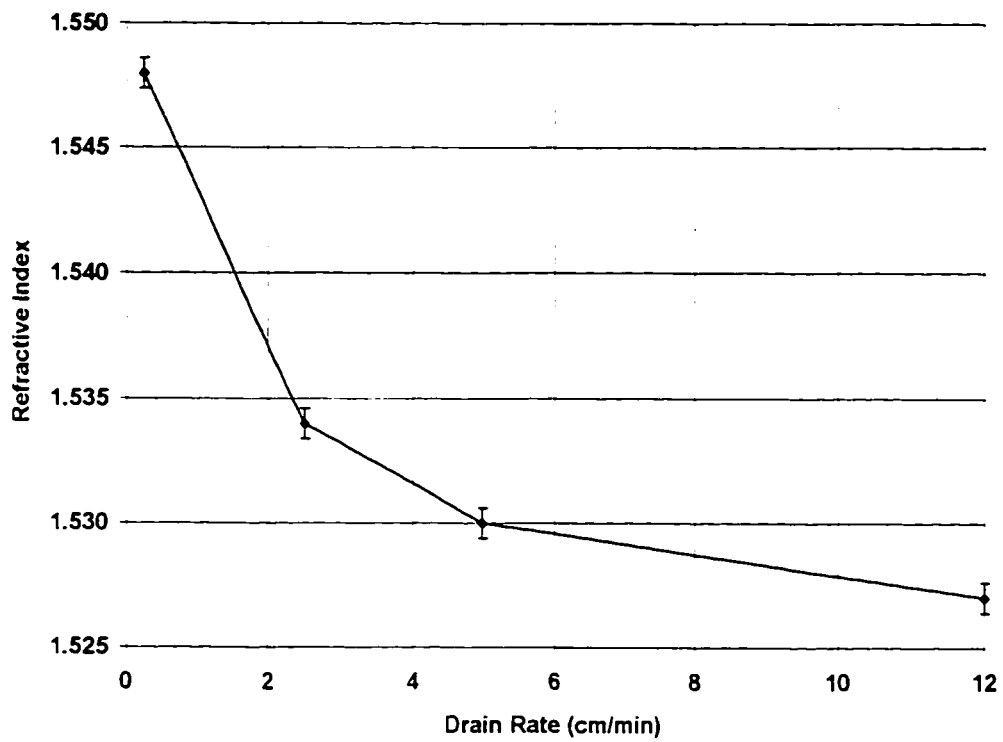


Fig. 26. Effect of drain rate on the refractive index of titania-silica sol-gel films.

Each data point represents the average values obtained from 10 measurements.

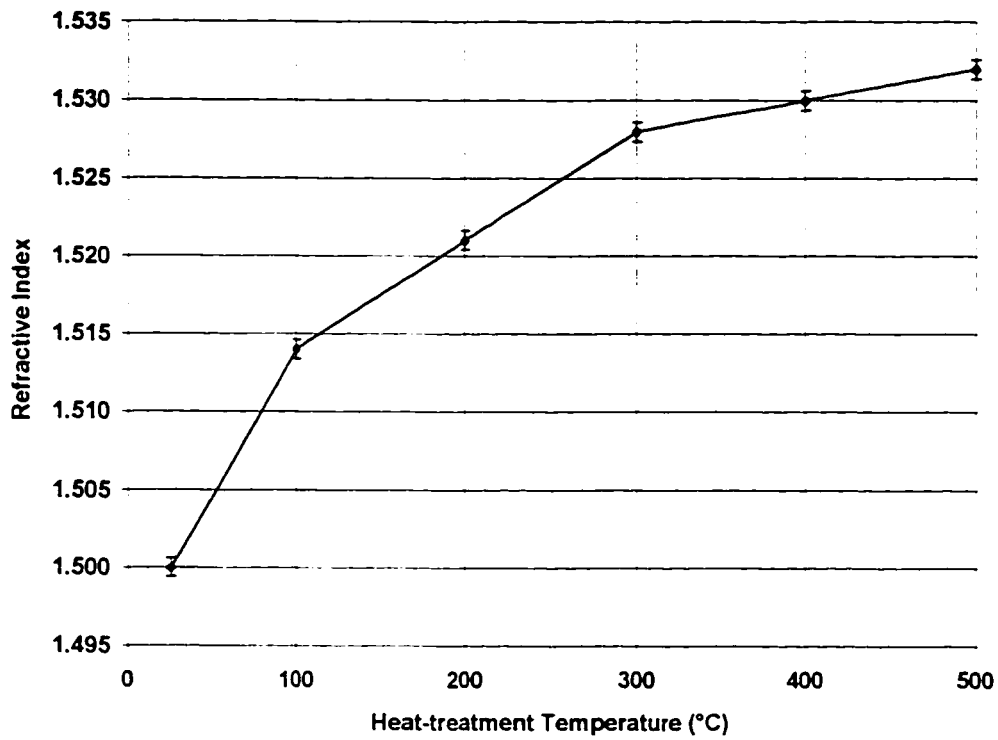


Fig. 27. Effect of heat-treatment temperature on the refractive index of titania-silica sol-gel films. Each data point represents the average values obtained from 10 measurements.

The occurrence of unwettable regions and several pin holes in the deposited films, with increased viscosity, was observed with the addition of greater amounts of PEG. When the PEG concentration in the solution was above 2 vol. %, good quality films could not be obtained.

Thermochemical changes during heat-treatment in the PEG containing bulk gels were studied via differential scanning calorimetry (DSC). DSC traces from 25 to 375°C for bulk gels under different PEG concentrations in the solution are shown in Figure 28. The starting transient, which is instrument specific, occurred at about 50°C, and a large exothermic peak, which results from the decomposition of added PEG, was observed at around 225°C. At temperatures over 325°C, amorphous gels may begin to crystallize. The DSC curves remained unchanged at temperatures between 50°C and 200°C without any peaks. Two more major peaks were expected to be observed in the DSC curve, but the experimental results did not meet this expectation. One is an endothermic peak at about 150°C, associated with the removal of residual solvent and water. Another exothermic peak is usually observed at temperatures between 250°C and 300°C, which is related to the burning of residual organic compounds in the gel.⁽⁴³⁾ However, only one exothermic peak was observed in the curve, probably due to the small size of the sample. The reason for this may also be linked to the nearly complete removal of water and residual organic groups during drying.

The increase in viscosity of the coating solutions, by the addition of PEG, brought about an increase in the thickness of the as-deposited films, as shown in Figure 29.

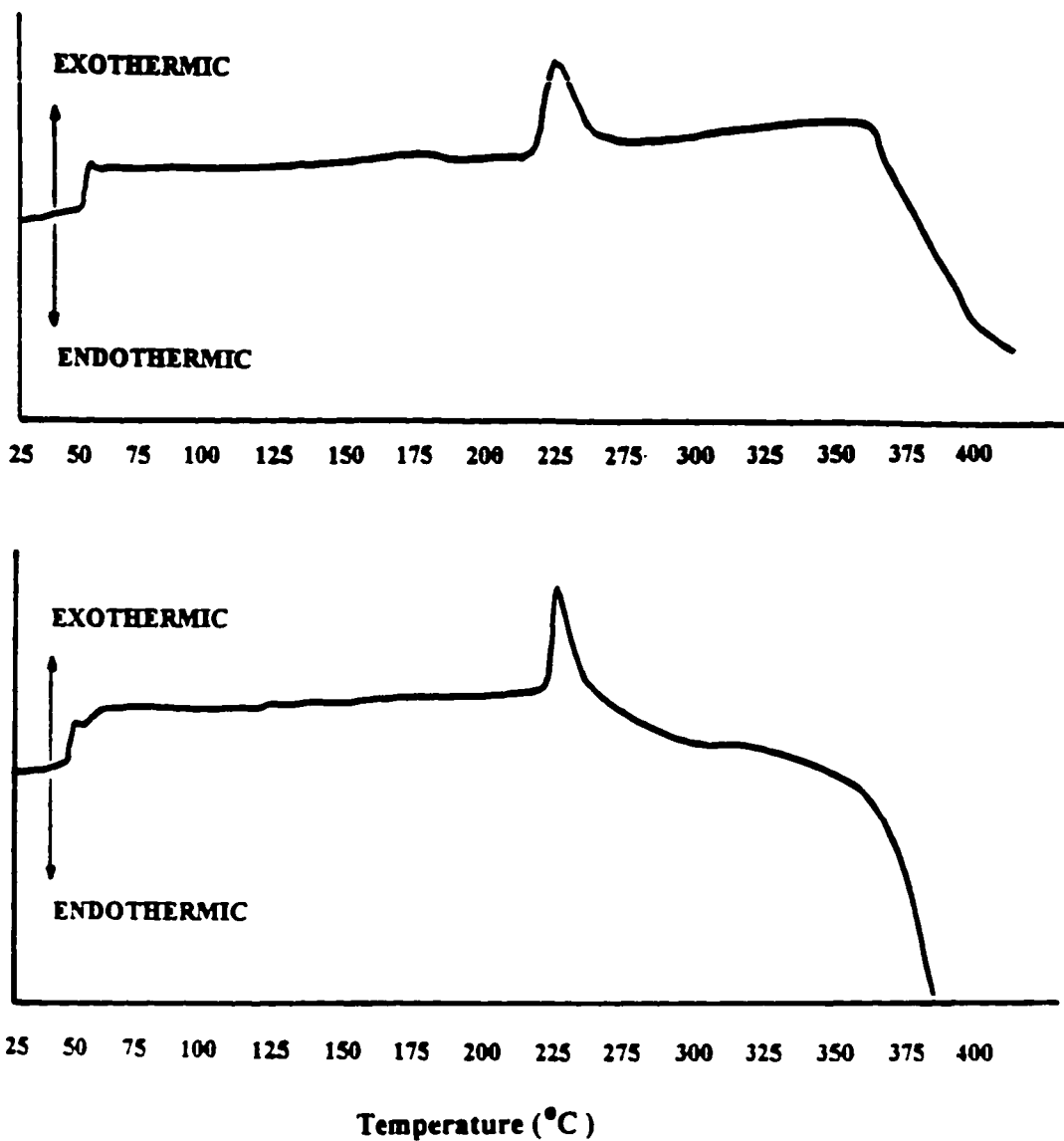


Fig. 28. Schematic illustration of DSC curves of PEG containing gels.
 (The heating rate was 10°C/min up to 400°C)

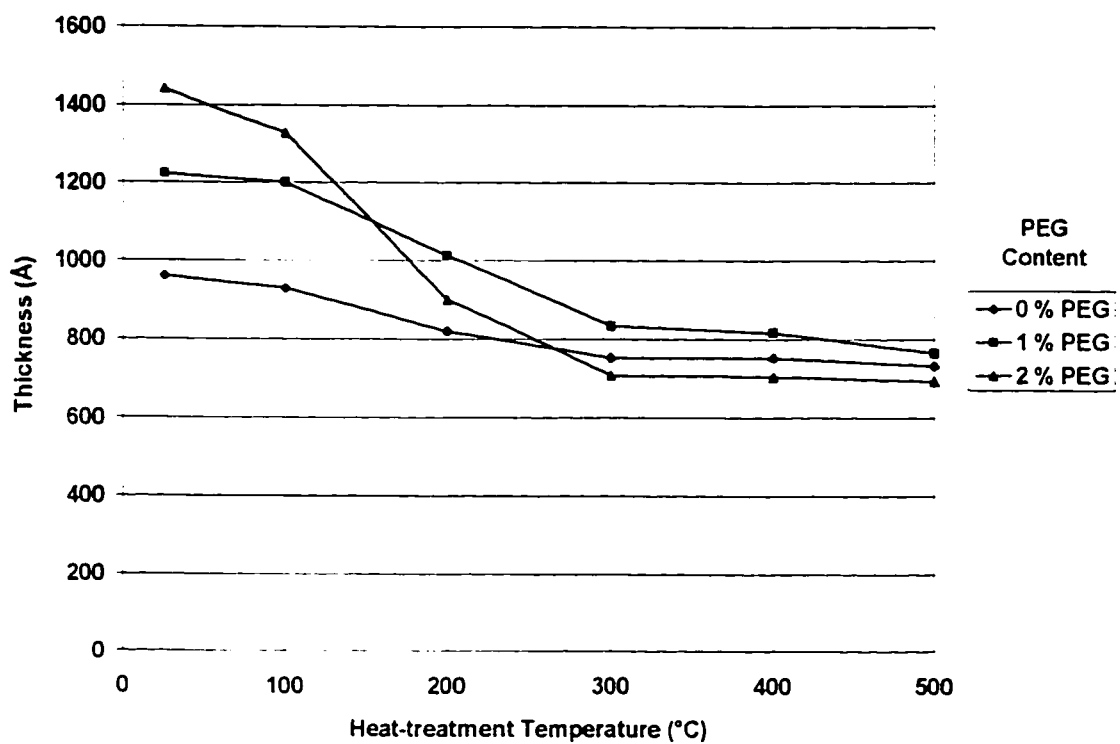


Fig. 29. Effect of the addition of PEG on the thickness of titania-silica sol-gel films.

Each data point represents the average values obtained from 7 measurements.

The decrease in film thickness during heat-treatment is also shown in Figure 29. As the heat-treatment temperature increased, the PEG-containing films shrank considerably, especially in a range of 100° to 300°C, as shown in Figure 30. The shrinkage in this temperature range is mainly due to the decomposition of added PEG during heat-treatment. As the concentration of PEG increased, the shrinkage also increased. The maximum shrinkage of the film without PEG was about 24 %, whereas that of the film obtained with the addition of 2 vol. % PEG was about 52 %. This indicates that the films prepared with the addition of PEG is highly porous. Figure 31 shows variations of the refractive index of the films during heat-treatment, for films obtained with and without the addition of PEG. The difference in the refractive index of the as-deposited films prepared with and without the addition of PEG may be due to the presence of PEG within the films. The change in the refractive index at temperatures over 350°C can be ascribed to the difference in the porosity of the films due to decomposition of PEG within the films. Table 6 lists the porosity of the bulk gels and refractive indices of films prepared with and without the addition of PEG. The addition of PEG into the solution led to a lower refractive index after heat-treatment at temperatures over 300°C. The reflectivity of the films could be varied through proper control of the film thickness and refractive index by adding PEG into the solution to introduce porosity. Figure 32 shows the percent specular reflectivity of the TiO₂-SiO₂ sol-gel films. The incorporation of PEG with 2 vol. % into TiO₂-SiO₂ solution led to a lower reflectivity of the coated Si wafer at wavelength around 700 nm.

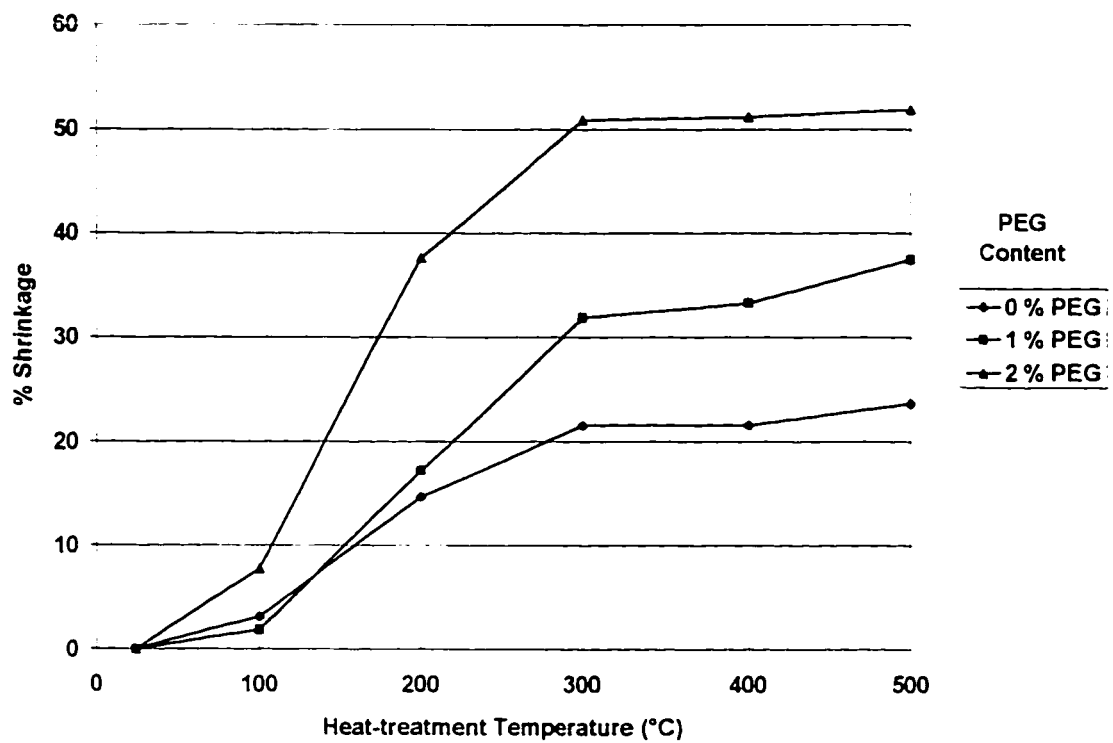


Fig. 30. Effect of the addition of PEG on the shrinkage of titania-silica sol-gel films.

Each data point represents the average values obtained from 7 measurements.

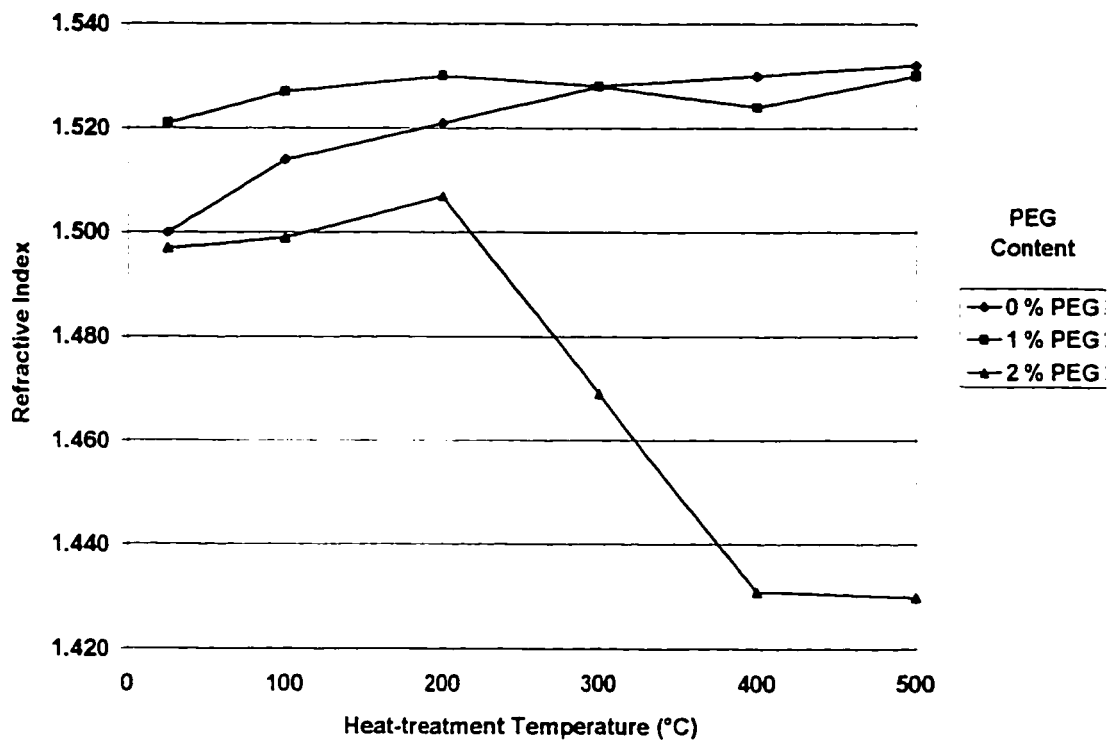


Fig. 31. Effect of the addition of PEG on the refractive index of titania-silica sol-gel films. (Each data point represents the average values obtained from 7 measurements.)

Table 6 Porosity of bulk titania-silica gels and refractive index of films on Si wafers as a function of the addition of PEG (2 vol. %).

Samples	Total Pore Volume, cc/g	Average Pore Radius, Å	Surface Area m²/g	Refractive Index
A	0.1868	15.3	244	1.500
B	0.003	31.6	1.88	1.497
C	0.324	12.9	502	1.528
D	0.390	14.4	541	1.430

A: Gels without PEG heated at 100°C,

B: Gels with PEG heated at 100°C

C: Gels without PEG heated at 300°C,

D: Gels with PEG heated at 300°C

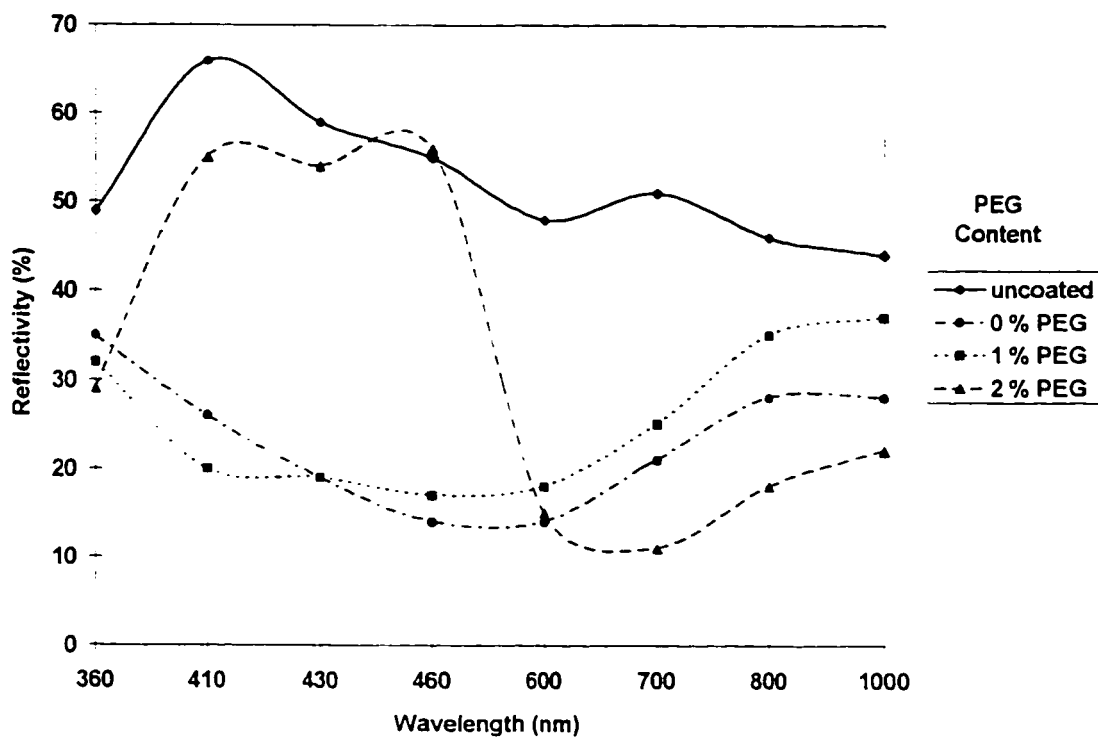


Fig. 32. Effect of the addition of PEG on the reflectivity of titania-silica sol-gel films.

Each data point represents the average values obtained from 6 measurements.

But this specimen had a reflection curve which showed higher reflectivities in the range of 410-460 nm unlike the samples coated with films containing no PEG at all.

An understanding of the porous structure of the bulk gels was deduced from the nitrogen adsorption/desorption isotherms. When the quantity of the gas adsorbed onto or desorbed from the surface of bulk gel is measured over a wide range of relative pressures at a constant temperature, the result is an adsorption/desorption isotherm.

The adsorption/desorption isotherms for the gels obtained with and without the addition of PEG are shown in Figure 33. The isotherm obtained for the gel without PEG, after heat-treatment at 300°C, shows a Type I isotherm, typical of a sample containing micropores. This is shown in Figure 33 (b). The Type I isotherm exhibits a larger adsorbed volume at low relative pressures and a plateau in the volume adsorbed at intermediate pressures, which indicates a large volume of extremely small pores.⁽⁴⁴⁾ The gels prepared with the addition of PEG and heat-treated at 300°C exhibits a Type IV isotherm, which showed a monotonic increase in adsorption with increasing relative pressure. Types I and IV usually exhibit hysteresis between the adsorption and desorption isotherms. The Type IV isotherm is normally found for samples having less microporosity and a broader distribution of pores with diameter of 20-500 Å. The difference in isotherms between the gels obtained with and without the addition of PEG is caused by different pore structures after heat-treatment due to the decomposition of PEG. The surface area and total pore volume of the as-dried gel was significantly lower with the addition of PEG, as compared with that of the gel produced without PEG.

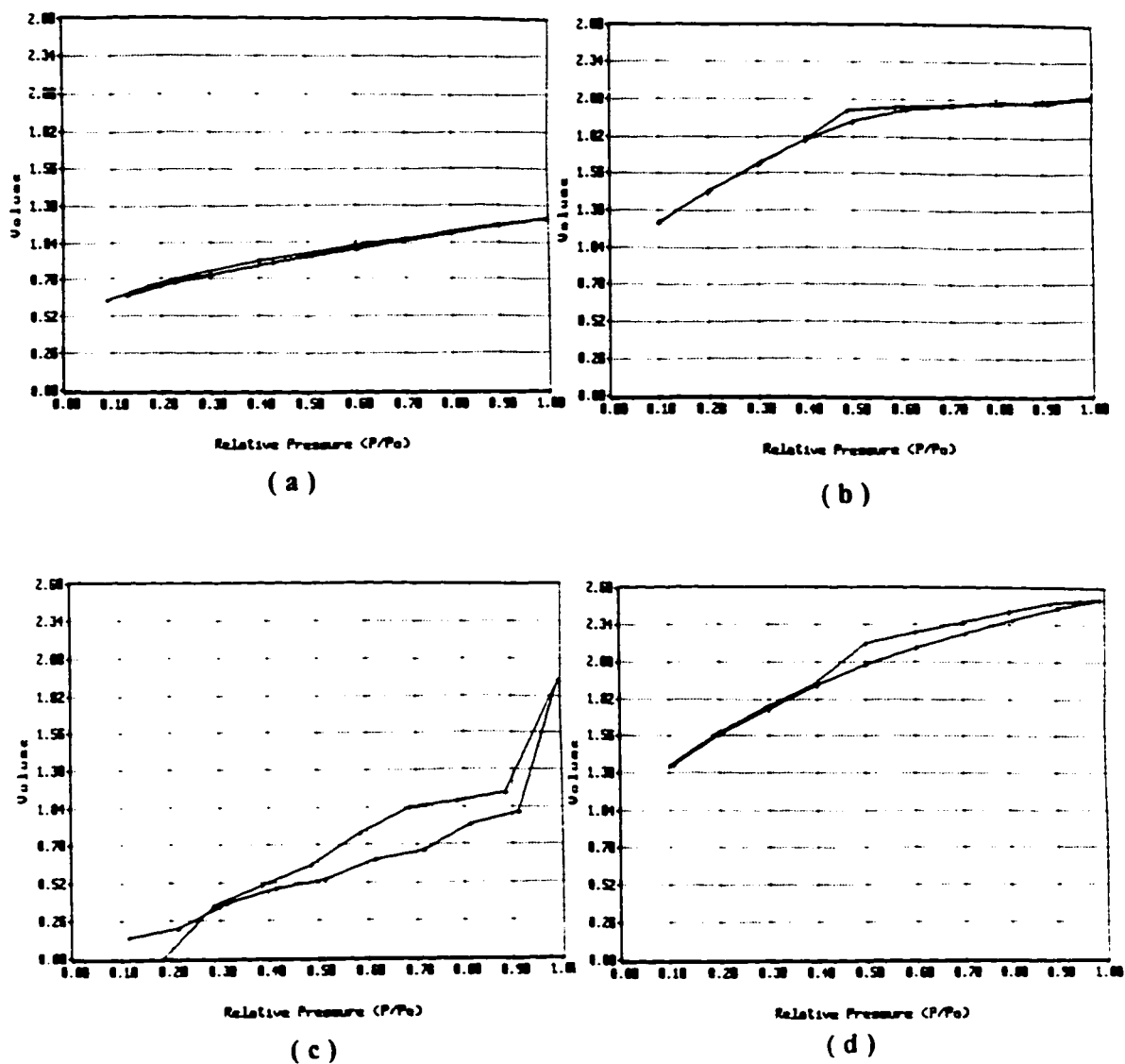


Fig. 33. N₂ adsorption/desorption isotherms of titania-silica bulk gels prepared from sol with and without PEG. (a) 0 % PEG and heat-treated at 100°C, (b) 0 % PEG and heat-treated at 300°C, (c) 2 % PEG and heat-treated at 100°C, (d) 2 % PEG and heat-treated at 300°C.

The average pore size of the as-dried gel increased from 15.3 to 31.6 Å with the addition of PEG. The as-dried gel produced with the addition of PEG is practically a non-porous gel with relatively few large pores. The decomposition of PEG in the bulk gels after heat-treatment at 300°C led to increases in pore volume, pore size and surface area, compared to those of gels prepared without the addition of PEG. Figure 34 shows the change in the pore size distribution of the bulk gels prepared with and without the addition of PEG. The pore distributions in the gels prepared with the addition of PEG were significantly different from those of the gels prepared without PEG addition. In the case of the as-dried gels prepared without the addition of PEG, the pore size distribution was broader than that of heat-treated gels at 300°C, as shown in Figures 34 (a) and (b). The heat-treatment led to a narrower pore size distribution in the gel, containing mostly small pores with radii less than 50 Å. Figures 34 (c) and (d) show the pore size distribution of the gels prepared with the addition of PEG. The as-dried gel prepared with the addition of PEG showed a very narrow pore size distribution. The addition of PEG may lead to a decrease in the number of larger pores with radii 50 to 500 Å, as a result of the PEG trapped in the larger pores or voids. A slightly broader pore size distribution and a considerable shift toward larger average pore size were observed with gels heat-treated at 300°C as shown in Figure 34 (d). This resulted from the change in porosity of the gels due to the combustion of PEG during heat-treatment.

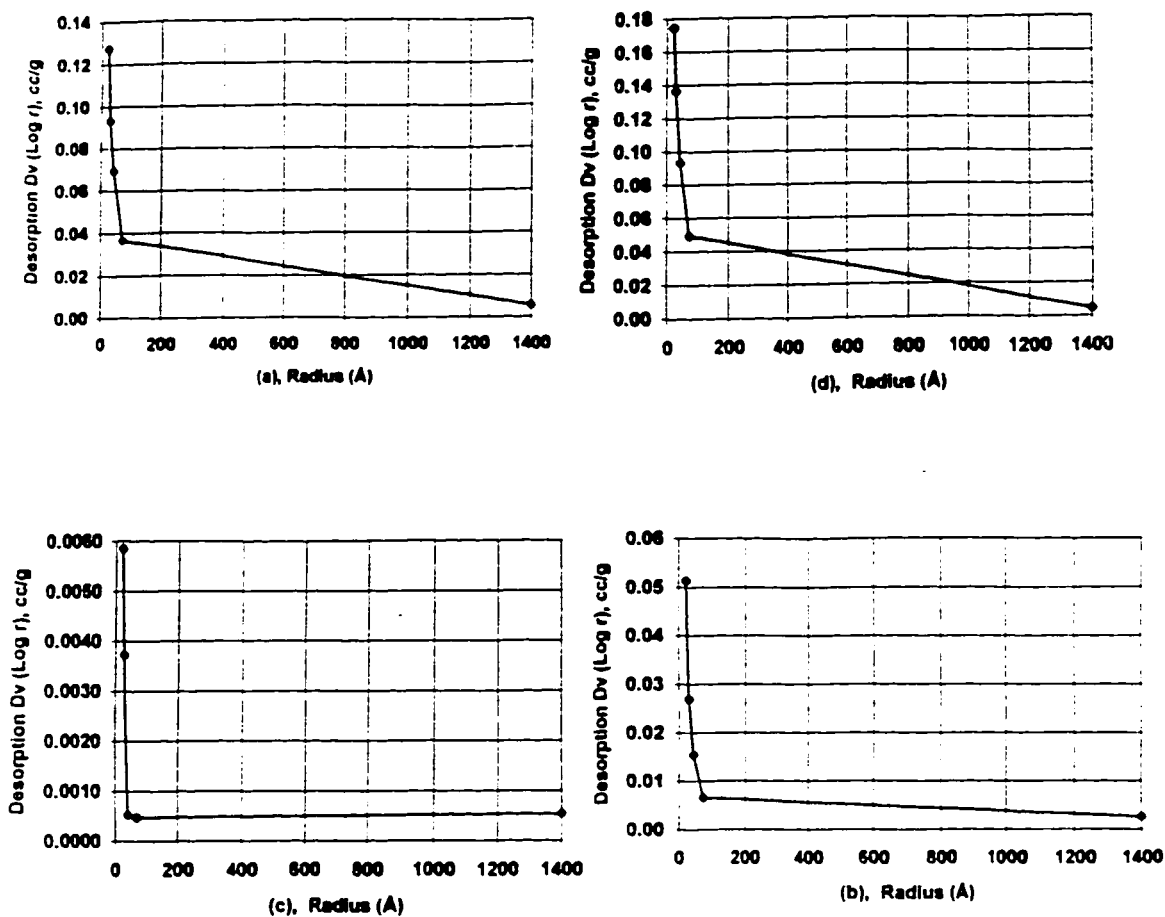


Fig. 34. Pore size distributions of titania-silica bulk gels prepared by 2 vol. % PEG containing sol and sol without PEG. (a) no PEG and dried at 100°C, (b) no PEG and heat-treated at 300°C, (c) 2 vol. % PEG and dried at 100°C, (d) 2 vol. % PEG and heat-treated at 300°C.

5.4. Effect of Water Concentration

In order to obtain uniform coatings of the substrates, a suitable amount of water is required to react with the alkoxides used. The amount of water must be sufficient for the full hydrolysis and polycondensation reactions. But greater amounts of water usually resulted in a decrease of the gelation time and failure in the preparation of the desired coating solution. The amount of water not only affected the solution but also the nature of the deposited films. The solution prepared with low water concentration ($H_2O/TEOS < 1$) caused opaque deposition, while the solution obtained using a higher water concentration ($H_2O/TEOS > 5$) led to poor coating properties such as unwettability or discontinuous films. Low and high water concentration solutions are designated with L and H, respectively, in Table 5. Generally, hydrolysis is assisted by using sufficient amounts of water. However, even with excess water, the reaction does not go to completion. Although increased amounts of water often promotes the hydrolysis, when the ratio of H_2O/Si or Ti is increased, while maintaining a constant ratio of solvent/oxide, the oxide concentration is reduced. This in turn reduces the hydrolysis and condensation rates, causing poor wettability due to an over-diluted solution.⁽⁴⁵⁾ Therefore, the amount of water is a very important factor influencing the overall sol-gel processing.

The change in porosity of the gel by varying the concentration of water was not as clear as in the case of gels obtained with and without the addition of PEG. The effect of different water concentrations, $H_2O/TEOS$, on the porosity of bulk gels and the refractive index of the gel films are reported in Table 7. Major differences in pore volume, surface

area, and refractive index were not observed between gels made at low and high water:alkoxide ratios. It was found from isotherm plots that the pore structure of the bulk gel varied by changing the concentration of water. The gels with lower water concentration ($H_2O/TEOS = 1.5, 2$) showed a Type IV isotherm with a broader pore size distribution than that of higher water gels ($H_2O/TEOS = 3, 4$) as shown in Figures 35 and 36. It was also shown from Type I isotherms of higher water gels that higher water concentration led to the formation of microporous structures with small pores. Increasing the water concentration from $H_2O/TEOS = 1.5$ to $H_2O/TEOS = 4$ decreased the average pore radius from 15.6 to 12.4 Å. At lower water concentrations, larger pore size values may be related to the polycondensation of incomplete hydrolyzed species causing a less cross-linked structure. Higher water concentrations (excess water) leads to the formation of highly condensed species. This indicates that high water concentrations may serve to tighten the gel structure and form smaller pores. It was found from Figures 36 (c) and (d) that higher water gels have a narrower pore size distribution than lower water gels. The concentration of water had no significant effect on the refractive index of the films. However, the deposited films with various ratios of $H_2O/TEOS$ showed essentially uniform antireflections over a wide range of wavelengths, as shown in Figure 37.

Table 7 Porosity of bulk titania-silica gels and refractive index of films on Si wafers as a function of water concentration.

$\text{H}_2\text{O} / \text{TEOS}^{\text{@}}$	Total Pore Volume, cc/g	Average Pore Radius, Å	Surface Area m^2/g	Refractive Index
1.5	0.1425	15.6	183	1.531
2.0	0.1868	15.3	244	1.545
3.0	0.1363	12.3	222	1.540
4.0	0.2192	12.4	354	1.523

@ Different water concentration in volume, $\text{H}_2\text{O}/\text{M}(\text{OR})_n$

-Theoretical ratio for complete hydrolysis and condensation = $n/2$

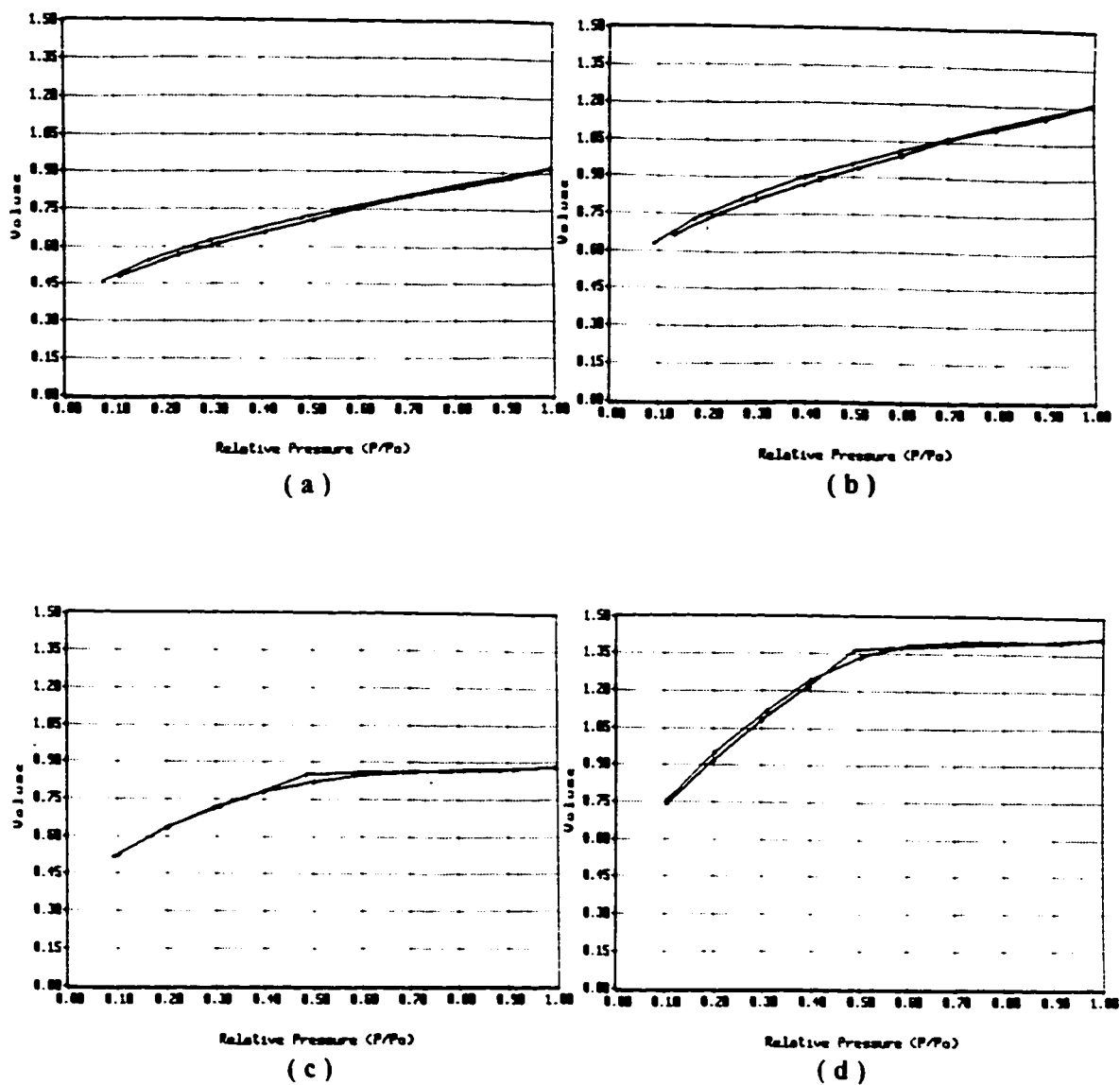


Fig. 35. N₂ adsorption/desorption isotherms of titania-silica bulk gels at various water concentrations. (a) water/TEOS = 1.5, (b) water/TEOS = 2, (c) water/TEOS = 3, (d) water/TEOS = 4 (All gels were heat-treated at 300°C)

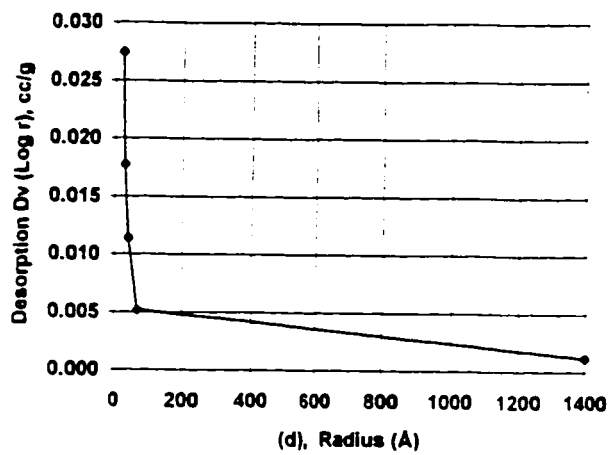
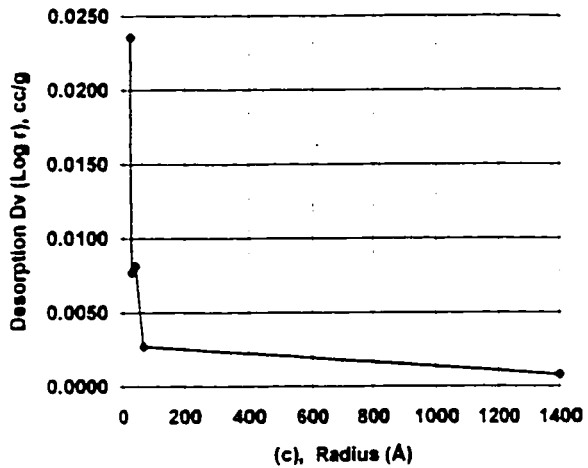
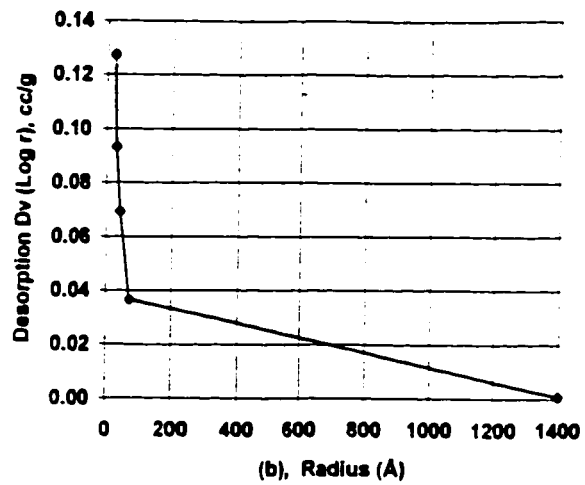
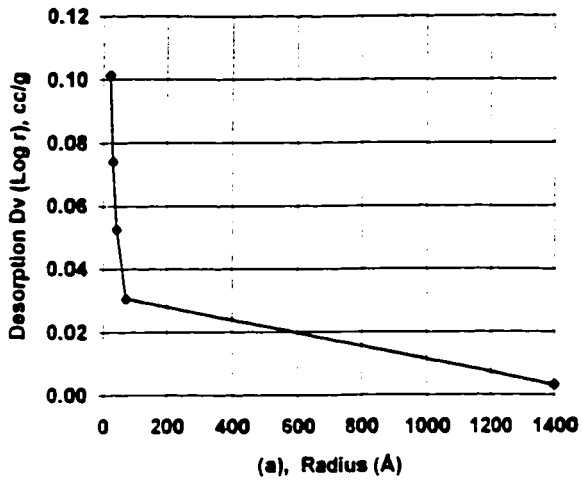


Fig. 36. Pore size distribution of titania-silica bulk gels at various water concentrations. (a) water/TEOS = 1.5, (b) water/TEOS = 2, (c) water/TEOS = 3, (d) water/TEOS = 4 (All gels were heat-treated at 300°C.)

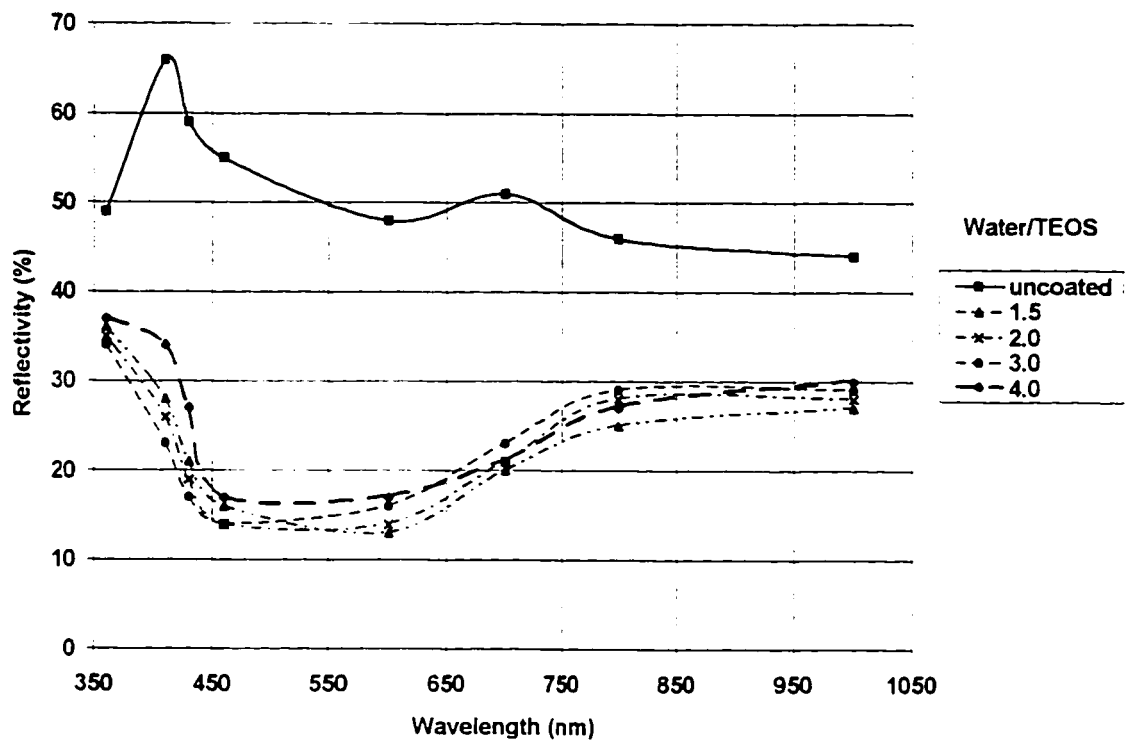


Fig. 37. Effect of water concentration on the reflectivity of titania-silica sol-gel films.

Each data point represents the average values obtained from 6 measurements.

5.5. Effect of Aging Times

It was found that both pore volume and surface area of the bulk gels increased as the aging time increased, as reported in Table 8. This indicates that the gels prepared from solutions aged for longer periods have more porous structures than gels obtained from those aged for shorter periods. The aging may involve further condensation and change the structure of the entrained inorganic species in the original sol. The aging leads to growth of the entrained fractal species in the sol, which causes an increase of pore volume, pore size, and surface area of the gels.⁽²³⁾ However, little change in pore size was observed by varying the aging times within the two week period.

By increasing the aging times, the refractive index of the films decreased due to an increase of the porosity. An inspection of the isotherms showed that the aged gels had Type I isotherms, typical of a sample containing micropores, as shown in Figure 38. Narrower pore size distributions were obtained for all gels aged over a time period of several days, as shown in Figure 39. Figure 40 shows the reflectivity of TiO₂/SiO₂-coated silicon wafers prepared from solutions aged at various times. The reflectivity of the coated Si wafers closely approached minimum reflectances at around 600nm with increasing aging times of from 4 to 14 days.

Table 8 Porosity of bulk titania-silica gels and refractive index of films on Si wafers as a function of aging times

Aging Times	Total Pore	Average Pore	Surface Area	Refractive
(Day)	Volume, cc/g	Radius, Å	m²/g	Index
unaged	0.1363	12.3	222	1.546
4	0.1924	13.5	286	1.429
7	0.2125	13.0	326	1.396
14	0.2515	13.2	382	1.340

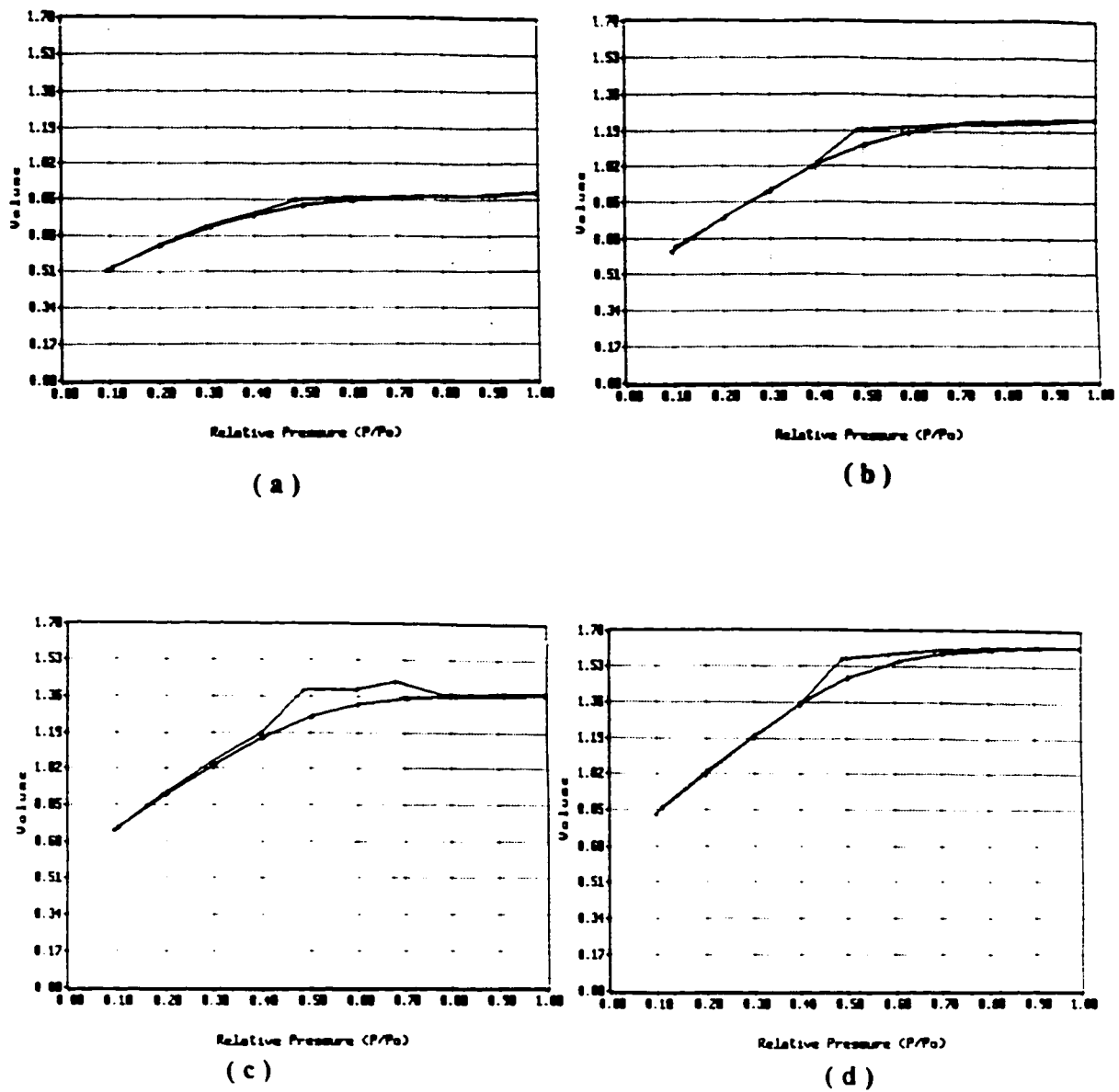


Fig. 38. N₂ adsorption/desorption isotherms of titania-silica bulk gels at various sol aging times. (a) no aging, (b) 4 day aged, (c) 7 day aged, (d) 14 day aged

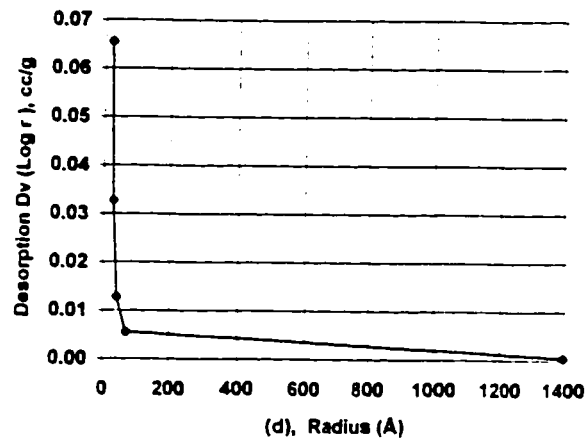
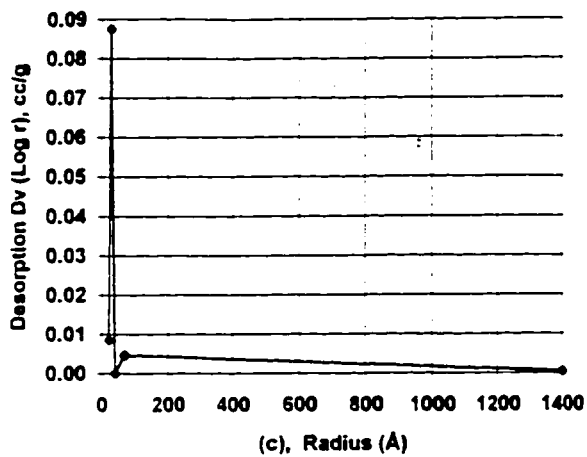
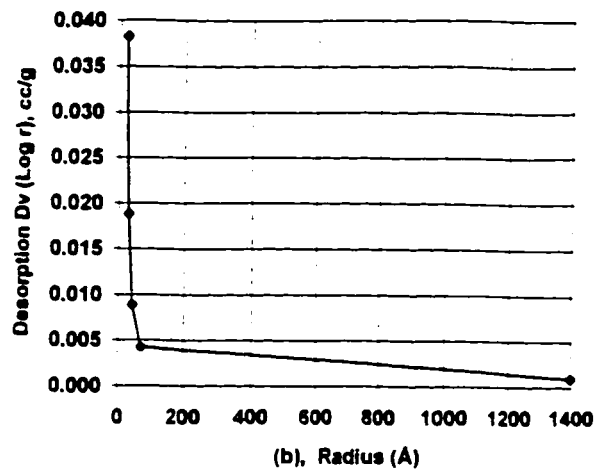
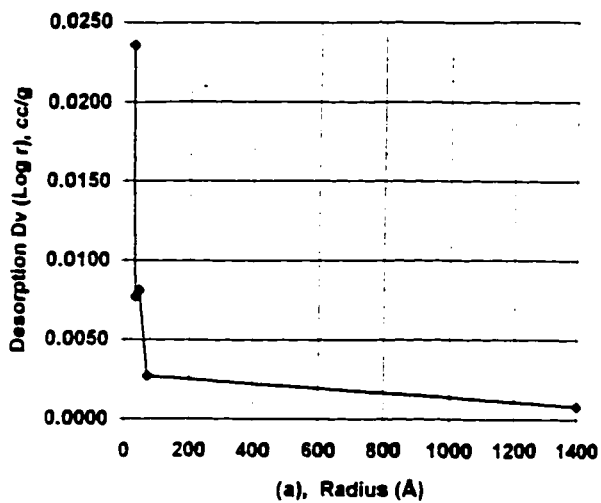


Fig. 39. Pore size distribution of titania-silica bulk gels at various sol aging times.

(a) no aging, (b) 4 day aged, (c) 7 day aged, (d) 14 day aged

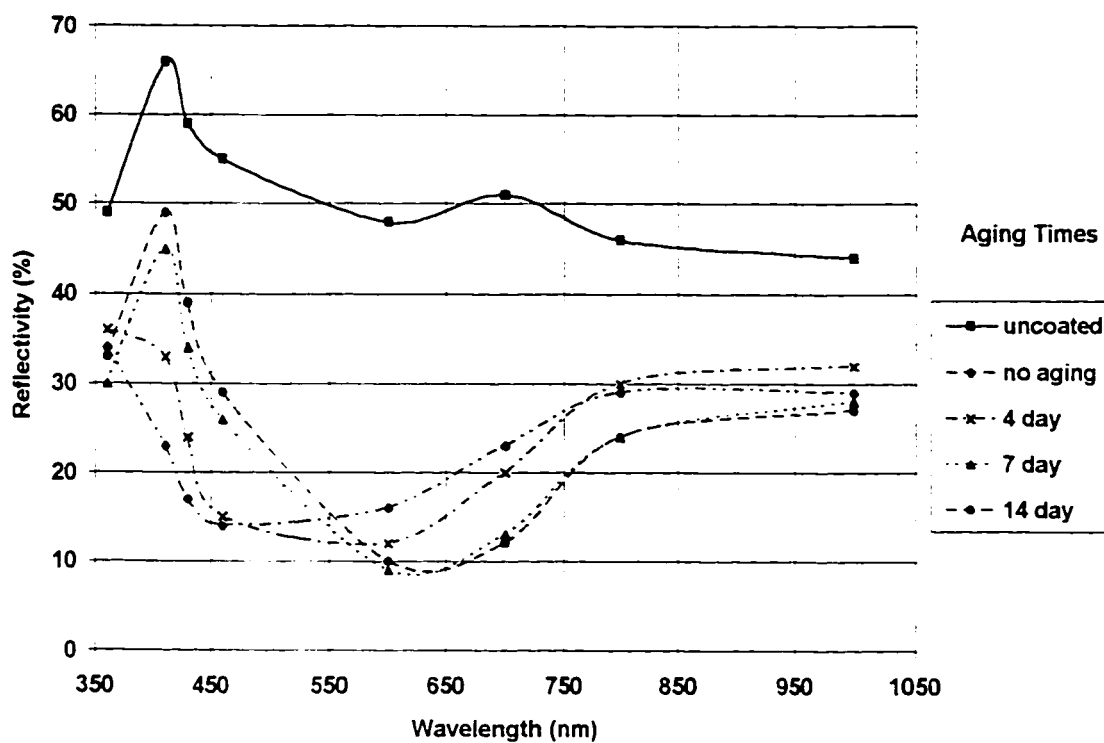


Fig. 40. Effect of sol aging times on the reflectivity titania-silica sol-gel films.

Each data point represents the average values obtained from 6 measurements.

5.6. Effect of Heat-treatment Temperature After Deposition

When sol-gel derived films or bulk gels are subjected to heat-treatment for densification, the change in properties of the gels with heat-treatment is dependent upon the pore structures of the gels. Heating densifies the gel structure and leads to uniform reduction in pore size, causing an increase in the refractive index as shown in Table 9. Densification is essentially a sintering process, by which the pore of the gel is reduced or eliminated.⁽⁴⁶⁾ The thickness of the films could also be modified by heat-treatment. The isotherms of the gels heat-treated above 300°C show a Type I isotherm, which indicates microporous structures of the gels as shown in Figure 41. It was shown from Table 9 that the pore volume increase up to 300°C was due to the evaporation of water adhering to the micropore walls of the gel, and also the formation of fine pores as a result of the decomposition of residual organic compounds. The decrease in pore volume above 300°C is probably due to the shrinkage of the pores. A narrower pore size distribution along with smaller pores were obtained from the gels heat-treated at higher temperatures, as shown in Figure 42.

5.7. Effect of Alkoxide Composition

Titanium isopropoxide hydrolyzed much faster than tetraethylorthosilicate, which led to a cloudy solution (precipitation) or fast gelation when large amounts of $\text{Ti}(\text{O}^i\text{Pr})_4$ were rapidly added to the TEOS solution. A higher content of $\text{Ti}(\text{O}^i\text{Pr})_4$ also caused less stability during aging, leading to rapid gelation.

Table 9 Porosity of bulk titania-silica gels and refractive index of films on Si wafers as a function of heat-treatment temperature.

Temperature	Total Pore	Average Pore	Surface Area	Refractive
(°C)	Volume, cc/g	Radius, Å	m²/g	Index
100	0.1816	15.3	244	1.500
200	0.3164	13.6	464	1.514
300	0.3240	12.9	502	1.521
400	0.2302	12.9	356	1.528
500	0.2697	12.7	424	1.530
600	0.2512	12.7	395	1.532

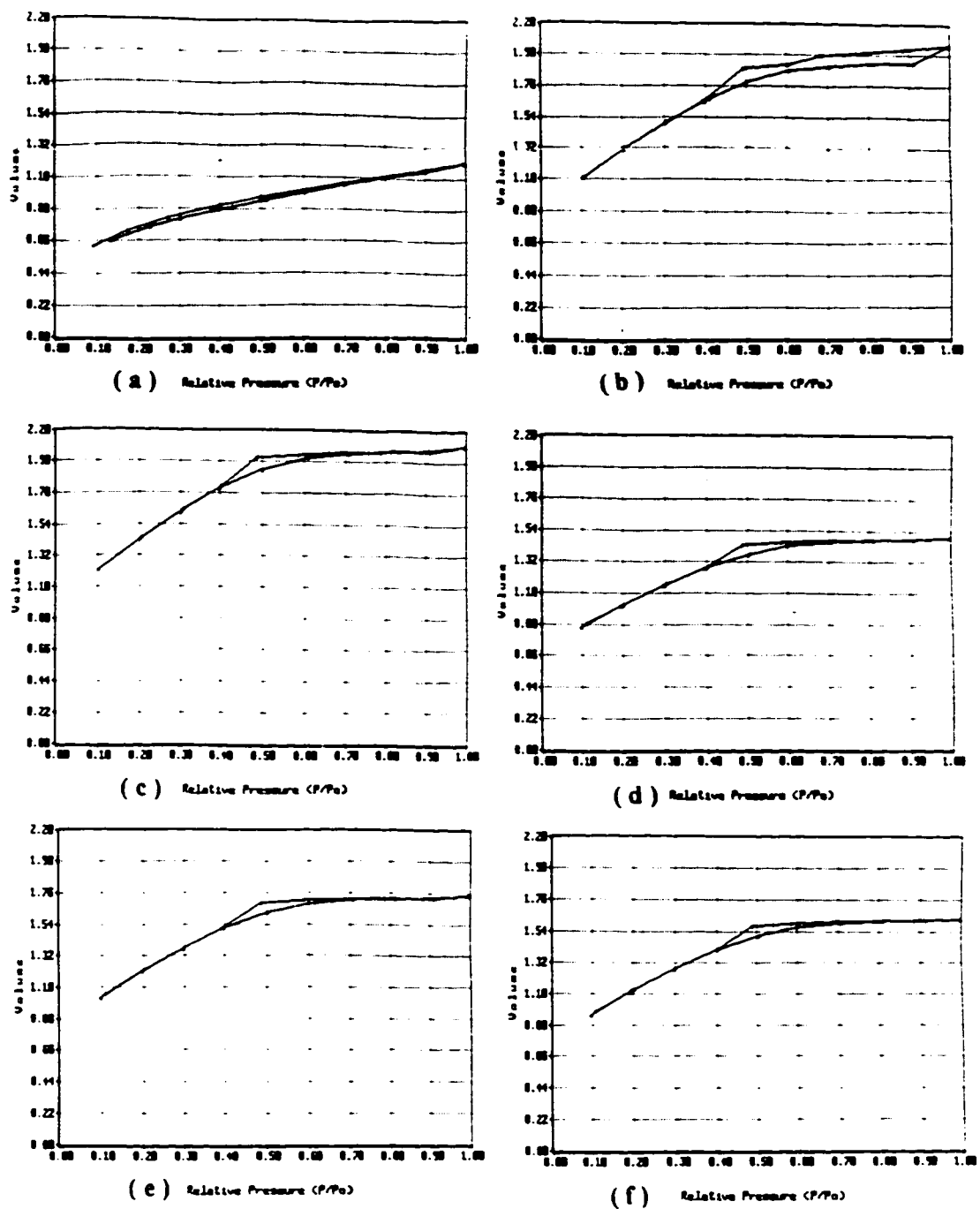


Fig. 41. N_2 adsorption/desorption isotherms of titania-silica bulk gels at various heat-treatment temperature. (a) 100°C, (b) 200°C, (c) 300°C, (d) 400°C, (e) 500°C, (f) 600°C

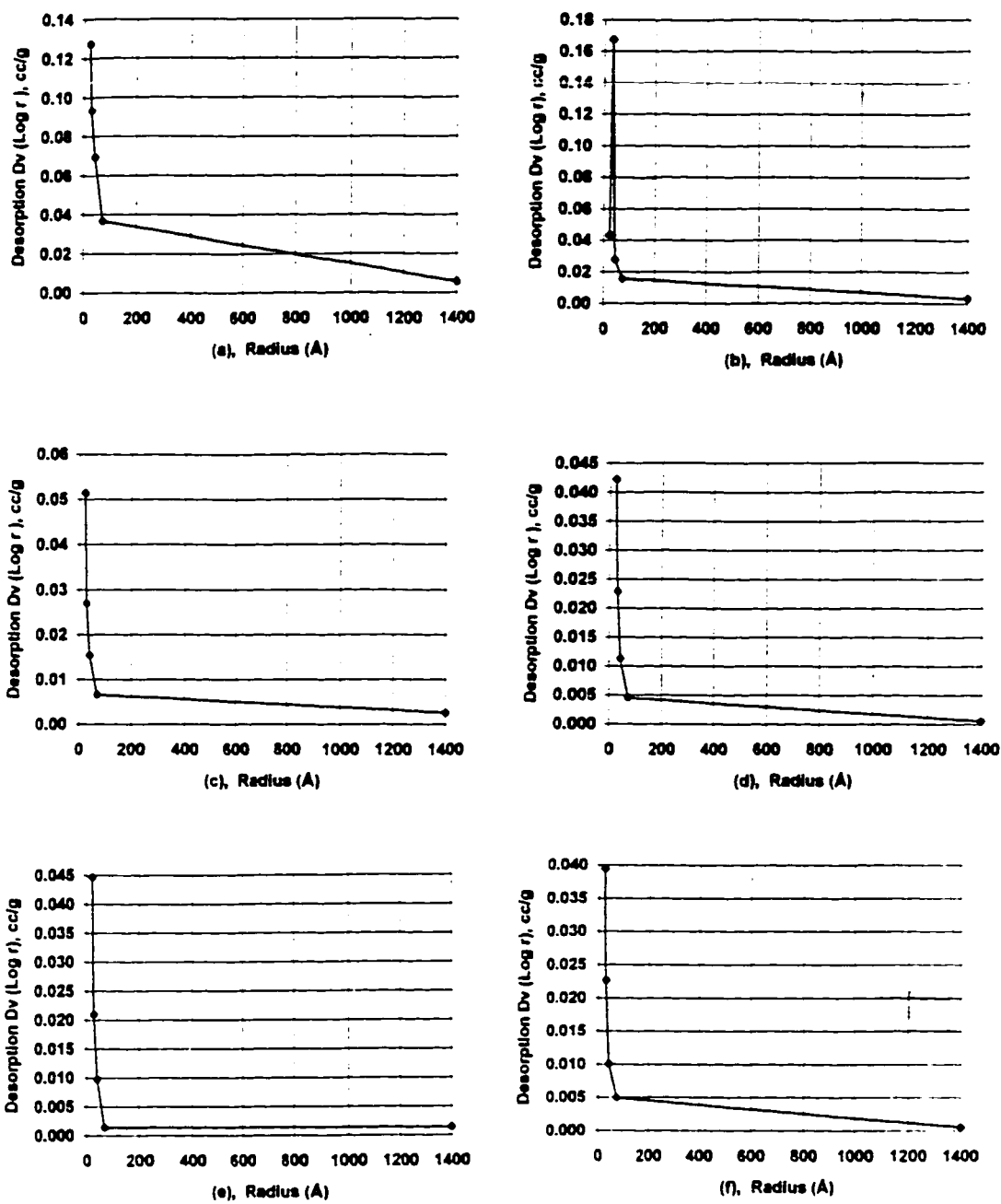


Fig. 42. Pore size distribution of titania-silica bulk gels at various heat-treatment temperature. (a) 100°C, (b) 200°C, (c) 300°C, (d) 400°C, (e) 500°C, (f) 600°C

When a higher concentration of $\text{Ti}(\text{O}^i\text{Pr})_4$ was used, further dilution of the solution was required to avoid premature gelation, resulting from an increased condensation rate of $\text{Ti}(\text{O}^i\text{Pr})_4$. In this investigation, clear and good coating solutions were more easily obtained by using a lower $\text{Ti}(\text{O}^i\text{Pr})_4$ concentration (i.e., $\text{TiO}_2/\text{SiO}_2 = 1/4$). The titania-silica films containing higher TiO_2 caused opacity, probably due to phase separation and crystallization during heat-treatment.⁽⁴⁷⁾ The refractive index of the films prepared by the mixing of two materials (TiO_2 and SiO_2) may be varied by using different alkoxide compositions. Figure 43 shows that the refractive index decreased as the TiO_2 content increased, due to the much higher refractive index of TiO_2 ($n = 2.3$) than SiO_2 ($n = 1.46$). In addition to composition, the refractive index also depends on other factors such as porosity, thickness, and structural defects. Therefore, in this investigation, solutions prepared from lower TiO_2 concentrations ($\text{TiO}_2 / \text{SiO}_2 = 1/4$) were studied to investigate the possible variations in the refractive index that could be varied as a function of process factors such as aging times, heat-treatment, and addition of PEG. The reflectivity as a function of the alkoxide composition is shown in Figure 44. The solution prepared with a ratio of $\text{TiO}_2/ \text{SiO}_2 = 4$ gave a coating having the lowest reflectances over a wide range of wavelengths.

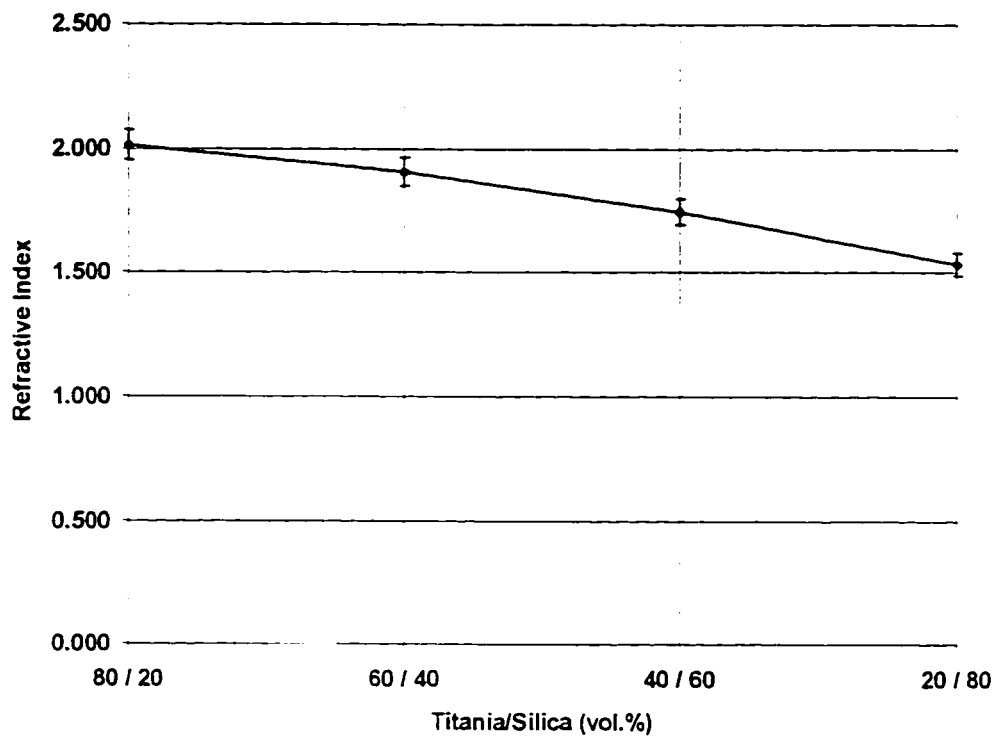


Fig. 43. Refractive index as a function of alkoxide composition ($\text{TiO}_2/\text{SiO}_2$).

Each data point represents the average values obtained from 10 measurements.

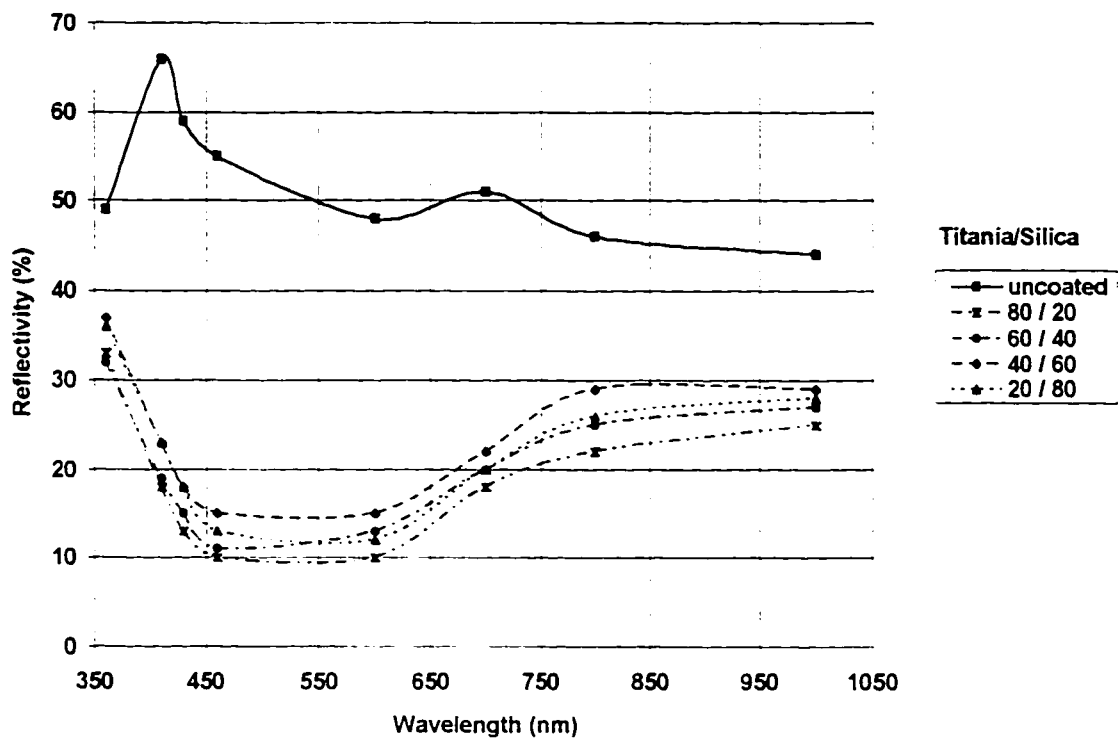


Fig. 44. Effect of alkoxide composition on the reflectivity of titania-silica sol-gel films. (Each data point represents the average values obtained from 10 measurements.)

CHAPTER 6

CONCLUSIONS

In this study, several parameters that affect the optical properties and pore structures of sol-gel derived $\text{TiO}_2/\text{SiO}_2$ films were identified and their specific effects were described. The pore characterization was performed by measuring the porosity of bulk gels which was used as a reference for an evaluation of pore structure of the films. The pore structure as well as physical and optical properties of sol-gel derived films are significantly governed by process conditions.

The film thickness was significantly affected by the coating application rate (drain rate), the number of coating cycles and heat-treatment temperatures after the deposition of the film. It was found that an increase in drain rate increased the film thickness whereas the thickness decreased with increased heat-treatment temperatures. For a given drain rate, the film thickness was linearly proportional to the number of deposited layers.

The refractive index of the sol-gel derived films can be tailored by varying the drain rate, heat-treatment temperature, aging times and addition of PEG. The spectral reflectance of the silicon wafer substrate decreased with the deposition of sol-gel films.

The addition of water soluble polymers such as PEG had a significant effect on the pore structure and optical properties of the films and led to a large shrinkage in the vertical direction of the films. It has also been found that there is an optimal concentration

of PEG, approximately 2 vol. % of solution and an increase in PEG content above this level made the shrinkage of the film excessive and resulted in poor coating qualities.

The preparation of the desired coating solution and good qualities of the deposited films were obtained by using suitable amounts of water ($H_2O/TEOS$ volume ratio = 2 to 5). Gels made with a high water-to-TEOS ratio had smaller pores than those prepared from sols with lower water concentrations.

The control of aging times and heat-treatment were also found to affect the porosity of the gels. It was found that an increase in aging times increased both pore volume and surface area of gels and led to a narrower pore size distribution. A narrower pore size distribution with small pores could be obtained by increasing the heat-treatment temperatures.

There are now many commercialized sol-gel derived coatings and an increasing amount of research in this field. The chemistry and technology of the sol-gel process are inseparable and mutually dependent. Therefore, a concerted research effort into sol-gel chemistry will gain new insights into the basic principles, provide us with innovative ideas for its capabilities, and will lead us to new and useful applications in the future.

Much attention has been paid recently to the precise tailoring of pore structure and optical properties of the films prepared via sol-gel process modified with the addition of several kinds of polymers. Especially, further work is needed to study the effects of water soluble polymers on the sol-gel coating structures and properties.

CHAPTER 7

REFERENCES

1. L. C. Klein, "Sol-Gel Technology for Thin Films, Fibers, Preforms, Electronics, and Specialty Shapes", Noyes Publications, New Jersey, 1988, p. 51.
2. H. Schmidt, "Chemistry of Materials Preparation by the Sol-gel Process", *J. Non-Cryst. Solids*, **100** (1988) 51-52.
3. S. Sakka and K. Kamiya, "Glasses from Metal Alkoxides", *J. Non-Cryst. Solids*, **42** (1980) 403-422.
4. I. M. Thomas, "Optical Coatings by the Sol-Gel Process", *Opt. News*, **12** (1986) 18-12.
5. J. D. Mackenzie in "Ultrastructure Processing of Glasses, Ceramics and Composites" eds., L. L. Hench and D. R. Ulrich, Wiley, New York, 1984, p. 15.
6. C. J. Brinker and G. W. Scherer, "Sol-Gel Science, The Physics and Chemistry of Sol-Gel Processing", Academic Press Inc., New York, 1990, p. 787-834.
7. D. R. Uhlmann and G. P. Rajendran in "Ultrastructure Processing of Advanced Ceramics", eds., J. D. Mackenzie and D. R. Ulrich, Wiley, New York, 1988, P. 241-251.
8. B. E. Yoldas and T. W. O' Keeffe, "Antireflective Coatings applied from Metal-Organic derived Liquid Precursors", *Appl. Opt.*, **18** (1979) 3133-3138
9. J. G. Wilder, "Porous Silica AR Coating for Use at 248 nm or 266 nm", *Appl. Opt.*, **23** (1984) 1448
10. D. C. Bradley, R. C. Mehrotra and D. P. Gaur, "Metal Alkoxides", Academic Press, New York, (1978).
11. S. Sakka, H. Kozuka and Sae-Hun Kim, in "Ultrastructure Processing of Advanced Ceramics", eds., J. D. Mackenzie and D. R. Ulrich, Wiley, New York, 1988, p. 159-170.

12. K. D. Keefer, in "Better Ceramics Through Chemistry", eds., C. J. Brinker, D. E. Clark and D. R. Ulrich, North-Holland, New York, 1984, p. 15-24.
13. S. Sakka and K. Kamiya, "The Sol-Gel Transition in the Hydrolysis of Metal Metal Alkoxides", *J. Non-Cryst. Solids*, **48** (1982) 31-46.
14. T. Hayashi, T. Yamada and H. Sato, "Preparation of Titania-Silica Glasses by Gel Method", *J. Mater. Sci.*, **18** (1983) 3137-3142.
15. L. Hu, T. Yoko, H. Kozuka and S. Sakka, "Effects of Solvent on Properties of Sol-Gel derived TiO₂ Coating Films", *Thin Solid Films*, **219** (1992) 18-23.
16. K. A. Vorotilov, E. V. Orlova and V. I. Petrovsky, "Sol-Gel Films on Silicon Substrates", *Thin Solid Films*, **207** (1992) 180-184.
17. K.C. Chen, T. Tsuchiya and J. D. Mackenzie, "Sol-Gel Processing of Silica I", *J. Non-Cryst. Solids*, **81** (1986) 227-238.
18. B. E. Yoldas, "Monolithic Glasses Formation by Chemical Polymerization", *J. Mater. Sci.*, **14** (1979) 1843-1849.
19. C. J. Brinker, K. D. Keefer, D. W. Shaefer, T. A. Assink, B. D. Kay and C. S. Ashley, "Sol-Gel Transition in Simple Silicates II", *J. Non-Cryst. Solids*, **63** (1984) 45-49.
20. R. Aelion, A. Loebel and F. Erich, "Hydrolysis of Ethyl Silicate", *J. Am. Chem. Soc.*, **72** (1950) 5705-5712.
21. Young-Joo Kim and L. F. Francis, "Processing and Characterization of Porous TiO₂ Coatings", *J. Am. Ceram. Soc.*, **76** (1993) 737-742.
22. Tin-Pin Zhong and D. E. Clark, "Interaction Between Colloidal Particles in SiO₂ and TiO₂ Sols", *J. Non-Cryst. Solids*, **160** (1993) 247-254.
23. C. J. Brinker, A. J. Hurd, P. R. Schunk, G. C. Frye and C. S. Ashley, "Review of Sol-Gel Film Formation", *J. Non-Cryst. Solids*, **147 & 148** (1992) 424-436.
24. Y. Takahashi and Y. Matsuoka, "Dip-coating of TiO₂ Films using a Sol-Gel Derived from Ti (O-i-Pr)₄-Diethanolamine-H₂O-i-PrOH System", *J. Mater. Sci.*, **23** (1988) 2259-2266.

25. L. E. Scriven, in "Better Ceramics Through Chemistry III", eds., C. J. Brinker, D. E. Clark and D. R. Ulrich, *Mat. Res. Soc. Symp. Proc.*, vol. 21, Materials Research Society, Pittsburgh, PA. 1988, p. 717-728.
26. P. Hinz and H. Dislich, *J. Non-Cryst. Solids*, **12** (1985) 134.
27. L. D. Landau and B. G. Levich, *Acta Physiochim*, URSS, **17** (1942) 42.
28. S. D. R. Wilson, *J. Eng. Math.*, **16** (1982) 201.
29. Jung-Won Lee, Chang-Whan Won, Byong-Sun Chun and H. Y. Sohn, "Dip Coating of Alumina Films by the Sol-Gel Method", *J. Mater. Res.*, **8** (1993) 3151-3157.
30. B. E. Yoldas, "Deposition and Properties of Optical Oxides Coatings from Polymerized Solutions", *Appl. Opt.*, **21** (1982) 2960.
31. V. Kozhukharov, Ch. trapalis, B. Samuneva. "Sol-Gel Processing of Titanium-containing Thin Coatings", *J. Mater. Sci.*, **28** (1993) 1283-1288.
32. Nilgun Ozer, "Reproducibility of the Coloration Processes in TiO₂ Films", *Thin Solid Films*, **214** (1992) 17-24.
33. C. J. Brinker, A. J. Hurd and K. J. Ward, in "Ultrastructure Processing of Advanced Ceramics", eds., J. D. Mackenzie and D. R. Ulrich, Wiley, New York, 1988, p. 223.
34. R. L. Nelson, J. D. F. Ramsay, J. L. Woodhead, J. A. Cairns and J. A. A. Crossley, "The Coating of Metals with Ceramic Oxides via Colloidal Intermediates", *Thin Solid Films*, **81** (1981) 329-337.
35. C. J. Brinker, G. C. Frye, A. J. Hurd and G. S. Ashley, "Fundamentals of Sol-Gel Dip Coating", *Thin Solid Films*.
36. C. J. Brinker, G. W. Scherer, *J. Non-Cryst. Solids*, **70** (1985) 301.
37. S. Sato, T. Murakada, T. Suzuki, T. Ohgawara, "Control of Pore Size Distributions of Silica Gel through Sol-Gel Process using Water Soluble Polymers as Additives", *J. Mater. Sci.*, **25** (1990) 4880-4885.
38. A. Matsuda, Y. Matsuno, S. Katayama, T. Tsuno, N. Tohge and T. Minami, "Physical and Chemical Properties of Titania-Silica Films derived from PEG containing Gels", *J. Am. Ceram. Soc.*, **77** (1990) 2217-2221.

39. B. E. Yoldas and D. P. Partlow, "Formation of broad Band Antireflective Coatings on fused Silica", *Thin Solid Films*, **129** (1985) 1-14.
40. B. E. Yoldas and T. W. O' Keeffe, "Antireflective Coatings applied from Metal-organic derived Liquid Precursors". *Appl. Opt.*, **18** (1979) 3133-3138.
41. B. E. Yoldas and D. P. Partlow, "Wide Spectrum Antireflective Coating for fused Silica and other Glasses", *Appl. Opt.*, **23** (1984) 1418-1424.
42. B. E. Yoldas, "Investigation of porous Oxides as an Antireflective Coating for Glass Surfaces", *Appl. Opt.*, **19** (1980) 1425-1429.
43. C. J. Brinker and S. P. Mukherjee, "Comparison of Sol-Gel derived Thin Films with Monoliths". *Thin Solid Films*, **77** (1981) 141-148.
44. S. Lowell and J. E. Shields, "Powder Surface Area and Porosity", 2d eds., Chapman and Hall, New York, 1984
45. L. C. Klein, *Ann. Res. Mater. Sci.*, **15** (1985) 227-248.
46. J. Zarzycki, M. Prassas and J. Phalippon, "Synthesis of Glasses from Gels", *J. Mater. Sci.*, **17** (1982) 3391-3399.
47. S. M. Melpolder, A. W. West, C. L. Barnes and T. N. Blanton, "Phase Transformation in TiO₂-SiO₂ Sol-Gel Films", *J. Mater. Sci.*, **26** (1991) 3585-3592.
48. R. J. Archer, "Manual on Ellipsometry", Gaertner Scientific Co., 1968.
49. "Instruction Manual". Dyn-optics Inc., 1983.
50. S. J. Gregg and K. S. W. Sing, "Adsorption, Surface Area and Porosity", Academic Press, New York, 1982.

APPENDIX A

ELLIPSOMETRY

Ellipsometry is the measurement and interpretation of differences between the states of polarization of the incident and reflected He-Ne laser beams.⁽⁴⁸⁾ Ellipsometry is widely used for measuring the thickness and refractive index of thin films on dielectric or metallic surfaces such as silicon oxide and silicon nitride films on silicon surfaces.

Ellipsometers are optical instruments which measure the amplitude and phase changes in the state of polarization of collimated light waves of monochromatic polarized light caused by reflection from a surface of sample. Gaertner Ellipsometer Model 117 consists of a helium-neon laser, polarizer, compensator, specimen table, analyzer and photodetector as shown in Figure 45. The light from the helium-neon laser is first linearly polarized by passing through the polarizer and then elliptically polarized by passing through the compensator. When a light wave reflects from a surface of specimen under measurement, the polarization of the light changes in accordance with specimen film thickness and optical characteristics of the film and substrate. This light then passes through the analyzer and is sensed by the photodetector.

Ellipsometry has several advantages over other methods of thickness measurements:

- (1) It can measure the film thickness at least an order of magnitude smaller than can be measured by other methods such as interferometry and reflectometry.
- (2) It can permit determination of the refractive index of thin films with unknown thickness.

(3) It can make measurements in optically-transparent environments such as liquid or air.

(4) It does not require special conditions such as vacuum, heat, or electron bombardment that may change the optical properties of surfaces being studied.

(5) Since the lower intensity of the laser enables normal room operation without need for an enclosure and unwanted background reflected light through a filter, the measurements can be made in normal room conditions.

SPECIFICATIONS OF GAERTER ELLIPSOMETER L117

Light Source	He-Ne 6328 Å laser 2 mw
Beam Size at Object	1 mm spot diameter
Angles of Incidence	set at 30°, 50°, and 70° by pre-adjusted pin locks
Sample Orientation	horizontal
Extinction Meter	built in, solid state amplifier
Measuring Range	from a few Angstroms to thick films
Accuracy	2.5 Å to 10 Å over most of the measuring range

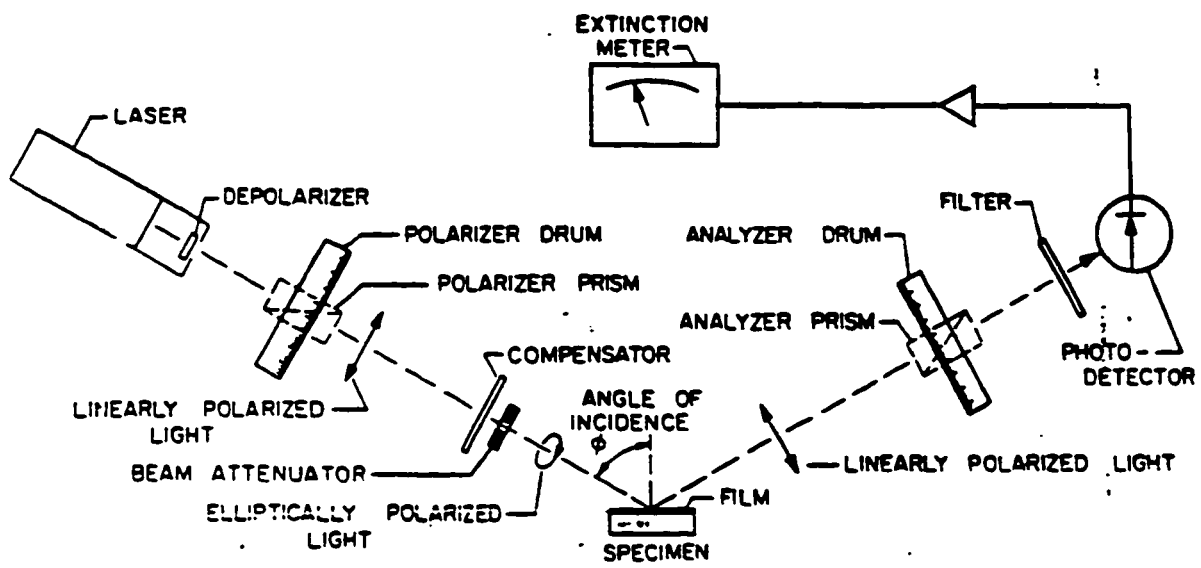


Fig. 45. Ellipsometer components at measurement.⁽⁴⁸⁾

APPENDIX B

Reflection Measurement by using Reflectometer

The Dyn-Optics 224 Reflectometer can measure the specular and diffused reflectivity at normal incidence from 350 nm to 1100 nm.⁽⁴⁹⁾ This can be operated in full room light without affecting accuracy. The specular reflectance of optical elements, mirrors, photomasks, and silicon wafers can be quickly measured with this instrument. Diffuse reflectance of such items as paper, fabric, paint, and metallic surfaces can also be measured.

The light beam is projected downward onto the test sample which is mounted on adjustable stages as shown in Figure 46. The detector is located above the test sample in a position where the reflected light falls. The wavelengths are defined by four filters in a cassette.

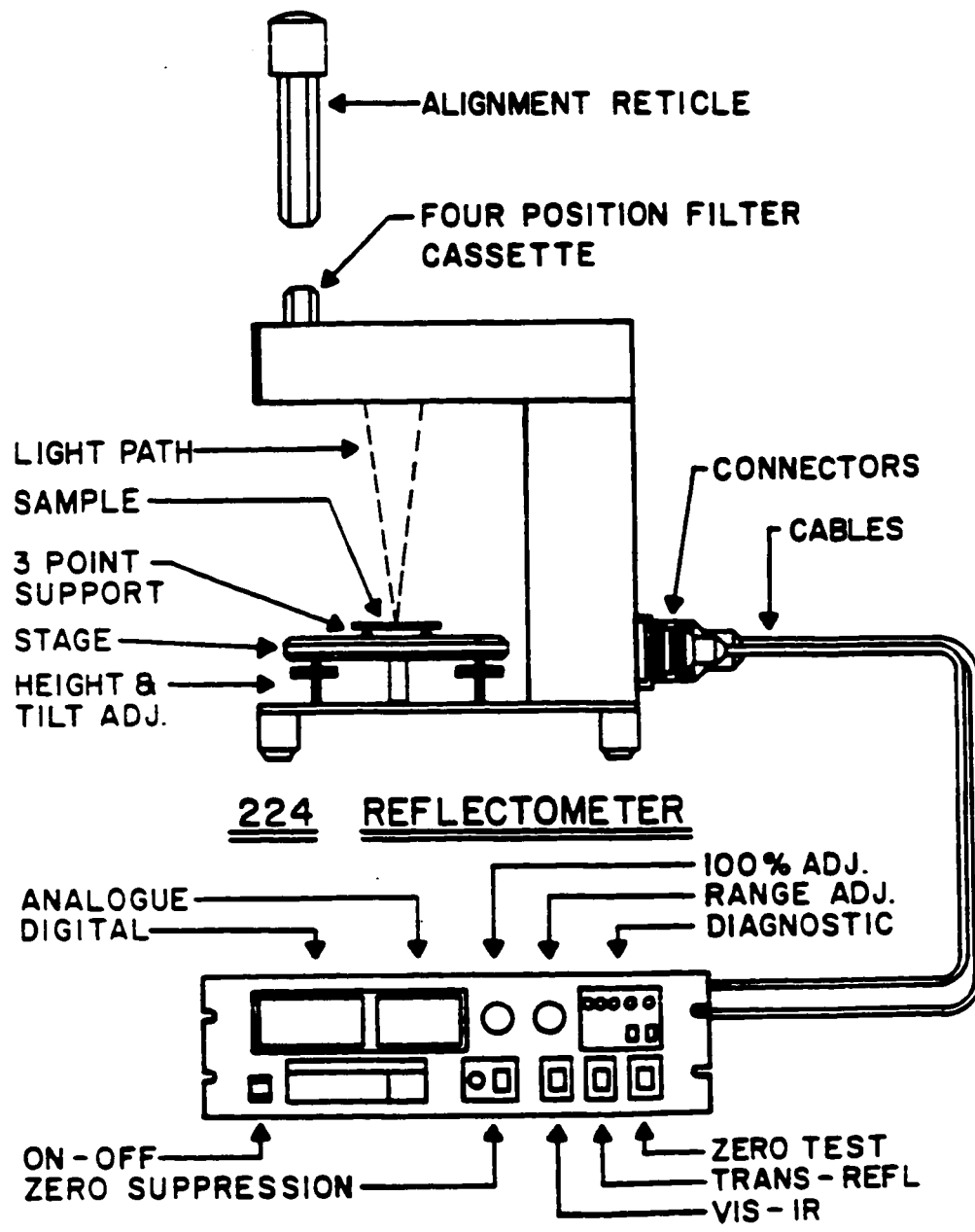


Fig. 46. Typical configuration of Dyn-Optics 224 Reflectometer.⁽⁴⁹⁾

APPENDIX C

Porosity Measurement with Quantachrome Autosorb-1

The porosity within the solid can be determined by measuring the quantity of gas adsorbed onto or desorbed from a solid surface at some equilibrium vapor pressure by the static volumetric method with BET (Bruner-Emmet-Teller) apparatus such as Autosorb-1. The data of porosity measurements are obtained by admitting or removing a known quantity of adsorbate gas into or out of a sample cell containing the solid adsorbent maintained at a constant temperature below the critical temperature of the adsorbate. As adsorption or desorption occurs, the pressure in the sample cell changes until equilibrium is established. The amount of gas adsorbed or desorbed at the equilibrium pressure is the difference between the amount of gas admitted or removed and amount required to fill the space around the adsorbent. Nitrogen adsorption at its boiling point is generally used as the adsorbate because it gives the most consistent and reproducible results.⁽⁵⁰⁾

The Autosorb-1 has the capability of measuring adsorbed volumes of nitrogen at relative pressure in the range 0.001 to slightly under 1.0. A typical Autosorb-1 is shown in Figure 47. The background theories for surface area and porosity measurements are briefly discussed below.

(1) Surface Area

The BET method is the most widely used procedure for the determination of the surface area of solid materials. The BET equation is given by:⁽⁵⁰⁾

$$1/W ((P_o / P) - 1) = 1/W_m C + C-1/W_m C (P/P_o) \quad [9]$$

where W is the weight of gas adsorbed at a relative pressure P/P_o and W_m is the weight of adsorbate constituting a monolayer of surface coverage. The term C , BET constant, is related to the energy of adsorption in the first adsorbed layer and consequently its value is an indication of the magnitude of the adsorbent / adsorbate interaction. The above BET equation requires a linear plot of $1/(W (P_o/P) - 1)$ vs. P/P_o . A typical BET plot is shown in Figure 48. The weight of adsorbate W_m can be obtained from the slope s and intercept i of the BET plot. That is,

$$s = c - 1/W_m C \quad [10]$$

$$i = 1/W_m C \quad [11]$$

$$W_m = 1/s + I \quad [12]$$

The total surface area S_t of the sample can be expressed as:

$$S_t = W_m N A_{cs} / M \quad [13]$$

where N is the Avogadro's number, A_{cs} is the molecular cross-sectional area of the adsorbate molecule, and M is the molecular weight of the adsorbate. Eventually the specific surface area S of the solid can be calculated from total surface area S_t and the sample weight w . That is, $S = S_t / w$

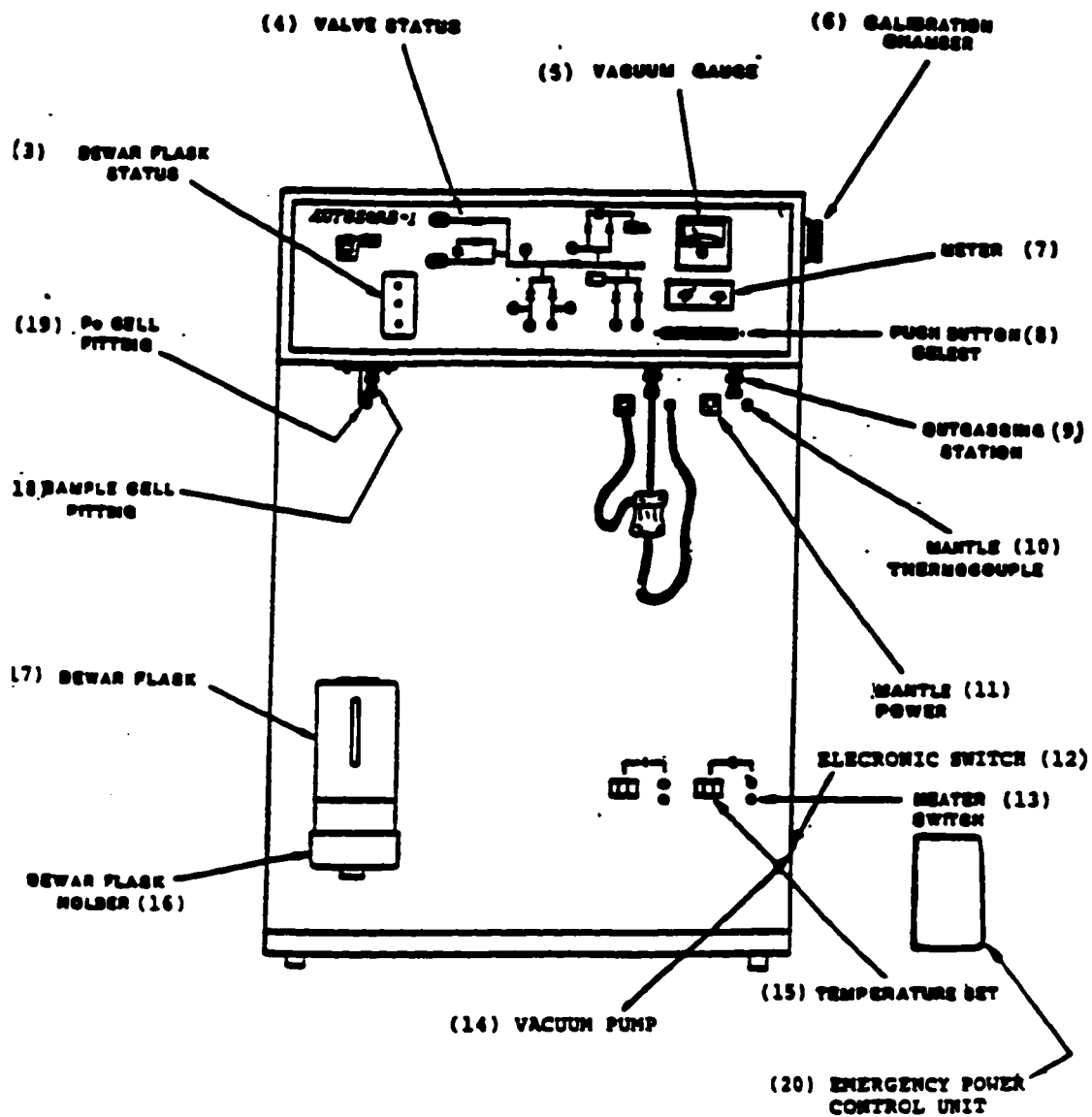


Fig. 47. Quantachrome's Autosorb-1

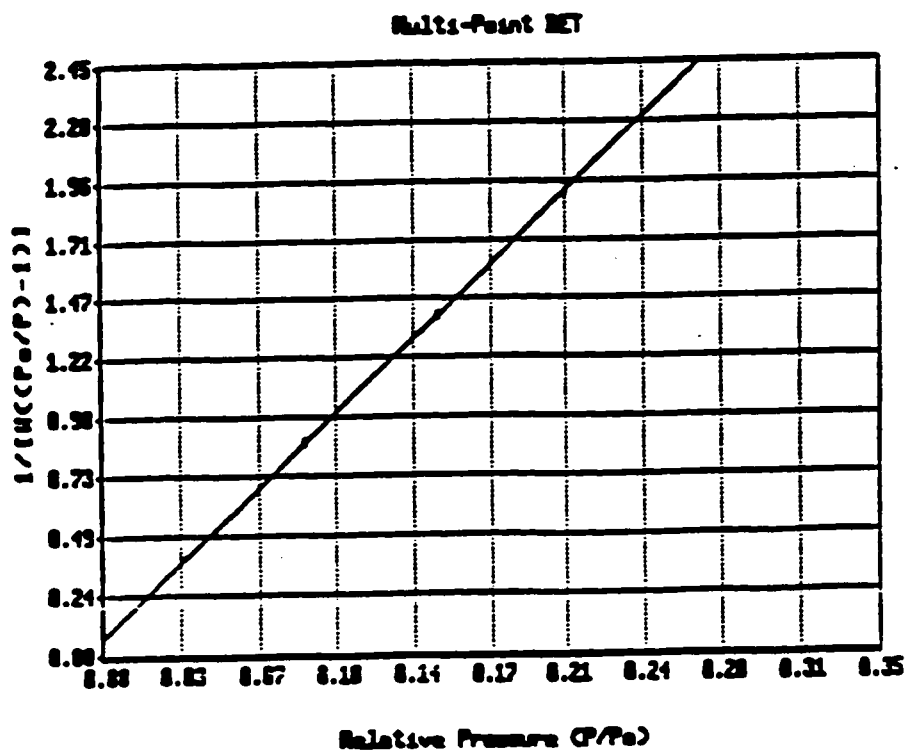


Fig. 48. A typical BET plot.⁽⁵⁰⁾

(2) Isotherms

The adsorption/desorption isotherms can be used to determine the surface area and porosity of an adsorbent. The nitrogen adsorption isotherm is obtained by determining the volume of nitrogen adsorbate on the sample surface as a function of the relative saturation of nitrogen, P/P_0 , where P and P_0 are the partial pressure and saturation vapor pressure of N_2 , respectively. Similarly, desorption isotherms can be obtained by measuring the quantities of gas removed from the sample as the relative vapor pressure decreases back to zero. The adsorption isotherm is obtained point-by-point on the Autosorb-1 by admitting to the adsorbent successive known volumes of nitrogen and measuring the equilibrium pressure. All adsorption isotherms may be grouped into one of the five types shown in Figure 49.⁽⁴⁴⁾

(a) Type I isotherms are concave to P/P_0 axis and the amount of adsorbate approaches a limiting value as P/P_0 approaches 1. Type I isotherm is a typical of sample containing micropores with relatively small external surfaces. The limiting uptake of adsorbate is governed by the accessible micropore volume rather than by the internal surface area. Probably, no additional adsorption occurs after micropores have been filled.

(b) Type II isotherms are the normal form of isotherm obtained with a nonporous or macroporous adsorbent. This type of isotherm represents unrestricted monolayer-multilayer adsorption. Point B, the start of the linear central section of the isotherm, is usually taken to indicate the relative pressure at which monolayer coverage is complete.

(c) Type III isotherms are convex to the P/P_0 axis over its entire range. This type of isotherm is rarely encountered. A well-known example is the adsorption of water vapor on nonporous carbons. The absence of a distinct point b on type III isotherm is caused by stronger adsorbate-adsorbate than adsorbate-adsorbent interactions.

(d) Type IV isotherms are normally found for samples having mesopores with radius of 20-500 Å. This type of isotherm shows a sharp rise in adsorption at higher relative pressures followed by a leveling off at relative pressures near 1.

(e) Type V isotherms are uncommon, corresponding to the type III, except that pores in the mesopore range are present.

CHARACTERIZATION OF PORES ACCORDING TO THEIR SIZES

Macropores	Pores with openings exceeding 500 Å in radius
Micropores	Pores with radii not exceeding 20 Å
Mesopores	Pores of intermediate size (20-500 Å)

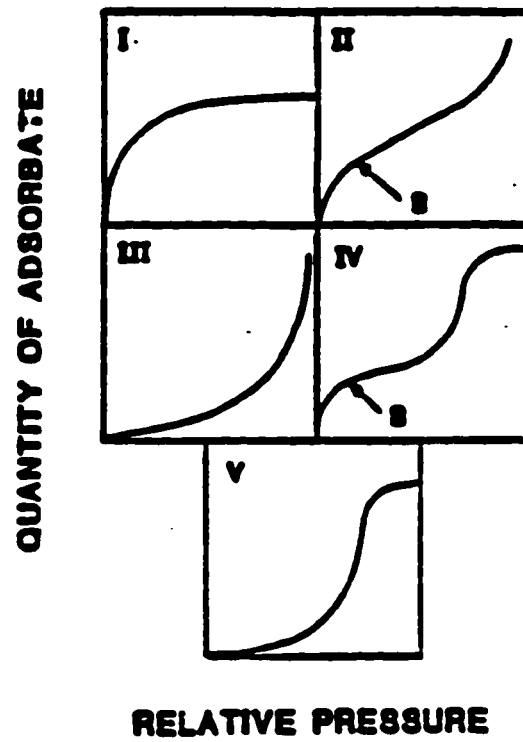


Fig. 49. Isotherm types classified by BDDT.⁽⁴⁴⁾

APPENDIX D

Calculation for percent change in thickness of TiO₂-SiO₂ sol-gel films prepared from various PEG concentrations vs. heat-treatment temperature.

The percent change in thickness (i.e. shrinkage) of the films on heat-treatment was estimated as

$$d = ((d_1 - d_2) / d_1) \times 100\%$$

where d_1 is the thickness of the as-deposited film and d_2 is the thickness of the heat-treated film.

(1) % shrinkage of the film prepared without the addition of PEG

d_2 (Å)	% Shrinkage of the Film
961 (= d_1) at 25°C	$((961-961)/961) \times 100 = 0\%$
930 at 100°C	$((961-930)/961) \times 100 = 3.2\%$
820 at 200°C	$((961-820)/961) \times 100 = 14.7\%$
753 at 300°C	$((961-753)/961) \times 100 = 21.6\%$
753 at 400°C	$((961-753)/961) \times 100 = 21.6\%$
733 at 500°C	$((961-733)/961) \times 100 = 23.7\%$

(2) % shrinkage of the film prepared with the addition of 1 vol.% PEG

d_2 (Å)	% Shrinkage of the Film
1224 (= d_1) at 25°C	$((1224-1224)/1224) \times 100 = 0 \%$
1201 at 100°C	$((1224-1201)/1224) \times 100 = 1.88 \%$
1013 at 200°C	$((1224-1013)/1224) \times 100 = 17.2 \%$
833 at 300°C	$((1224-833)/1224) \times 100 = 31.9 \%$
811 at 400°C	$((1224-811)/1224) \times 100 = 33.3 \%$
765 at 500°C	$((1224-765)/1224) \times 100 = 37.5 \%$

(3) % shrinkage of the film prepared with the addition of 2 vol. % PEG

d_2 (Å)	% Shrinkage of the Film
1442 (= d_1) at 25°C	$((1442-1442)/1442) \times 100 = 0 \%$
1329 at 100°C	$((1442-1329)/1442) \times 100 = 7.8 \%$
900 at 200°C	$((1442-900)/1442) \times 100 = 37.6 \%$
708 at 300°C	$((1442-708)/1442) \times 100 = 50.9 \%$
704 at 400°C	$((1442-704)/1442) \times 100 = 51.2 \%$
694 at 500°C	$((1442-694)/1442) \times 100 = 51.9 \%$

APPENDIX E

Ellipsometric Measurements for Thickness and Refractive Index of TiO₂-SiO₂ Thin Films on Silicon Wafers

• Nomenclature and Dimensional Units:

n_f = refractive index of film being measured (TiO₂-SiO₂)

n_s = refractive index of substrate carrying film (Silicon Wafer)

d = thickness of film being measured in angstroms (10^{-10} m)

ϕ = angle of incidence selectable at 70, 50 or 30°

λ = wavelength of incident light using He-Ne laser

DEL = Δ , phase difference in degrees

PSI = ψ , amplitude ratio in degrees

= the number of measurements

@ Measurement Conditions:

n_s of silicon wafer = 3.85-0.02i

k_s of Si = -0.02

ϕ = 70°

λ = 6328 Å

number of measurement = 10 to 15

1. Thickness and Refractive Index vs. Drain Rate (by one coating cycle)

(1) Drain Rate = 0.25 cm/min

Thickness, d (Å)	n_r	PSI	DEL
254	1.543	15.46	117.78
275	1.581	16.29	113.18
180	1.593	13.37	129.52
258	1.555	15.63	116.76
282	1.541	16.35	113.62
251	1.548	15.38	118.10
281	1.540	16.30	113.10
255	1.538	15.48	117.77
274	1.506	15.93	116.77
276	1.539	16.13	114.65

(2) Drain Rate = 2.5 cm/min

d, Å	n_r	PSI	DEL
384	1.521	19.59	102.09
388	1.535	19.82	101.03
395	1.533	20.05	100.39
389	1.530	19.81	101.21
387	1.535	19.80	101.11
371	1.535	19.25	102.84
368	1.535	19.15	103.17
376	1.535	19.42	102.29
373	1.538	19.35	102.46
369	1.532	19.17	103.20
365	1.535	19.06	103.48
361	1.542	18.98	103.57
370	1.532	19.19	103.11
369	1.524	19.12	103.53
353	1.540	18.70	104.55

(3) Drain Rate = 5 cm/min

d, Å	n_r	PSI	DEL
498	1.531	23.45	91.51
495	1.533	23.38	91.60
501	1.531	23.54	91.31
498	1.528	23.43	91.63
490	1.525	23.15	92.38
479	1.534	22.86	92.82
507	1.534	23.78	90.68
502	1.530	23.57	91.27
507	1.524	23.70	91.17
477	1.527	22.70	93.40
474	1.530	22.64	93.44
505	1.532	23.70	90.91
545	1.527	24.97	88.39
518	1.533	24.13	89.94
514	1.530	23.99	90.33

(4) Drain Rate = 12 cm/min

d, Å	n_r	PSI	DEL
803	1.523	34.17	76.75
823	1.528	35.16	75.84
820	1.531	35.10	75.72
827	1.529	35.39	75.67
862	1.526	36.93	75.07
842	1.523	35.86	75.79
797	1.524	33.97	76.82
797	1.529	34.10	76.45
839	1.531	35.97	75.24
841	1.533	36.14	75.03
848	1.533	36.43	74.90
844	1.525	36.01	75.58
859	1.529	36.86	74.93
872	1.526	37.41	74.92
870	1.525	37.27	75.01

2. Thickness and Refractive Index vs. H₂O/TEOS

(1) H₂O/TEOS = 1.5

d, Å	n _r	PSI	DEL
736	1.529	31.95	77.54
734	1.532	31.91	77.45
739	1.531	32.05	77.37
746	1.533	32.38	76.96
762	1.530	32.98	76.58
749	1.535	32.45	77.06
738	1.532	31.74	77.59
747	1.530	42.41	77.16
751	1.538	32.49	76.98
728	1.520	31.55	77.87

(2) H₂O/TEOS = 2

d, Å	n _r	PSI	DEL
796	1.546	35.08	74.90
812	1.544	35.74	74.61
797	1.546	35.12	74.86
830	1.542	36.54	74.28
849	1.545	37.58	73.65
856	1.546	37.97	73.40
818	1.546	35.40	74.69
821	1.545	36.26	74.32
808	1.543	35.65	74.62
843	1.547	37.71	73.52

(3) H₂O/TEOS = 3

d, Å	n_r	PSI	DEL
755	1.539	32.86	76.25
745	1.539	32.49	76.58
728	1.539	31.80	77.22
743	1.539	32.39	76.66
760	1.540	33.09	76.03
752	1.539	32.77	76.32
763	1.538	33.17	76.03
743	1.540	32.37	76.68
738	1.539	32.24	76.88
739	1.539	32.30	76.91

(4) H₂O/TEOS = 4

d, Å	n_r	PSI	DEL
694	1.533	30.43	78.97
693	1.534	30.40	78.96
685	1.534	30.14	79.26
684	1.534	30.09	79.35
758	1.534	32.87	76.48
756	1.531	32.72	76.78
743	1.531	32.21	77.24
673	1.534	29.66	74.91
701	1.533	30.68	78.76
700	1.531	30.61	78.75

3. Thickness and Refractive Index vs. Heat-treatment Temperature (single coating with 12cm/min)

(1) as-deposited (25°C)

d, Å	n_r	PSI	DEL
988	1.501	42.78	75.75
1012	1.500	44.37	75.80
1051	1.503	47.50	75.59
960	1.501	41.11	75.85
929	1.498	39.21	76.33
941	1.502	40.06	75.91
997	1.500	43.39	75.79
970	1.499	41.61	75.96
988	1.495	42.49	76.23
959	1.493	40.68	76.50
967	1.501	41.51	75.83
941	1.500	39.97	76.09
910	1.500	38.33	76.39
929	1.497	39.16	76.43
878	1.499	36.76	76.88

(2) 100°C

d, Å	n_r	PSI	DEL
918	1.508	38.85	76.25
927	1.511	39.16	76.43
921	1.519	39.11	75.27
925	1.514	39.75	75.19
919	1.512	39.14	76.41
937	1.514	39.98	75.43
929	1.514	38.95	76.13
931	1.515	39.49	75.87
934	1.514	39.31	76.05
959	1.519	40.63	76.31

(3) 200°C

d, Å	n _r	PSI	DEL
759	1.524	32.45	77.99
812	1.525	34.60	76.34
851	1.521	36.23	75.72
842	1.520	35.76	76.03
821	1.516	34.78	76.75
781	1.522	33.28	77.41
857	1.519	36.44	75.73
855	1.521	36.40	75.63
852	1.522	36.31	75.59
815	1.524	34.73	76.31
777	1.524	33.15	77.40
789	1.521	33.57	77.23
833	1.519	35.37	76.24
832	1.517	35.26	76.40
802	1.518	34.01	77.12

(4) 300°C

d, Å	n _r	PSI	DEL
709	1.531	30.68	79.41
742	1.527	31.84	78.40
757	1.528	32.42	77.83
704	1.520	3.33	80.27
760	1.530	32.60	77.56
825	1.527	35.21	75.87
798	1.527	34.04	76.62
790	1.527	33.72	76.90
773	1.526	33.10	77.16
755	1.530	32.43	77.62
731	1.532	31.48	78.60
728	1.528	31.34	78.85
740	1.524	31.69	78.70
750	1.523	32.06	78.38

(5) 400°C

d, Å	n _r	PSI	DEL
731	1.532	31.53	78.44
786	1.532	33.69	76.58
801	1.530	34.26	76.27
816	1.529	34.89	75.95
764	1.529	32.74	77.48
749	1.535	32.25	77.63
774	1.531	33.18	77.02
729	1.533	31.46	78.49
771	1.529	33.03	77.23
736	1.527	31.59	78.65
773	1.529	33.10	77.18
741	1.529	31.85	78.31
710	1.527	30.65	79.63
725	1.526	31.17	79.12
718	1.531	31.02	79.03

(6) 500°C

d, Å	n _r	PSI	DEL
712	1.532	30.82	79.21
763	1.532	32.74	77.34
768	1.530	32.93	77.26
769	1.532	33.00	77.14
721	1.533	31.15	78.77
704	1.534	30.55	79.41
742	1.533	31.96	77.97
783	1.527	33.45	77.01
750	1.535	32.32	77.53
733	1.533	31.61	78.34
704	1.532	30.52	79.52
720	1.530	31.06	79.01
718	1.533	31.04	78.91
720	1.529	31.06	79.05
706	1.529	30.53	79.54

4. Thickness and Refractive Index vs. PEG Concentration

4.1 1 % PEG in the solution

(1) as-deposited (25°C)

d, Å	n_r	PSI	DEL
1249	1.521	74.76	62.92
1205	1.520	67.76	69.51
1254	1.521	75.48	62.05
1219	1.521	70.00	67.94
1223	1.521	70.58	67.63
1182	1.522	64.32	70.96

(2) 100°C

d, Å	n_r	PSI	DEL
1127	1.526	57.56	71.84
1182	1.526	65.03	69.53
1223	1.527	71.46	64.74
1220	1.527	71.03	65.22
1178	1.528	64.64	69.35
1256	1.526	76.70	56.83
1244	1.526	74.86	60.25

(3) 200°C

d, Å	n_r	PSI	DEL
1003	1.528	45.55	73.07
1199	1.529	67.98	67.16
1000	1.528	45.31	73.06
1025	1.530	47.50	72.62
967	1.531	43.12	73.11
965	1.532	43.04	73.06
1046	1.530	49.32	72.41
1038	1.529	48.45	72.68
1250	1.530	76.38	55.43

(4) 300°C

d, Å	n_r	PSI	DEL
826	1.526	35.26	75.89
829	1.528	35.42	75.71
846	1.530	36.26	75.15
850	1.532	36.48	74.95
810	1.530	34.65	76.03
854	1.528	36.60	75.11
838	1.527	35.81	75.55

(5) 400°C

d, Å	n _r	PSI	DEL
741	1.524	31.77	78.59
810	1.526	34.56	76.33
822	1.527	35.08	75.97
817	1.528	34.89	76.02
733	1.530	31.57	78.51
854	1.519	36.32	75.78
917	1.522	39.63	74.46
911	1.521	39.21	74.68
850	1.519	36.14	75.86

(6) 500°C

d, Å	n _r	PSI	DEL
706	1.530	30.55	79.61
769	1.532	32.98	77.16
777	1.526	33.20	77.24
740	1.530	31.84	78.25
732	1.530	31.55	78.51
797	1.532	43.12	76.30
773	1.530	33.14	77.08

4.2. 2 % PEG in the solution

(1) as-deposited (25°C)

d, Å	n_r	PSI	DEL
1423	1.498	76.75	287.84
1460	1.505	68.55	285.93
1434	1.495	75.64	285.60
1448	1.496	73.12	284.50
1448	1.496	73.03	284.54
1332	1.495	84.01	56.84
1440	1.495	74.59	285.02

(2) 100°C

d, Å	n_r	PSI	DEL
1200	1.498	63.09	76.68
1278	1.498	75.15	73.42
1321	1.497	82.65	60.53
1306	1.499	80.30	66.34
1327	1.499	83.84	53.14
1332	1.498	84.40	49.84
1407	1.498	79.45	291.39
1440	1.501	72.99	286.39

(3) 200°C

d, Å	n_r	PSI	DEL
869	1.510	36.70	76.21
894	1.512	37.99	75.64
907	1.509	38.57	75.68
897	1.510	38.06	75.76
896	1.507	37.92	76.00
893	1.507	37.73	76.06
897	1.501	37.71	76.46
909	1.499	38.25	76.43

(4) 300°C

d, Å	n_r	PSI	DEL
723	1.472	30.09	82.74
705	1.469	29.43	83.63
716	1.467	29.76	83.32
737	1.467	30.44	82.63
707	1.470	29.51	83.47
660	1.481	28.16	84.70
677	1.470	28.52	84.71
704	1.463	29.28	84.09
740	1.464	30.49	82.74
713	1.466	29.63	83.53

(5) 400°C

d, Å	n _r	PSI	DEL
698	1.431	28.44	86.50
709	1.429	28.74	86.22
699	1.428	28.43	86.64
704	1.431	28.64	86.28
714	1.429	28.91	86.05
697	1.431	28.43	86.50
692	1.425	28.14	87.13
708	1.437	28.89	85.69
709	1.432	28.82	86.01
705	1.433	28.73	86.06

(6) 500°C

d, Å	n _r	PSI	DEL
674	1.438	27.82	87.01
685	1.433	28.07	86.88
685	1.434	28.12	86.76
695	1.426	28.26	86.94
708	1.429	28.73	86.25
670	1.433	27.60	87.52
704	1.427	28.54	86.59
710	1.425	28.70	86.47
704	1.429	28.61	86.37
704	1.425	28.50	86.69

5. The Number of Deposition vs. Thickness at Various Coating Rate

# of Deposition	0.25 cm / min	2.5 cm / min	5 cm / min	12 cm / min
1	258, 252, 276	368, 371, 369,	483, 489, 487,	897, 896, 889,
	271, 148	367, 365	479, 497	902, 911
2	389, 394, 391.	529, 531, 534,	731, 739, 716,	1300, 1299,
	387, 394	536, 530	728, 741	1312,
				1306, 1313
3	531, 539, 553.	742, 737, 746,	957, 959, 963,	1749, 1756,
	545, 527	741, 739	969, 967	1769,
				1753, 1753
4	678, 679, 685.	923, 929, 931,	1159, 1163,	2249, 2255,
	693, 685	930, 932	1166,	2261,
			1172, 1170	2251, 2259
5	831, 825, 846.	1112, 1107.	1378, 1383,	2784, 2771,
	837, 831	1120,	1371,	2779,
		1109, 1097	1382, 1376	2789, 2797
6	989, 982, 973,	1289, 1291,	1651, 1659,	3341, 3345,
	992, 979	1287,	1653,	3348,
		1281, 1287	1647, 1635	3343, 3348

6. Refractive Index Measurements at various Alkoxide Compositions

TiO₂/SiO₂ (vol. %)	Refractive Index
80/20	2.012, 2.010, 1.983, 2.080, 2.015, 2.010, 2.014, 1.997, 2.013, 2.012, AVG. = 2.015
60/40	1.892, 1.899, 1.904, 1.920, 1.912, 1.884, 1.906, 1.918, 1.917, 1.920, AVG. = 1.907
40/60	1.741, 1.770, 1.739, 1.732, 1.765, 1.739, 1.743, 1.751, 1.739, 1.742, AVG. = 1.746
20/80	1.535, 1.538, 1.535, 1.542, 1.531, 1.533, 1.529, 1.531, 1.533, 1.539, AVG. = 1.535

APPENDIX F

Reflectivity Measurement (% Reflectance)

1. Reflectivity vs. PEG Concentration

Wavelength (nm)	0 % PEG	1 % PEG	2 % PEG
360	34.7, 33.2, 34.1	30.9, 31.1, 32.4	28.6, 29.4, 27.9
	35.8, 35.9, 37.0	32.8, 33.6, 31.2	29.1, 30.2, 28.8
410	25.2, 25.8, 24.9	20.1, 18.2, 19.3	54.4, 53.5, 54.1
	25.9, 26.3, 27.9	19.9, 20.5, 22.0	55.9, 55.8, 57.0
430	18.7, 19.3, 17.9	18.1, 17.3, 18.5	53.7, 52.9, 53.5
	19.2, 20.1, 18.8	18.9, 19.4, 21.8	54.8, 55.2, 53.9
460	13.7, 13.5, 12.9	17.2, 16.1, 15.9	55.8, 54.9, 55.2
	13.9, 14.8, 15.2	18.8, 18.1, 15.9	55.9, 57.9, 56.3
600	13.8, 14.2, 12.3	18.3, 16.2, 17.8	14.7, 14.1, 13.2
	14.9, 15.1, 13.7	17.8, 18.1, 19.8	15.9, 15.8, 17.0
700	21.0, 21.2, 20.3	24.9, 25.3, 25.5	11.2, 11.3, 11.0
	22.3, 22.8, 18.4	26.1, 26.4, 21.8	11.8, 11.4, 11.3
800	26.2, 25.9, 27.3	34.8, 33.5, 34.2	15.8, 17.4, 16.2
	29.2, 28.2, 31.2	35.9, 35.7, 35.9	21.3, 18.1, 19.2
1000	27.3, 25.7, 27.0	37.2, 36.1, 35.9	21.2, 20.3, 19.9
	28.6, 29.8, 29.6	35.9, 38.2, 38.8	23.4, 22.9, 24.3

2. Reflectivity vs. H₂O/TEOS

Wavelength (nm)	H ₂ O/TEOS = 1.5	H ₂ O/TEOS = 2	H ₂ O/TEOS = 3	H ₂ O/TEOS = 4
360	36.1, 36.5, 35.2	34.3, 35.2, 33.9	34.2, 33.9, 34.2	36.8, 36.5, 37.2
	35.9, 36.8, 35.5	36.8, 37.1, 32.7	33.4, 34.0, 34.3	37.0, 37.3, 36.2
410	28.1, 26.2, 26.4	26.1, 26.3, 26.4	22.1, 23.0, 22.6	34.2, 34.0, 34.1
	29.3, 29.1, 28.9	25.8, 26.9, 25.5	22.4, 23.5, 24.4	33.5, 34.0, 34.2
430	20.2, 20.0, 20.3	16.9, 18.2, 19.0	16.8, 16.7, 17.0	24.8, 29.0, 26.7
	21.7, 22.0, 21.8	17.9, 19.8, 22.2	17.1, 17.2, 16.2	28.1, 27.2, 26.2
460	16.5, 16.3, 16.0	14.2, 14.2, 13.9	14.0, 14.2, 14.1	16.9, 16.6, 18.0
	15.7, 16.8, 15.7	13.2, 14.0, 14.5	13.5, 14.0, 14.2	16.1, 16.2, 17.2
600	12.1, 13.0, 12.8	14.5, 14.2, 13.6	16.3, 16.2, 16.3	16.1, 16.6, 17.2
	12.2, 13.9, 14.0	14.3, 14.2, 13.2	15.8, 16.7, 15.7	16.9, 16.4, 17.2
700	21.1, 18.7, 19.5	20.0, 20.5, 20.0	22.0, 23.1, 22.8	20.5, 19.7, 20.0
	22.0, 21.5, 17.2	21.8, 22.3, 21.4	22.2, 24.4, 23.5	22.0, 22.3, 21.5
800	23.9, 24.3, 25.2	28.0, 26.5, 26.2	27.3, 28.2, 28.8	23.2, 23.9, 24.8
	26.8, 27.1, 22.7	29.3, 29.1, 28.9	27.9, 29.8, 32.0	26.8, 29.0, 34.3
1000	26.8, 27.0, 22.7	28.3, 26.2, 26.7	28.8, 28.0, 27.1	31.1, 30.8, 28.0
	27.1, 28.2, 26.2	28.4, 29.1, 29.3	27.4, 29.8, 32.5	33.1, 28.6, 28.4

3. Reflectivity vs. TiO₂/SiO₂

Wavelength (nm)	20 / 80	40 / 60	60 / 40	80 / 20
360	36.0, 36.5, 35.5	36.7, 36.6, 37.3	34.1, 29.1, 28.7	29.8, 31.2, 28.7
	35.6, 36.4, 35.9	36.9, 37.5, 36.6	36.1, 38.2, 25.8	34.9, 35.0, 37.6
410	22.1, 23.0, 22.9	22.7, 22.6, 22.9	16.9, 18.3, 18.9	15.7, 16.9, 17.9
	22.1, 24.8, 22.9	22.4, 24.5, 22.9	17.5, 21.2, 22.2	17.0, 18.4, 22.1
430	15.9, 16.7, 17.0	16.9, 16.3, 17.4	13.4, 13.2, 13.4	11.7, 13.4, 12.3
	17.9, 18.5, 22.0	16.9, 18.2, 22.3	15.6, 16.9, 17.5	12.7, 13.8, 14.1
460	12.0, 13.1, 12.6	12.9, 13.2, 13.9	8.9, 9.2, 10.4	9.7, 10.4, 8.5
	12.4, 13.7, 14.2	15.8, 16.7, 17.5	12.7, 11.5, 13.3	9.8, 10.9, 10.7
600	12.3, 11.1, 11.8	12.4, 13.7, 13.8	11.9, 12.3, 13.4	10.1, 8.3, 8.8
	12.8, 13.3, 11.7	15.9, 16.9, 17.3	14.7, 11.9, 13.8	8.9, 11.3, 12.6
700	21.7, 18.1, 19.5	22.3, 21.4, 21.5	21.0, 18.8, 19.5	15.8, 16.8, 17.3
	22.0, 21.0, 17.7	22.8, 22.3, 21.7	22.0, 21.7, 17.0	17.6, 18.3, 22.2
800	26.5, 26.0, 26.0	27.1, 27.9, 26.9	22.4, 23.7, 23.8	20.8, 18.0, 17.5
	25.1, 26.4, 25.9	29.9, 33.1, 29.1	25.8, 26.9, 27.4	24.0, 21.9, 16.8
1000	25.9, 25.8, 26.3	26.8, 28.2, 26.4	25.3, 24.9, 26.8	20.9, 22.3, 23.8
	28.7, 29.0, 32.3	30.4, 33.3, 28.9	26.9, 27.6, 30.5	25.6, 26.2, 31.2

4. Reflectivity vs. Aging Times

Wavelength (nm)	No Aging	4 Day	7 Day	14 Day
360	33.1, 32.9, 33.3	33.9, 35.7, 35.9	31.4, 30.5, 29.2	31.9, 32.4, 34.0
	34.8, 35.9, 34.0	35.9, 36.3, 38.3	32.5, 28.2, 28.2	31.8, 35.4, 32.5
410	21.9, 23.2, 22.6	31.7, 32.6, 34.2	43.1, 43.9, 44.3	48.1, 44.5, 46.1
	22.4, 24.0, 23.4	31.8, 35.2, 32.5	45.8, 47.3, 45.6	48.4, 48.9, 58.0
430	16.8, 16.7, 18.2	21.9, 22.7, 23.1	34.5, 33.7, 34.2	37.8, 36.9, 39.2
	16.1, 16.0, 17.2	23.9, 23.9, 28.5	33.4, 34.1, 34.1	40.3, 41.1, 38.7
460	14.3, 14.1, 13.9	12.9, 13.3, 13.9	26.3, 25.3, 26.1	27.6, 26.9, 29.4
	13.0, 14.2, 14.5	14.9, 15.9, 19.1	25.5, 27.8, 25.0	30.4, 31.1, 28.6
600	16.5, 16.2, 16.1	12.1, 10.8, 11.0	7.8, 7.2, 8.4	8.1, 8.9, 8.9
	15.8, 16.7, 15.7	13.9, 12.2, 12.0	8.7, 8.1, 13.8	12.3, 8.8, 13.0
700	22.1, 23.5, 22.1	21.0, 18.8, 19.1	12.1, 13.2, 12.6	12.2, 10.7, 11.9
	22.3, 23.6, 24.4	22.4, 21.5, 17.2	12.4, 13.7, 14.0	13.0, 12.4, 11.8
800	28.9, 27.9, 27.4	31.2, 30.7, 28.6	22.1, 21.9, 23.3	22.8, 21.2, 23.4
	27.1, 29.8, 32.5	33.1, 28.0, 28.4	26.1, 25.2, 25.4	26.1, 25.1, 25.4
1000	27.0, 28.5, 28.6	30.1, 29.9, 33.1	28.4, 26.2, 26.1	26.6, 27.2, 26.5
	28.1, 29.7, 32.1	34.9, 31.8, 32.2	29.1, 29.3, 28.9	27.3, 28.3, 26.1

APPENDIX G

Autorsorb-1' data for porosity measurements:

(1) Surface area-pore volume-pore size summary

(2) Tabular data for isotherms

SURFACE AREA-PORE VOLUME-PORE SIZE SUMMARY

Quantachrome Corporation
Quantachrome Autosorb Automated Gas Adsorption System Report
ASORB2PC Version 1.04

Sample ID..... titania-silica gel
 Sample Description..... No PEG
 Comments..... dried at 100 C, Water/TEOS=2
 Gas Type..... NITROGEN
 Cross-Sec Area.. 16.2 Å² Corr Factor.. 6.580E-05 Molec Wgt.. 28.0114
 Sample Weight... 0.0500 g P/Po Toler... 4 File Name.. ASWATE02.RAW
 Analysis Time... 237.7 min Equil Time... 2 Operator... Young-Min Kw
 Outgas Time..... 3.0 hrs Outgas Temp.. 24 °C Station #.. 1
 End of Run.....

AREA-VOLUME-PORE SIZE SUMMARY

SURFACE AREA DATA

Multi-Point BET.....	2.435E+02	m ² /g
Langmuir Surface Area.....	6.093E+02	m ² /g
Meso Pore Area.....	1.264E+02	m ² /g
* t-Method Micro Pore Area.....	1.171E+02	m ² /g
* MP-Method Micro Pore Area.....	1.234E+02	m ² /g
DR-Method Micro Pore Area.....	4.111E+02	m ² /g
Cumulative Adsorption Surface Area.....	1.844E+01	m ² /g
Cumulative Desorption Surface Area.....	2.820E+01	m ² /g

PORE VOLUME DATA

Total Pore Volume for pores with Radius less than 2595.2 Å at P/Po = 0.9963.....	1.868E-01	cc/g
* t-Method Micro Pore Volume.....	5.902E-02	cc/g
* MP-Method Micro Pore Volume.....	7.124E-02	cc/g

PORE SIZE DATA

Average Pore Radius.....	1.534E+01	Å
--------------------------	-----------	---

* Note: MP and t-Method values based on data points with t-Tags.

Date: 2-09-95

Page 1

Quantachrome Corporation
Quantachrome Autosorb Automated Gas Adsorption System Report
ASORB2PC Version 1.04

Sample ID..... titania-silica gel
Sample Description..... containing 2 % PEG
Comments..... dried at 100 C for 30 min
Gas Type..... NITROGEN
Cross-Sec Area.. 16.2 Å² Corr Factor.. 6.580E-05 Molec Wgt.. 28.0134
Sample Weight... 0.0500 g P/Po Toler... 4 File Name.. AS2PEG01.RAW
Analysis Time... 118.1 min Equil Time... 2 Operator... Young-Min Kw
Outgas Time..... 3.0 hrs Outgas Temp.. 24 °C Station #.. 1
End of Run.....

AREA-VOLUME-PORE SIZE SUMMARY

SURFACE AREA DATA

Multi-Point BET.....	1.881E+00	m ² /g
Langmuir Surface Area.....	-2.322E+01	m ² /g
Meso Pore Area.....	1.881E+00	m ² /g
* t-Method Micro Pore Area.....	0.000E+00	m ² /g
DR-Method Micro Pore Area.....	2.503E+00	m ² /g
Cumulative Adsorption Surface Area.....	2.873E-01	m ² /g
Cumulative Desorption Surface Area.....	9.463E-01	m ² /g

PORE VOLUME DATA

Total Pore Volume for pores with Radius less than 15926.8 Å at P/Po = 0.9994.....	2.971E-03	cc/g
* t-Method Micro Pore Volume.....	0.000E+00	cc/g

PORE SIZE DATA

Average Pore Radius.....	3.159E+01	Å
--------------------------	-----------	---

* Note: MP and t-Method values based on data points with t-Tags.

Quantachrome Corporation
Quantachrome Autosorb Automated Gas Adsorption System Report
ASORB2PC Version 1.04

Sample ID..... titania-silica gel
 Sample Description..... heat-treated at 300 C without PEG
 Comments..... Water / TEOS = 2
 Gas Type..... NITROGEN
 Cross-Sec Area.. 16.2 A² Corr Factor.. 6.580E-05 Molec Wgt.. 28.0134
 Sample Weight... 0.0500 g P/Po Toler... 4 File Name.. ASHEAT02.RAW
 Analysis Time... 158.9 min Equil Time... 2 Operator... Young-Min
 Outgas Time..... 3.0 hrs Outgas Temp.. 24 °C Station #.. 1
 End of Run.....

AREA-VOLUME-PORE SIZE SUMMARY

SURFACE AREA DATA

Multi-Point BET.....	5.024E+02	m ² /g
Langmuir Surface Area.....	1.014E+03	m ² /g
Meso Pore Area.....	2.523E+02	m ² /g
* t-Method Micro Pore Area.....	2.501E+02	m ² /g
* MP-Method Micro Pore Area.....	4.488E+02	m ² /g
DR-Method Micro Pore Area.....	8.346E+02	m ² /g
Cumulative Adsorption Surface Area.....	6.911E+00	m ² /g
Cumulative Desorption Surface Area.....	8.995E+00	m ² /g

PORE VOLUME DATA

Total Pore Volume for pores with Radius less than 15926.8 Å at P/Po = 0.9994.....	3.240E-01	cc/g
* t-Method Micro Pore Volume.....	1.171E-01	cc/g
* MP-Method Micro Pore Volume.....	2.916E-01	cc/g

PORE SIZE DATA

Average Pore Radius.....	1.290E+01	Å
--------------------------	-----------	---

* Note: MP and t-Method values based on data points with t-Tags.

Quantachrome Corporation
Quantachrome Autosorb Automated Gas Adsorption System Report
ASORB2PC Version 1.04

Sample ID..... titania-silica gel
 Sample Description..... 2 % PEG contained
 Comments..... heat-treated at 300 C for 30 min
 Gas Type..... NITROGEN
 Cross-Sec Area.. 16.2 Å² Corr Factor.. 6.580E-05 Molec Wgt.. 28.0134
 Sample Weight... 0.0500 g P/Po Toler... 4 File Name.. AS2PEG02.RAW
 Analysis Time... 181.1 min Equil Time... 2 Operator... Young-Min Kw
 Outgas Time..... 3.0 hrs Outgas Temp.. 24 °C Station #.. 1
 End of Run.....

AREA-VOLUME-PORE SIZE SUMMARY

SURFACE AREA DATA

Multi-Point BET.....	5.411E+02	m ² /g
Langmuir Surface Area.....	1.258E+03	m ² /g
Meso Pore Area.....	2.885E+02	m ² /g
* t-Method Micro Pore Area.....	2.526E+02	m ² /g
* MP-Method Micro Pore Area.....	4.029E+02	m ² /g
DR-Method Micro Pore Area.....	8.956E+02	m ² /g
Cumulative Adsorption Surface Area.....	2.935E+01	m ² /g
Cumulative Desorption Surface Area.....	3.929E+01	m ² /g

PORE VOLUME DATA

Total Pore Volume for pores with Radius less than 1238.5 Å at P/Po = 0.9922.....	3.898E-01	cc/g
* t-Method Micro Pore Volume.....	1.193E-01	cc/g
* MP-Method Micro Pore Volume.....	2.483E-01	cc/g

PORE SIZE DATA

Average Pore Radius.....	1.441E+01	Å
--------------------------	-----------	---

* Note: MP and t-Method values based on data points with t-Tags.

Quantachrome Corporation
Quantachrome Autosorb Automated Gas Adsorption System Report
ASORB2PC Version 1.04

Sample ID..... titania-silica gel
 Sample Description..... Water / TEOS = 1.5
 Comments..... Dried at 100C for 30 min
 Gas Type..... NITROGEN
 Cross-Sec Area.. 16.2 Å² Corr Factor.. 6.580E-05 Molec Wgt.. 28.0134
 Sample Weight... 0.0500 g P/Po Toler... 4 File Name.. ASWATE01.RAW
 Analysis Time... 210.7 min Equil Time... 2 Operator... Young-Min Kw
 Outgas Time..... 3.0 hrs Outgas Temp.. 23 °C Station #.. 1
 End of Run.....

AREA-VOLUME-PORE SIZE SUMMARY

SURFACE AREA DATA

Multi-Point BET.....	1.832E+02	m ² /g
Langmuir Surface Area.....	4.638E+02	m ² /g
Meso Pore Area.....	9.812E+01	m ² /g
* t-Method Micro Pore Area.....	8.510E+01	m ² /g
* MP-Method Micro Pore Area.....	9.357E+01	m ² /g
DR-Method Micro Pore Area.....	3.050E+02	m ² /g
Cumulative Adsorption Surface Area.....	1.253E+01	m ² /g
Cumulative Desorption Surface Area.....	2.314E+01	m ² /g

PORE VOLUME DATA

Total Pore Volume for pores with Radius less than 15926.8 Å at P/Po = 0.9994.....	1.425E-01	cc/g
* t-Method Micro Pore Volume.....	4.253E-02	cc/g
* MP-Method Micro Pore Volume.....	5.498E-02	cc/g

PORE SIZE DATA

Average Pore Radius.....	1.555E+01	Å
--------------------------	-----------	---

* Note: MP and t-Method values based on data points with t-Tags.

Quantachrome Corporation
Quantachrome Autosorb Automated Gas Adsorption System Report
ASORB2PC Version 1.04

Sample ID..... titania-silica gel
 Sample Description..... Water / TEOS = 2
 Comments..... used as sample for heating and PEG effec
 Gas Type..... NITROGEN
 Cross-Sec Area.. 16.2 Å² Corr Factor.. 6.580E-05 Molec Wgt.. 28.0134
 Sample Weight... 0.0500 g P/Po Toler... 4 File Name.. ASWATE02.RAW
 Analysis Time... 237.7 min Equil Time... 2 Operator... Young-Min Kw
 Outgas Time..... 3.0 hrs Outgas Temp.. 24 °C Station #.. 1
 End of Run.....

AREA-VOLUME-PORE SIZE SUMMARY

SURFACE AREA DATA

Multi-Point BET.....	2.435E+02	m ² /g
Langmuir Surface Area.....	6.093E+02	m ² /g
Meso Pore Area.....	1.264E+02	m ² /g
* t-Method Micro Pore Area.....	1.171E+02	m ² /g
* MP-Method Micro Pore Area.....	1.234E+02	m ² /g
DR-Method Micro Pore Area.....	4.111E+02	m ² /g
Cumulative Adsorption Surface Area.....	1.844E+01	m ² /g
Cumulative Desorption Surface Area.....	2.820E+01	m ² /g

PORE VOLUME DATA

Total Pore Volume for pores with Radius less than 2595.2 Å at P/Po = 0.9963.....	1.868E-01	cc/g
* t-Method Micro Pore Volume.....	5.902E-02	cc/g
* MP-Method Micro Pore Volume.....	7.124E-02	cc/g

PORE SIZE DATA

Average Pore Radius.....	1.534E+01	Å
--------------------------	-----------	---

* Note: MP and t-Method values based on data points with t-Tags.

Quantachrome Corporation
Quantachrome Autosorb Automated Gas Adsorption System Report
ASORB2PC Version 1.04

Sample ID..... titania-silica gel
 Sample Description..... Water / TEOS = 3
 Comments..... used as no aging sample
 Gas Type..... NITROGEN
 Cross-Sec Area.. 16.2 Å² Corr Factor.. 6.580E-05 Molec Wgt.. 28.0134
 Sample Weight... 0.0500 g P/Po Toler... 4 File Name.. ASWATE03.RAW
 Analysis Time... 144.1 min Equil Time... 2 Operator... Young-Min Kw
 Outgas Time..... 3.0 hrs Outgas Temp.. 24 °C Station #.. 1
 End of Run.....

AREA-VOLUME-PORE SIZE SUMMARY

SURFACE AREA DATA

Multi-Point BET.....	2.220E+02	m ² /g
Langmuir Surface Area.....	4.208E+02	m ² /g
Meso Pore Area.....	9.658E+01	m ² /g
* t-Method Micro Pore Area.....	1.254E+02	m ² /g
* MP-Method Micro Pore Area.....	2.274E+02	m ² /g
DR-Method Micro Pore Area.....	3.630E+02	m ² /g
Cumulative Adsorption Surface Area.....	2.832E+00	m ² /g
Cumulative Desorption Surface Area.....	3.811E+00	m ² /g

PORE VOLUME DATA

Total Pore Volume for pores with Radius less than 15926.8 Å at P/Po = 0.9994.....	1.363E-01	cc/g
* t-Method Micro Pore Volume.....	5.751E-02	cc/g
* MP-Method Micro Pore Volume.....	1.368E-01	cc/g

PORE SIZE DATA

Average Pore Radius.....	1.228E+01	Å
--------------------------	-----------	---

* Note: MP and t-Method values based on data points with t-Tags.

Quantachrome Corporation
Quantachrome Autosorb Automated Gas Adsorption System Report
ASORB2PC Version 1.04

Sample ID..... titania-silica gel
 Sample Description..... Water / TEOS = 4
 Comments..... dried at 100C for 30 min
 Gas Type..... NITROGEN
 Cross-Sec Area.. 16.2 Å² Corr Factor.. 6.580E-05 Molac Wgt.. 28.0134
 Sample Weight... 0.0500 g P/Po Toler... 4 File Name.. ASWATE04.RAW
 Analysis Time... 172.8 min Equil Time... 2 Operator... Young-Min Kw
 Outgas Time..... 3.0 hrs Outgas Temp.. 24 °C Station #.. 1
 End of Run.....

AREA-VOLUME-PORE SIZE SUMMARY

SURFACE AREA DATA

Multi-Point BET.....	3.540E+02	m ² /g
Langmuir Surface Area.....	6.995E+02	m ² /g
Meso Pore Area.....	1.930E+02	m ² /g
* t-Method Micro Pore Area.....	1.610E+02	m ² /g
* MP-Method Micro Pore Area.....	4.366E+02	m ² /g
DR-Method Micro Pore Area.....	5.925E+02	m ² /g
Cumulative Adsorption Surface Area.....	2.672E+00	m ² /g
Cumulative Desorption Surface Area.....	5.493E+00	m ² /g

PORE VOLUME DATA

Total Pore Volume for pores with Radius less than 15926.8 Å at P/Po = 0.9994.....	2.192E-01	cc/g
* t-Method Micro Pore Volume.....	6.637E-02	cc/g
* MP-Method Micro Pore Volume.....	2.717E-01	cc/g

PORE SIZE DATA

Average Pore Radius.....	1.239E+01	Å
--------------------------	-----------	---

* Note: MP and t-Method values based on data points with t-Tags.

Date: 2-10-95

Page 1

Quantachrome Corporation
Quantachrome Autosorb Automated Gas Adsorption System Report
ASORB2PC Version 1.04

Sample ID..... Titania-silica gel
Sample Description..... No Aged
Comments..... Water / TEOS = 3
Gas Type..... NITROGEN
Cross-Sec Area.. 16.2 Å² Corr Factor.. 6.580E-05 Molec Wgt.. 28.0134
Sample Weight... 0.0500 g P/Po Toler... 4 File Name.. ASWATE03.RAW
Analysis Time... 144.1 min Equil Time... 2 Operator... Young-Min Kw
Outgas Time..... 3.0 hrs Outgas Temp.. 24 °C Station #.. 1
End of Run.....

AREA-VOLUME-PORE SIZE SUMMARY

SURFACE AREA DATA

Multi-Point BET.....	2.220E+02	m ² /g
Langmuir Surface Area.....	4.208E+02	m ² /g
Meso Pore Area.....	9.658E+01	m ² /g
* t-Method Micro Pore Area.....	1.254E+02	m ² /g
* MP-Method Micro Pore Area.....	2.274E+02	m ² /g
DR-Method Micro Pore Area.....	3.630E+02	m ² /g
Cumulative Adsorption Surface Area.....	2.832E+00	m ² /g
Cumulative Desorption Surface Area.....	3.811E+00	m ² /g

PORE VOLUME DATA

Total Pore Volume for pores with Radius less than 15926.8 Å at P/Po = 0.9994.....	1.363E-01	cc/g
* t-Method Micro Pore Volume.....	5.751E-02	cc/g
* MP-Method Micro Pore Volume.....	1.368E-01	cc/g

PORE SIZE DATA

Average Pore Radius.....	1.228E-01	Å
--------------------------	-----------	---

* Note: MP and t-Method values based on data points with t-Tags.

Quantachrome Corporation
 Quantachrome Autosorb Automated Gas Adsorption System Report
 ASORB2PC Version 1.04

Sample ID..... titania-silica gel
 Sample Description..... 4 Day Aged
 Comments..... Water / TEOS = 3
 Gas Type..... NITROGEN
 Cross-Sec Area.. 16.2 Å² Corr Factor.. 6.580E-05 Molec Wgt.. 28.0134
 Sample Weight... 0.0500 g P/Po Toler... 4 File Name.. AS4AGE01.RAW
 Analysis Time... 168.9 min Equil Time... 2 Operator... Young-Min Kw
 Outgas Time..... 3.0 hrs Outgas Temp.. 23 °C Station #.. 1
 End of Run.....

AREA-VOLUME-PORE SIZE SUMMARY

SURFACE AREA DATA

Multi-Point BET.....	2.860E+02	m ² /g
Langmuir Surface Area.....	6.354E+02	m ² /g
Meso Pore Area.....	1.748E+02	m ² /g
* t-Method Micro Pore Area.....	1.113E+02	m ² /g
* MP-Method Micro Pore Area.....	2.711E+02	m ² /g
DR-Method Micro Pore Area.....	4.857E+02	m ² /g
Cumulative Adsorption Surface Area.....	8.035E+00	m ² /g
Cumulative Desorption Surface Area.....	6.360E+00	m ² /g

PORE VOLUME DATA

Total Pore Volume for pores with Radius less than 15926.8 Å at P/Po = 0.9994.....	1.924E-01	cc/g
* t-Method Micro Pore Volume.....	4.829E-02	cc/g
* MP-Method Micro Pore Volume.....	1.801E-01	cc/g

PORE SIZE DATA

Average Pore Radius.....	1.345E+01	Å
--------------------------	-----------	---

* Note: MP and t-Method values based on data points with t-Tags.

Quantachrome Corporation
Quantachrome Autosorb Automated Gas Adsorption System Report
ASORB2PC Version 1.04

Sample ID..... titania-silica gel
 Sample Description..... 1 Week Aged
 Comments..... Water / TEOS = 1
 Gas Type..... NITROGEN
 Cross-Sec Area.. 16.2 Å² Corr Factor.. 6.580E-05 Molec Wgt.. 28.0134
 Sample Weight... 0.0500 g P/Po Toler... 4 File Name.. AS7AGE02.RAW
 Analysis Time... 152.9 min Equil Time... 2 Operator... Young-Min Kw
 Outgas Time..... 3.0 hrs Outgas Temp.. 24 °C Station #.. 1
 End of Run.....

AREA-VOLUME-PORE SIZE SUMMARY

SURFACE AREA DATA

Multi-Point BET.....	3.263E+02	m ² /g
Langmuir Surface Area.....	6.861E+02	m ² /g
Meso Pore Area.....	1.892E+02	m ² /g
* t-Method Micro Pore Area.....	1.371E+02	m ² /g
* MP-Method Micro Pore Area.....	3.224E+02	m ² /g
DR-Method Micro Pore Area.....	5.493E+02	m ² /g
Cumulative Adsorption Surface Area.....	5.892E+00	m ² /g
Cumulative Desorption Surface Area.....	7.592E+00	m ² /g

PORE VOLUME DATA

Total Pore Volume for pores with Radius less than 15926.8 Å at P/Po = 0.9994.....	2.125E-01	cc/g
* t-Method Micro Pore Volume.....	6.008E-02	cc/g
* MP-Method Micro Pore Volume.....	2.111E-01	cc/g

PORE SIZE DATA

Average Pore Radius.....	1.302E+01	Å
--------------------------	-----------	---

* Note: MP and t-Method values based on data points with t-Tags.

Quantachrome Corporation
 Quantachrome Autosorb Automated Gas Adsorption System Report
 ASORB2PC Version 1.04

Sample ID..... titania-silica gel
 Sample Description..... 2 Weeks Aged
 Comments..... Water/TEOS = 3
 Gas Type..... NITROGEN
 Cross-Sec Area.. 16.2 Å² Corr Factor.. 6.580E-05 Molec Wgt.. 28.0134
 Sample Weight... 0.0500 g P/Po Toler... 4 File Name.. AS14AG03.RAW
 Analysis Time... 152.4 min Equil Time... 2 Operator... Young-Min Kw
 Outgas Time..... 3.0 hrs Outgas Temp.. 24 °C Station #.. 1
 End of Run.....

AREA-VOLUME-PORE SIZE SUMMARY

SURFACE AREA DATA

Multi-Point BET.....	3.815E+02	m ² /g
Langmuir Surface Area.....	8.261E+02	m ² /g
Meso Pore Area.....	2.311E+02	m ² /g
* t-Method Micro Pore Area.....	1.504E+02	m ² /g
* MP-Method Micro Pore Area.....	3.805E+02	m ² /g
DR-Method Micro Pore Area.....	6.449E+02	m ² /g
Cumulative Adsorption Surface Area.....	8.079E+00	m ² /g
Cumulative Desorption Surface Area.....	1.047E+01	m ² /g

PORE VOLUME DATA

Total Pore Volume for pores with Radius less than 15926.8 Å at P/Po = 0.9994.....	2.515E-01	cc/g
* t-Method Micro Pore Volume.....	6.343E-02	cc/g
* MP-Method Micro Pore Volume.....	2.502E-01	cc/g

PORE SIZE DATA

Average Pore Radius.....	1.319E+01	Å
--------------------------	-----------	---

* Note: MP and t-Method values based on data points with t-Tags.

Quantachrome Corporation
Quantachrome Autosorb Automated Gas Adsorption System Report
ASORB2PC Version 1.04

Sample ID..... titania-silica gel
 Sample Description..... heat-treated at 100 C for 30 min.
 Comments..... Water / TEOS = 2
 Gas Type..... NITROGEN
 Cross-Sec Area.. 16.2 Å² Corr Factor.. 6.580E-05 Molec Wgt.. 28.0134
 Sample Weight... 0.0500 g P/Po Toler... 4 File Name.. ASWATE02.RAW
 Analysis Time... 237.7 min Equil Time... 2 Operator... Young-Min Kw
 Outgas Time..... 3.0 hrs Outgas Temp.. 24 °C Station #.. 1
 End of Run.....

AREA-VOLUME-PORE SIZE SUMMARY

SURFACE AREA DATA

Multi-Point BET.....	2.435E+02	m ² /g
Langmuir Surface Area.....	6.093E+02	m ² /g
Meso Pore Area.....	1.264E+02	m ² /g
* t-Method Micro Pore Area.....	1.171E+02	m ² /g
* MP-Method Micro Pore Area.....	1.234E+02	m ² /g
DR-Method Micro Pore Area.....	4.111E+02	m ² /g
Cumulative Adsorption Surface Area.....	1.844E+01	m ² /g
Cumulative Desorption Surface Area.....	2.820E+01	m ² /g

PORE VOLUME DATA

Total Pore Volume for pores with Radius less than 2595.2 Å at P/Po = 0.9963.....	1.868E-01	cc/g
* t-Method Micro Pore Volume.....	5.902E-02	cc/g
* MP-Method Micro Pore Volume.....	7.124E-02	cc/g

PORE SIZE DATA

Average Pore Radius.....	1.534E-01	Å
--------------------------	-----------	---

* Note: MP and t-Method values based on data points with t-Tags.

Quantachrome Corporation
quantachrome Autosorb Automated Gas Adsorption System Report
ASORB2PC Version 1.04

Sample ID..... titania-silica gel
 Sample Description..... heat-treated at 200 C for 30 min
 Comments..... Water / TEOS = 2
 Gas Type..... NITROGEN
 Cross-Sec Area.. 16.2 Å² Corr Factor.. 6.580E-05 Molec Wgt.. 28.0114
 Sample Weight... 0.0500 g P/Po Toler... 4 File Name.. ASHEAT01.RAW
 Analysis Time... 189.8 min Equil Time... 2 Operator... Young-Min Kw
 Outgas Time..... 1.0 hrs Outgas Temp.. 24 °C Station #.. 1
 End of Run.....

AREA-VOLUME-PORE SIZE SUMMARY

SURFACE AREA DATA

Multi-Point BET.....	4.640E+02	m ² /g
Langmuir Surface Area.....	9.815E+02	m ² /g
Meso Pore Area.....	2.476E+02	m ² /g
* t-Method Micro Pore Area.....	2.165E+02	m ² /g
* MP-Method Micro Pore Area.....	4.248E+02	m ² /g
DR-Method Micro Pore Area.....	7.754E+02	m ² /g
Cumulative Adsorption Surface Area.....	7.325E+00	m ² /g
Cumulative Desorption Surface Area.....	2.006E+01	m ² /g

PORE VOLUME DATA

Total Pore Volume for pores with Radius less than 2908.0 Å at P/Po = 0.9967.....	3.164E-01	cc/g
* t-Method Micro Pore Volume.....	9.959E-02	cc/g
* MP-Method Micro Pore Volume.....	2.775E-01	cc/g

PORE SIZE DATA

Average Pore Radius.....	1.364E+01	Å
--------------------------	-----------	---

* Note: MP and t-Method values based on data points with t-Tags.

Date: 3-04-95

Page 1

Quantachrome Corporation
Quantachrome Autosorb Automated Gas Adsorption System Report
ASORB2PC Version 1.04

Sample ID..... titania-silica gel
Sample Description..... heat-treated at 300 C for 30 min
Comments..... Water / TEOS = 2
Gas Type..... NITROGEN
Cross-Sec Area.. 16.2 A² Corr Factor.. 6.580E-05 Molec Wgt.. 28.0134
Sample Weight... 0.0500 g P/Po Toler... 4 File Name.. ASHEAT02.RAW
Analysis Time... 158.9 min Equil Time... 2 Operator... Young-Min
Outgas Time..... 3.0 hrs Outgas Temp.. 24 °C Station #.. 1
End of Run.....

AREA-VOLUME-PORE SIZE SUMMARY

SURFACE AREA DATA

Multi-Point BET..... 5.024E+02 m²/g
Langmuir Surface Area..... 1.014E+03 m²/g
Meso Pore Area..... 2.523E+02 m²/g
* t-Method Micro Pore Area..... 2.501E+02 m²/g
* MP-Method Micro Pore Area..... 4.488E+02 m²/g
DR-Method Micro Pore Area..... 8.346E+02 m²/g
Cumulative Adsorption Surface Area..... 6.911E+00 m²/g
Cumulative Desorption Surface Area..... 8.995E+00 m²/g

PORE VOLUME DATA

Total Pore Volume for pores with Radius
less than 15926.8 Å at P/Po = 0.9994..... 3.240E-01 cc/g
* t-Method Micro Pore Volume..... 1.171E-01 cc/g
* MP-Method Micro Pore Volume..... 2.916E-01 cc/g

PORE SIZE DATA

Average Pore Radius..... 1.290E+01 Å

* Note: MP and t-Method values based on data points with t-Tags.

Quantachrome Corporation
Quantachrome Autosorb Automated Gas Adsorption System Report
ASOR22PC Version 1.04

Sample ID..... titania-silica gel
 Sample Description..... heat-treated at 400 C for 30 min
 Comments..... Water / TEOS = 2
 Gas Type..... NITROGEN
 Cross-Sec Area.. 16.2 Å² Corr Factor.. 6.580E-05 Molac Wgt.. 28.0134
 Sample Weight... 0.0500 g P/Po Toler... 4 File Name.. ASHEAT03.RAW
 Analysis Time... 151.0 min Equil Time... 2 Operator... Young-Min
 Outgas Time..... 3.0 hrs Outgas Temp.. 24 °C Station #.. 1
 End of Run.....

AREA-VOLUME-PORE SIZE SUMMARY

SURFACE AREA DATA

Multi-Point BET.....	3.559E+02	m ² /g
Langmuir Surface Area.....	7.282E+02	m ² /g
Meso Pore Area.....	1.814E+02	m ² /g
* t-Method Micro Pore Area.....	1.745E+02	m ² /g
* MP-Method Micro Pore Area.....	2.996E+02	m ² /g
DR-Method Micro Pore Area.....	5.974E+02	m ² /g
Cumulative Adsorption Surface Area.....	6.817E+00	m ² /g
Cumulative Desorption Surface Area.....	7.291E+00	m ² /g

PORE VOLUME DATA

Total Pore Volume for pores with Radius less than 15926.8 Å at P/Po = 0.9994.....	2.302E-01	cc/g
* t-Method Micro Pore Volume.....	8.291E-02	cc/g
* MP-Method Micro Pore Volume.....	1.956E-01	cc/g

PORE SIZE DATA

Average Pore Radius.....	1.294E+01	Å
--------------------------	-----------	---

* Note: MP and t-Method values based on data points with t-Tags.

Quantachrome Corporation
Quantachrome Autosorb Automated Gas Adsorption System Report
ASORB2PC Version 1.04

Sample ID..... titania-silica gel
 Sample Description..... heat-treated at 500 C for 30 min
 Comments..... Water / TEOS = 2
 Gas Type..... NITROGEN
 Cross-Sec Area.. 16.2 Å² Corr Factor.. 6.580E-05 Molec Wgt.. 28.0134
 Sample Weight... 0.0500 g P/Po Toler... 4 File Name.. ASHEAT04.RAW
 Analysis Time... 150.0 min Equil Time... 2 Operator... Young-Min
 Outgas Time..... 3.0 hrs Outgas Temp.. 24 °C Station #.. 1
 End of Run.....

AREA-VOLUME-PORE SIZE SUMMARY

SURFACE AREA DATA

Multi-Point BET.....	4.240E+02	m ² /g
Langmuir Surface Area.....	8.433E+02	m ² /g
Meso Pore Area.....	2.064E+02	m ² /g
* t-Method Micro Pore Area.....	2.175E+02	m ² /g
* MP-Method Micro Pore Area.....	3.718E+02	m ² /g
DR-Method Micro Pore Area.....	7.063E+02	m ² /g
Cumulative Adsorption Surface Area.....	6.015E+00	m ² /g
Cumulative Desorption Surface Area.....	6.980E+00	m ² /g

PORE VOLUME DATA

Total Pore Volume for pores with Radius less than 15926.8 Å at P/Po = 0.9994.....	2.697E-01	cc/g
* t-Method Micro Pore Volume.....	1.027E-01	cc/g
* MP-Method Micro Pore Volume.....	2.399E-01	cc/g

PORE SIZE DATA

Average Pore Radius.....	1.272E+01	Å
--------------------------	-----------	---

* Note: MP and t-Method values based on data points with t-Tags.

Quantachrome Corporation
 Quantachrome Autosorb Automated Gas Adsorption System Report
 ASORB2PC Version 1.04

Sample ID..... titania-silica gel
 Sample Description..... heat-treated at 600 C
 Comments..... Water / TEOS = 2
 Gas Type..... NITROGEN
 Cross-Sec Area.. 16.2 Å² Corr Factor.. 6.580E-05 Molec Wgt.. 28.0134
 Sample Weight... 0.0500 g P/Po Toler... 4 File Name.. ASHEAT05.RAW
 Analysis Time... 148.4 min Equil Time... 2 Operator... Young-Min
 Outgas Time..... 3.0 hrs Outgas Temp.. 24 °C Station #.. 1
 End of Run.....

AREA-VOLUME-PORE SIZE SUMMARY

SURFACE AREA DATA

Multi-Point BET.....	3.951E+02	m ² /g
Langmuir Surface Area.....	7.912E+02	m ² /g
Meso Pore Area.....	1.954E+02	m ² /g
* t-Method Micro Pore Area.....	1.997E+02	m ² /g
* MP-Method Micro Pore Area.....	3.483E+02	m ² /g
DR-Method Micro Pore Area.....	6.593E+02	m ² /g
Cumulative Adsorption Surface Area.....	6.680E+00	m ² /g
Cumulative Desorption Surface Area.....	6.940E+00	m ² /g

PORE VOLUME DATA

Total Pore Volume for pores with Radius less than 15926.8 Å at P/Po = 0.9994.....	2.512E-01	cc/g
* t-Method Micro Pore Volume.....	9.374E-02	cc/g
* MP-Method Micro Pore Volume.....	2.238E-01	cc/g

PORE SIZE DATA

Average Pore Radius.....	1.272E+01	Å
--------------------------	-----------	---

* Note: MP and t-Method values based on data points with t-Tags.

TABULAR DATA FOR ISOTHERMS

Date: 2-08-95

Page 1

Quantachrome Corporation
quantachrome Autosorb Automated Gas Adsorption System Report
ASORB2PC Version 1.04

Sample ID..... titania-silica gel
Sample Description..... Water / TEOS = 2
Comments..... used as sample for heating and PEG effec
Gas Type..... NITROGEN
Cross-Sec Area.. 16.2 Å² Corr Factor.. 6.580E-05 Molec Wgt.. 28.0134
Sample Weight... 0.0500 g P/Po Toler... 4 File Name.. ASWATE02.RAW
Analysis Time... 237.7 min Equil Time... 2 Operator... Young-Min Kw
Outgas Time..... 3.0 hrs Outgas Temp.. 24 °C Station #.. 1
End of Run.....

ISOTHERM

P/Po	Volume cc/g STP
0.1301	66.500
0.2259	75.240
0.2999	80.620
0.4311	89.040
0.5104	93.680
0.6029	98.920
0.6975	105.500
0.8008	110.460
0.9005	115.660
0.9963	120.700
0.8921	115.740
0.7919	110.840
0.6943	105.720
0.5953	100.700
0.4973	95.320
0.4014	90.160
0.2711	81.060
0.1728	72.800
0.0880	62.780

Quantachrome Corporation
 Quantachrome Autosorb Automated Gas Adsorption System Report
 ASORB2PC Version 1.04

Sample ID..... titania-silica gel
 Sample Description..... containing 2 % PEG
 Comments..... dried at 100 C for 30 min
 Gas Type..... NITROGEN
 Cross-Sec Area.. 16.2 Å² Corr Factor.. 6.580E-05 Molec Wgt.. 28.0134
 Sample Weight... 0.0500 g P/Po Toler... 4 File Name.. AS2PEG01.RAW
 Analysis Time... 118.1 min Equil Time... 2 Operator... Young-Min Kw
 Outgas Time..... 3.0 hrs Outgas Temp.. 24 °C Station #.. 1
 End of Run.....

ISOTHERM

P/Po	Volume cc/g STP
0.1132	0.140
0.2144	0.200
0.3141	0.380
0.4140	0.480
0.5142	0.540
0.6139	0.680
0.7143	0.740
0.8137	0.920
0.9139	1.000
0.9994	1.920
0.8856	1.140
0.7854	1.080
0.6850	1.040
0.5855	0.860
0.4853	0.640
0.3856	0.500
0.2855	0.360
0.1853	0.000
0.0854	-0.220

Quantachrome Corporation
 Quantachrome Autosorb Automated Gas Adsorption System Report
 ASORB2PC Version 1.04

Sample ID..... titania-silica gel
 Sample Description..... heat-treated at 100 C for 30 min.
 Comments..... Water / TEOS = 2
 Gas Type..... NITROGEN
 Cross-Sec Area.. 16.2 A² Corr Factor.. 6.580E-05 Molec Wgt.. 28.0134
 Sample Weight... 0.0500 g P/Po Toler... 4 File Name.. ASHEAT02.RAW
 Analysis Time... 158.9 min Equil Time... 2 Operator... Young-Min
 Outgas Time..... 3.0 hrs Outgas Temp.. 24 °C Station #.. 1
 End of Run.....

ISOTHERM

P/Po	Volume cc/g STP
0.0996	121.540
0.2042	144.420
0.3054	163.720
0.3953	178.960
0.4985	192.320
0.6092	200.540
0.7065	203.680
0.8105	205.120
0.9115	205.960
0.9994	209.420
0.8862	205.780
0.7861	204.940
0.6860	203.820
0.5864	202.440
0.4876	200.420
0.4019	180.140
0.3013	162.500
0.1998	143.160
0.1001	121.100

Date: 2-11-95

Page 1

Quantachrome Corporation
Quantachrome Autosorb Automated Gas Adsorption System Report
ASORB2PC Version 1.04

Sample ID..... titania-silica gel
Sample Description..... 2 % PEG contained
Comments..... heat-treated at 300 C for 30 min
Gas Type..... NITROGEN
Cross-Sec Area.. 16.2 Å² Corr Factor.. 6.580E-05 Molec Wgt.. 28.0134
Sample Weight... 0.0500 g P/Po Toler... 4 File Name... AS2PEG02.RAW
Analysis Time... 181.1 min Equil Time... 2 Operator... Young-Min Kw
Outgas Time..... 3.0 hrs Outgas Temp.. 24 °C Station #.. 1
End of Run.....

ISOTHERM

P/Po	Volume cc/g STP
0.1068	134.780
0.2065	158.180
0.2986	175.340
0.3988	191.500
0.5007	205.660
0.6026	217.840
0.7040	228.040
0.8059	236.900
0.9023	245.820
0.9922	251.900
0.8891	248.800
0.7978	242.820
0.6999	235.740
0.5995	228.240
0.4993	220.620
0.3906	191.880
0.2929	176.120
0.1951	157.780
0.0987	134.400

Date: 2-06-95

Page 1

Quantachrome Corporation
Quantachrome Autosorb Automated Gas Adsorption System Report
ASORB2PC Version 1.04

Sample ID..... titania-silica gel
Sample Description..... Water / TEOS = 1.5
Comments..... Dried at 100C for 30 min
Gas Type..... NITROGEN
Cross-Sec Area.. 16.2 Å² Corr Factor.. 6.580E-05 Molec Wgt.. 28.0134
Sample Weight... 0.0500 g P/Po Toler... 4 File Name.. ASWATE01.RAW
Analysis Time... 210.7 min Equil Time... 2 Operator... Young-Min Kw
Outgas Time..... 3.0 hrs Outgas Temp.. 23 °C Station #.. 1
End of Run.....

ISOTHERM

P/Po	Volume cc/g STP
0.1097	48.100
0.2295	56.600
0.3108	61.100
0.4080	65.800
0.5092	70.420
0.6023	75.600
0.7100	80.280
0.8166	84.100
0.9151	88.080
0.9994	92.080
0.8883	87.640
0.7826	83.520
0.6810	79.460
0.5811	75.580
0.4826	71.400
0.3875	66.920
0.2930	62.160
0.1680	54.380
0.0767	45.920

Date: 2-08-95

Page 1

Quantachrome Corporation
Quantachrome Autosorb Automated Gas Adsorption System Report
ASORB2PC Version 1.04

Sample ID..... titania-silica gel
Sample Description..... Water / TEOS = 2
Comments..... used as sample for heating and PEG effec
Gas Type..... NITROGEN
Cross-Sec Area.. 16.2 A² Corr Factor.. 6.580E-05 Molec Wgt.. 28.0134
Sample Weight... 0.0500 g P/Po Toler... 4 File Name.. ASWATE02.RAW
Analysis Time... 237.7 min Equil Time... 2 Operator... Young-Min Kw
Outgas Time..... 3.0 hrs Outgas Temp.. 24 °C Station #.. 1
End of Run.....

ISOTHERM

P/Po	Volume cc/g STP
0.1301	66.500
0.2259	75.240
0.2999	80.620
0.4311	89.040
0.5104	93.680
0.6029	98.920
0.6975	105.500
0.8008	110.460
0.9005	115.660
0.9963	120.700
0.3921	115.740
0.7919	110.840
0.6943	105.720
0.5953	100.700
0.4973	95.320
0.4014	90.160
0.2711	81.060
0.1723	72.800
0.0880	62.780

Quantachrome Corporation
 Quantachrome Autosorb Automated Gas Adsorption System Report
 ASORB2PC Version 1.04

Sample ID..... titania-silica gel
 Sample Description..... Water / TEOS = 3
 Comments..... used as no aging sample
 Gas Type..... NITROGEN
 Cross-Sec Area.. 16.2 Å^2 Corr Factor.. 6.580E-05 Molec Wgt.. 28.0134
 Sample Weight... 0.0500 g P/Po Toler... 4 File Name.. ASWATE03.RAW
 Analysis Time... 144.1 min Equil Time... 2 Operator... Young-Min Kw
 Outgas Time..... 3.0 hrs Outgas Temp.. 24 °C Station #.. 1
 End of Run.....

ISOTHERM

P/Po	Volume cc/g STP
0.1032	53.020
0.2042	63.920
0.3080	72.240
0.3980	77.740
0.5020	82.060
0.6075	84.740
0.7112	85.980
0.8119	86.700
0.9126	87.060
0.9994	88.100
0.8859	86.980
0.7857	86.640
0.6861	86.060
0.5855	85.640
0.4856	84.720
0.3991	78.340
0.2960	71.320
0.1982	63.620
0.0917	51.680

Date: 2-13-95

Page 1

Quantachrome Corporation
Quantachrome Autosorb Automated Gas Adsorption System Report
ASORB2PC Version 1.04

Sample ID..... titania-silica gel
Sample Description..... Water / TEOS = 4
Comments..... dried at 100C for 30 min
Gas Type..... NITROGEN
Cross-Sec Area.. 16.2 A² Corr Factor.. 6.580E-05 Molec Wgt.. 28.0134
Sample Weight... 0.0500 g P/Po Toler... 4 File Name.. ASWATE04.RAW
Analysis Time... 172.8 min Equil Time... 2 Operator... Young-Min Kw
Outgas Time..... 3.0 hrs Outgas Temp.. 24 °C Station #.. 1
End of Run.....

ISOTHERM

P/Po	Volume cc/g STP
0.1055	75.780
0.2012	95.060
0.3095	111.840
0.3969	123.920
0.5042	134.000
0.6030	138.280
0.7114	139.660
0.8137	140.020
0.9135	140.160
0.9994	141.680
0.3860	139.980
0.7855	139.320
0.6862	138.500
0.5863	137.580
0.4866	136.460
0.3932	121.520
0.2986	107.940
0.1995	91.820
0.1025	74.260

Quantachrome Corporation
quantachrome Autosorb Automated Gas Adsorption System Report
ASORB2PC Version 1.04

Sample ID..... titania-silica gel
 Sample Description..... Water / TEOS = 3
 Comments..... used as no aging sample
 Gas Type..... NITROGEN
 Cross-Sec Area.. 16.2 A² Corr Factor.. 6.580E-05 Molec Wgt.. 28.0134
 Sample Weight... 0.0500 g P/Po Toler... 4 File Name.. ASWATE03.RAW
 Analysis Time... 144.1 min Equil Time... 2 Operator... Young-Min Kw
 Outgas Time..... 3.0 hrs Outgas Temp.. 24 °C Station #.. 1
 End of Run.....

ISOTHERM

P/Po	Volume cc/g STP
0.1032	53.020
0.2042	63.920
0.3080	72.240
0.3980	77.740
0.5020	82.060
0.6075	84.740
0.7112	85.980
0.8119	86.700
0.9126	87.060
0.9994	88.100
0.8859	86.980
0.7857	86.640
0.6861	86.060
0.5855	85.640
0.4856	84.720
0.3991	78.340
0.2960	71.820
0.1982	63.620
0.0917	51.680

Quantachrome Corporation
 Quantachrome Autosorb Automated Gas Adsorption System Report
 ASORB2PC Version 1.04

Sample ID..... titania-silica gel
 Sample Description..... 4 Day Aged
 Comments..... Water / TEOS = 3
 Gas Type..... NITROGEN
 Cross-Sec Area.. 16.2 Å² Corr Factor.. 6.580E-05 Molec Wgt.. 28.0134
 Sample Weight... 0.0500 g P/Po Toler... 4 File Name.. AS4AGE01.RAW
 Analysis Time... 168.9 min Equil Time... 2 Operator... Young-Min Kw
 Outgas Time..... 3.0 hrs Outgas Temp.. 23 °C Station #.. 1
 End of Run.....

ISOTHERM

P/Po	Volume cc/g STP
0.1039	64.340
0.2026	78.240
0.3013	90.600
0.4005	102.400
0.5034	112.280
0.5985	118.220
0.7237	122.820
0.8132	123.500
0.9143	123.680
0.9994	124.360
0.8863	123.020
0.7861	122.480
0.6868	121.840
0.5865	120.880
0.4868	119.380
0.3921	101.680
0.2922	89.660
0.2026	77.940
0.0945	62.060

Date: 2-18-95

Page 1

Quantachrome Corporation
Quantachrome Autosorb Automated Gas Adsorption System Report
ASORB2PC Version 1.04

Sample ID..... titania-silica gel
Sample Description..... 1 Week Aged
Comments..... Water / TEOS = 3
Gas Type..... NITROGEN
Cross-Sec Area.. 16.2 A² Corr Factor.. 6.580E-05 Molec Wgt.. 28.0134
Sample Weight... 0.0500 g P/Po Toler... 4 File Name.. AS7AGE02.RAW
Analysis Time... 152.9 min Equil Time... 2 Operator... Young-Min Kw
Outgas Time..... 3.0 hrs Outgas Temp.. 24 °C Station #.. 1
End of Run.....

ISOTHERM

P/Po	Volume cc/g STP
0.1031	74.400
0.2018	90.000
0.3010	103.760
0.4009	116.480
0.5043	126.560
0.5992	132.140
0.7075	134.880
0.8118	136.080
0.9133	136.580
0.9994	137.320
0.8850	136.860
0.7860	136.280
0.6787	142.680
0.5957	139.260
0.4861	138.580
0.3969	118.580
0.2928	104.360
0.1919	89.440
0.0933	72.940

Date: 2-25-95

Page 1

Quantachrome Corporation
Quantachrome Autosorb Automated Gas Adsorption System Report
ASORB2PC Version 1.34

Sample ID..... titania-silica gel
Sample Description..... 2 Weeks Aged
Comments..... Water/TEOS = 3
Gas Type..... NITROGEN
Cross-Sec Area.. 16.2 A² Corr Factor.. 6.580E-05 Molec Wgt.. 28.0134
Sample Weight... 0.0500 g P/Po Toler... 4 File Name.. AS14AG03.RAW
Analysis Time... 152.4 min Equil Time... 2 Operator... Young-Min Kw
Outgas Time..... 3.0 hrs Outgas Temp.. 24 °C Station #.. 1
End of Run.....

ISOTHERM

P/Po	Volume cc/g STP
0.1096	86.060
0.1996	103.060
0.2978	119.780
0.3977	135.160
0.5020	147.440
0.6092	155.500
0.7050	158.980
0.8097	160.960
0.9118	162.000
0.9994	162.560
0.3858	161.940
0.7855	161.240
0.6860	160.320
0.5871	158.700
0.4888	156.180
0.4003	135.180
0.2981	119.180
0.1965	101.980
0.0965	82.680

Date: 2-08-95

Page 1

Quantachrome Corporation
Quantachrome Autosorb Automated Gas Adsorption System Report
ASORB2PC Version 1.04

Sample ID..... titania-silica gel
Sample Description..... Water / TEOS = 2
Comments..... used as sample for heating and PEG effec
Gas Type..... NITROGEN
Cross-Sec Area.. 16.2 Å² Corr Factor.. 6.580E-05 Molec Wgt.. 28.0134
Sample Weight... 0.0500 g P/Po Toler... 4 File Name.. ASWATE02.RAW
Analysis Time... 237.7 min Equil Time... 2 Operator... Young-Min Kw
Outgas Time..... 3.0 hrs Outgas Temp.. 24 °C Station #.. 1
End of Run.....

ISOTHERM

P/Po	Volume cc/g STP
0.1301	66.500
0.2259	75.240
0.2999	80.620
0.4311	89.040
0.5104	93.680
0.6029	98.920
0.6975	105.500
0.8008	110.460
0.9005	115.660
0.9963	120.700
0.8921	115.740
0.7919	110.840
0.6943	105.720
0.5953	100.700
0.4973	95.320
0.4014	90.160
0.2711	81.060
0.1728	72.800
0.0880	62.780

Quantachrome Corporation
Quantachrome Autosorb Automated Gas Adsorption System Report
ASORB2PC Version 1.04

Sample ID..... titania-silica gel
 Sample Description..... heat-treated at 200 C for 30 min
 Comments..... Water / TEOS = 2
 Gas Type..... NITROGEN
 Cross-Sec Area.. 16.2 A² Corr Factor.. 6.580E-05 Molec Wgt.. 28.0134
 Sample Weight... 0.0500 g P/Po Toler... 4 File Name.. ASHEAT01.RAW
 Analysis Time... 189.8 min Equil Time... 2 Operator... Young-Min Kw
 Outgas Time..... 3.0 hrs Outgas Temp.. 24 °C Station #.. 1
 End of Run.....

ISOTHERM

P/Po	Volume cc/g STP
0.1003	110.260
0.2035	131.760
0.3038	150.120
0.4074	166.980
0.4990	178.420
0.6071	186.680
0.7056	189.920
0.8105	191.380
0.9110	192.320
0.9967	204.460
0.8865	201.580
0.7860	199.600
0.6863	197.580
0.6040	190.780
0.4908	188.120
0.3929	165.340
0.2987	149.160
0.2011	131.260
0.1014	110.440

Quantachrome Corporation
Quantachrome Autosorb Automated Gas Adsorption System Report
ASORB2PC Version 1.34

Sample ID..... titania-silica gel
 Sample Description..... heat-treated at 300 C for 30 min.
 Comments..... Water / TEOS = 2
 Gas Type..... NITROGEN
 Cross-Sec Area.. 16.2 A² Corr Factor.. 6.580E-05 Molec Wgt.. 28.0134
 Sample Weight... 0.0500 g P/Po Toler... 4 File Name.. ASHEAT02.RAW
 Analysis Time... 158.9 min Equil Time... 2 Operator... Young-Min
 Outgas Time..... 3.0 hrs Outgas Temp.. 24 °C Station #.. 1
 End of Run.....

ISOTHERM

P/Po	Volume cc/g STP
0.0996	121.540
0.2042	144.420
0.3054	163.720
0.3953	178.960
0.4985	192.320
0.6092	200.540
0.7065	203.680
0.8105	205.120
0.9115	205.960
0.9994	209.420
0.8862	205.780
0.7861	204.940
0.6860	203.820
0.5864	202.440
0.4876	200.420
0.4019	180.140
0.3013	162.500
0.1998	143.160
0.1001	121.100

Date: 3-07-95

Page 1

Quantachrome Corporation
Quantachrome Autosorb Automated Gas Adsorption System Report
ASORB2PC Version 1.64

Sample ID..... titania-silica gel
Sample Description..... heat-treated at 400 C for 30 min
Comments..... Water / TEOS = 2
Gas Type..... NITROGEN
Cross-Sec Area.. 16.2 A² Corr Factor.. 6.580E-05 Molec Wgt.. 28.0134
Sample Weight... 0.0500 g P/Po Toler... 4 File Name.. ASHEAT03.RAW
Analysis Time... 151.0 min Equil Time... 2 Operator... Young-Min
Outgas Time..... 3.0 hrs Outgas Temp.. 24 °C Station #.. 1
End of Run.....

ISOTHERM

P/Po	Volume cc/g STP
0.1094	88.720
0.2017	102.500
0.3007	115.700
0.4005	127.720
0.5038	137.220
0.5981	142.760
0.7061	145.940
0.8106	147.180
0.9113	147.960
0.9994	148.760
0.8865	147.980
0.7862	147.400
0.6863	146.580
0.5865	145.420
0.4873	143.760
0.3912	126.760
0.2923	114.620
0.1922	100.940
0.0942	85.640

Quantachrome Corporation
 Quantachrome Autosorb Automated Gas Adsorption System Report
 ASORB2PC Version 1.04

Sample ID..... titania-silica gel
 Sample Description..... heat-treated at 500 C for 30 min
 Comments..... Water / TEOS = 2
 Gas Type..... NITROGEN
 Cross-Sec Area.. 16.2 A² Corr Factor.. 6.580E-05 Molec Wgt.. 28.0134
 Sample Weight... 0.0500 g P/Po Toler... 4 File Name.. ASHEAT04.RAW
 Analysis Time... 150.0 min Equil Time... 2 Operator... Young-Min
 Outgas Time..... 3.0 hrs Outgas Temp.. 24 °C Station #.. 1
 End of Run.....

ISOTHERM

P/Po	Volume cc/g STP
0.1071	105.140
0.1999	121.880
0.2983	137.260
0.3990	151.300
0.5029	162.020
0.5982	167.980
0.7067	170.880
0.8113	171.900
0.9122	172.360
0.9994	174.280
0.8857	172.300
0.7852	172.120
0.6859	171.440
0.5867	170.400
0.4877	168.680
0.3931	150.500
0.2933	136.580
0.1949	120.980
0.0959	102.400

Date: 3-11-95

Page 1

Quantachrome Corporation
Quantachrome Autosorb Automated Gas Adsorption System Report
ASORB2PC Version 1.04

Sample ID..... titania-silica gel
Sample Description..... heat-treated at 600 C
Comments..... Water / TEOS = 2
Gas Type..... NITROGEN
Cross-Sec Area.. 16.2 Å² Corr Factor.. 6.580E-05 Molec Wgt.. 28.0134
Sample Weight... 0.0500 g P/Po Toler... 4 File Name.. ASHEAT05.RAW
Analysis Time... 148.4 min Equil Time... 2 Operator... Young-Min
Outgas Time..... 3.0 hrs Outgas Temp.. 24 °C Station #.. 1
End of Run.....

ISOTHERM

P/Po	Volume cc/g STP
0.1083	97.480
0.2008	113.260
0.2995	127.880
0.4003	141.000
0.5043	151.040
0.5985	156.640
0.7067	159.720
0.8106	161.040
0.9126	161.760
0.9994	162.340
0.8854	161.600
0.7866	160.980
0.6859	160.240
0.5864	159.100
0.4871	157.540
0.4046	141.700
0.2960	127.160
0.1941	111.960
0.0947	94.500